Universidade do Minho
Escola de Ciências

Cláudia Isabel Castro Oliveira

Characterization of natural extracts for cosmetic applications

outubro de 2023

Characterization of natural extracts for cosmetic applications
Cláudia Oliveira
UMinho | 20223

Universidade do Minho
Escola de Ciências

Cláudia Isabel Castro Oliveira

Characterization of natural extracts for cosmetic applications

Dissertação de Mestrado
Mestrado em Técnicas de Caracterização e Análise Química

Trabalho efetuado sob a orientação da
Doutora Carla Manuela Pereira Marinho da Silva
e da
Professora Doutora Susana Paula Graça da Costa

outubro de 2023

DIREITOS DE AUTOR E CONDIÇÕES DE UTILIZAÇÃO DO TRABALHO POR TERCEIROS

Este é um trabalho académico que pode ser utilizado por terceiros desde que respeitadas as regras e boas práticas internacionalmente aceites, no que concerne aos direitos de autor e direitos conexos.

Assim, o presente trabalho pode ser utilizado nos termos previstos na licença abaixo indicada.

Caso o utilizador necessite de permissão para poder fazer um uso do trabalho em condições não previstas no licenciamento indicado, deverá contactar o autor, através do RepositóriUM da Universidade do Minho.

Licença concedida aos utilizadores deste trabalho



Atribuição-NãoComercial-SemDerivações
CC BY-NC-ND

https://creativecommons.org/licenses/by-nc-nd/4.0/

ACKNOWLEDGEMENTS

Having completed another stage in my academic journey, I want to thank everyone who helped me make this work possible.

Firstly, I would like to thank my supervisors. To Doctor Carla Silva, whose guidance, support, and encouragement were essential in the completion of this thesis. To Professor Susana Costa for her availability, attention, and valuable feedback.

Thank you to all LBBN members for all the help provided. Especially to David, for always being available to answer my countless questions.

I would also like to thank my friends who accompanied me in the laboratory during this thesis year, Cátia, Tatiana, and Catarina, I will remember our time together both inside and outside the laboratory.

Thank you to all my friends for their encouragement and faith in me. A special thanks to Flávia, Francisca, Margarida, Catarina, and Mariana.

Finally, I want to express my gratitude to my parents and sister for supporting me throughout the years and allowing me to study and pursue my dreams.

Thank you all!

STATEMENT OF INTEGRITY

I hereby declare having conducted this academic work with integrity. I confirm that I have not used plagiarism of any form of undue use of information or falsification of results along the process leading to its elaboration.

I further declare that I have fully acknowledged the Code of Ethical Conduct of University of Minho.

Caracterização de extratos naturais para aplicações cosméticas

RESUMO

Os bioativos derivados de fontes naturais têm uma ampla gama de aplicações, principalmente em cosméticos. Os extratos naturais oferecem uma alternativa aos medicamentos potencialmente perigosos no tratamento de uma variedade de doenças dermatológicas, incluindo a hipo- e hiperpigmentação. A caracterização de extratos naturais é uma etapa essencial para a compreensão da sua composição química, bioatividade e potenciais aplicações na área cosmética. Nesta dissertação foi realizada a extração de compostos bioativos de cinco fontes naturais (lavanda, tomilho, eucalipto, cortiça e cacau), utilizando solventes convencionais (misturas de EtOH:H_2O em duas proporções) e solventes eutécticos (SE) (glicerol:ácido lático e glicerol:ácido cítrico), e três métodos de extração (pás, durante 30 e 90 minutos, e misturadora planetária). Após o processo de extração, os resultados indicaram que os solventes eutécticos exibiram eficiências de extração semelhantes ou superiores em comparação aos solvents hidroetanólicos. Adicionalmente, observou-se que a misturadora planetária demonstrou notável capacidade de extração. Os extratos foram posteriormente caracterizados quanto às suas propriedades físico-químicas. A cortiça apresentou maior teor de fenólicos e flavonoides (362,10 mg GAE/g extrato e 1481,50 mg QE/g extrato, respetivamente). No que diz respeito à atividade antioxidante, foi também o extracto de cortiça que apresentou maior poder de captação do radical 2,2-difenil-1-picrilhidrazil e 2,2'-azino-*bis*(ácido 3-etilbenzotiazolina-6-sulfónico) (EC_{50} de 0,35 mg/mL e 28,84 mg/mL, respetivamente). O extrato de lavanda apresentou alta capacidade de redução de iões férricos de 9,96 mg TE/g extrato. No entanto, nenhum dos extratos demonstrou atividade quelante férrica. Quanto à atividade antimicrobiana, destacaram-se a cortiça e o eucalipto pela sua atividade contra bactérias Gram-positivas e Gram-negativas. Foi também a cortiça que apresentou maior capacidade fotoprotetora (fator de proteção de 10,43). A análise por cromatografia gasosa acoplada a espetrometria de massa dos extratos obtidos utilizando solventes convencionais revelou açúcares e pequenos álcoois. Nos extratos à base de SE, a sua composição consiste principalmente em açúcares e menores quantidades de álcoois e ácidos, esteróides, compostos aromáticos, ácidos gordos e terpenóides. Por fim, avaliou-se o efeito inibitório de todos os extratos sobre a tirosinase e observou-se que o extrato de tomilho exibiu um efeito inibitório notável de 46,0%. As descobertas dos extratos demonstram características favoráveis que poderão ser potencialmente incorporadas em formulações cosméticas para tratar distúrbios pigmentares no futuro.

Palavras-chave: caracterização fisico-química; extração de bioativos; fontes naturais; formulações cosméticas; solventes eutécticos.

Characterization of natural extracts for cosmetic applications

ABSTRACT

Bioactives derived from natural sources have a wide range of applications, particularly in cosmetics. Natural extracts offer an alternative to potentially dangerous drugs in the treatment of a variety of dermatological disorders, including hypo- and hyperpigmentation. The characterization of natural extracts is an essential step in understanding their chemical composition, bioactivity, and potential applications in the cosmetic field. In this dissertation, the extraction of bioactive compounds from five natural sources was performed (lavender, thyme, eucalyptus, cork, and cocoa), using conventional solvents (EtOH:H_2O mixtures in two ratios) and deep eutectic solvents (DES) (glycerol:lactic acid and glycerol:citric acid), and three extraction methods (a mechanical impeller, for 30 and 90 minutes, and a planetary mixer). Upon the extraction process, the data indicated that eutectic solvents exhibited similar or superior extraction efficiencies compared to hydroethanolic solvents. Additionally, it was observed that the planetary mixer demonstrated a notable capacity for extraction. The extracts were posteriorly characterized in terms of their physicochemical properties. Cork showed the highest total phenolic and flavonoid content (362.10 mg GAE/g extract and 1481.50 mg QE/g extract, respectively). Regarding antioxidant activity, it also was the cork extract that showed the highest 2,2-diphenyl-1-picrylhydrazyl and 2,2′-azino-*bis*(3-ethylbenzothiazoline-6-sulfonic acid) radical scavenging action (EC_{50} of 0.35 mg/mL and 28.84 mg/mL, respectively). The lavender extract had a significant capacity to reduce ferric ions, as evidenced by a ferric ion reducing power of 9.96 mg TE/g extract. However, none of the extracts demonstrated any ferric chelating activity. Regarding antimicrobial activity, cork and eucalyptus stood out for their activity against both Gram-positive and Gram-negative bacteria. It was also the cork extract that presented the highest photoprotective capacity (sun protection factor of 10.43). The gas chromatography coupled to mass spectrometry analysis of the extracts obtained using conventional solvents revealed mainly sugars and small alcohols. In DES-based extracts, their composition mostly consists of sugars, and smaller quantities of alcohols and acids, steroids, aromatic compounds, fatty acids, and terpenoids. Finally, the inhibitory effect of all extracts on tyrosinase was assessed, and it was observed that thyme extract exhibited a notable inhibitory effect of 46.0%. The findings from the extracts demonstrate favourable characteristics that could be potentially incorporated into cosmetic formulations to address pigmentary disorders in the future.

Keywords: physiochemical characterization; bioactives extraction; natural sources; cosmetic formulations; deep eutectic solvents.

TABLE OF CONTENTS

Direitos de autor e condições de utilização do trabalho por terceiros ..... **ii**

Acknowledgements ..... **iii**

Statement of Integrity ..... **iv**

Resumo ..... **v**

Abstract ..... **vi**

List of Abbreviations and Symbols ..... **x**

List of Figures ..... **xiii**

List of Tables ..... **xvii**

1. Introduction **1**

1.1 Melanin 1

1.1.1 Synthesis of melanin 2

1.1.2 Melanin biosynthesis signal pathways 4

1.1.3 Pigmentation disorders 5

1.1.4 Melanogenesis inhibitors and stimulators from different sources 6

1.1.4.1 Synthetic compounds for tyrosinase regulation 6

1.1.4.2 Naturally occurring compounds for tyrosinase regulation 7

1.2 Cosmetic formulations 10

1.3 Natural sources 13

1.3.1 Lavender 13

1.3.2 Thyme 14

1.3.3 Eucalyptus 15

1.3.4 Cocoa 16

1.3.5 Cork 17

1.4 Extraction Methods 18

1.5 Characterization of natural extracts 22

1.5.1 Total phenolic content 22

1.5.2 Total flavonoid content 24
1.5.3 Antioxidant activity 26
1.5.3.1 2,2-Diphenyl-1-picrylhydrazyl (DPPH) radical scavenging assay 27
1.5.3.2 2,2′-Azino-bis(3-ethylbenzothiazoline-6-sulfonic acid) (ABTS) radical scavenging assay 28
1.5.3.3 Ferric ion reducing antioxidant power (FRAP) assay 29
1.5.3.4 Ferric chelating activity assay 30
1.5.4 Antimicrobial Activity 31
1.5.5 Sun Protection Factor 33
1.5.6 Identification of extracts' volatile compounds by gas chromatography-mass spectrometry.. 34
2. Motivation and aims of this work 36
3. Materials and Methods 37
3.1 Materials and chemicals 37
3.2 Extraction solvents development and characterization 38
3.2.1 Extraction solvents production 38
3.2.2 Characterization of the extraction solvents 39
3.2.2.1 Polarity 39
3.2.2.2 pH measurement 39
3.2.2.3 Viscosity 39
3.2.2.4 Density 40
3.2.2.5 Refraction index 40
3.2.2.6 Conductivity 40
3.3 Extraction of bioactive compounds from natural sources 40
3.4 Characterization of the extracts 42
3.4.1 Determination of total phenolic content (TPC) 42
3.4.2 Determination of total flavonoid content (TFC) 43
3.4.3 Determination of antioxidant activity 44
3.4.3.1 DPPH radical scavenging activity assay 44
3.4.3.2 ABTS radical scavenging activity assay 45
3.4.3.3 Ferric ion reducing antioxidant power (FRAP) assay 47
3.4.3.4 Ferric chelating activity assay 48

3.4.4 Determination of antimicrobial activity 49
3.4.4.1 Broth microdilution method (MICs and MBCs determination) 49
3.4.4.2 Agar-well diffusion method 51
3.4.5 Determination of sun protection factor (SPF) 52
3.4.6 Gas chromatography-mass spectroscopy (GC-MS) analysis 53
3.4.7 Tyrosinase inhibition assay 54
4. Results and Discussion 56
4.1 Characterization of the extraction solvents 56
4.2 Extraction of bioactive compounds from natural sources 58
4.3 Characterization of natural extracts 60
4.3.1. Total phenolic content (TPC) 60
4.3.2 Total flavonoid content (TFC) 62
4.3.3 Antioxidant activity 65
4.3.3.1 DPPH radical scavenging assay 65
4.3.3.2 ABTS radical scavenging assay 66
4.3.3.3 Ferric ion reducing antioxidant power (FRAP) assay 68
4.3.3.4 Ferric chelating activity assay 70
4.3.4 Determination of antimicrobial activity 72
4.3.4.1 Minimum inhibitory concentrations (MICs) and minimum bactericidal concentrations (MBCs) 72
4.3.4.2 Agar-well diffusion method 73
4.3.5 Sun Protection Factor (SPF) 74
4.3.6 Identification of extracts' volatile compounds by gas chromatography-mass spectrometry (GC-MS) 76
4.3.7 Tyrosinase inhibition assay 78
5. Conclusions and future perspectives 85
6. References 89

LIST OF ABBREVIATIONS AND SYMBOLS

ABTS	2,2′-Azino-*bis*(3-ethylbenzothiazoline-6-sulfonic acid)
AC	Adenylate cyclase
ACTH	Adrenocorticotrophic hormone
cAMP	Cyclic adenosine monophosphate
CFUs	Colony forming units
CRE	cAMP response element
CREB	cAMP response element-binding protein
DES	Deep eutectic solvent
DHI	5,6-Dihydroxyindole
DHICA	5,6-Dihydroindole-2-carboxylic acid
DMSO	Dimethyl sulfoxide
DPPH	2,2-Diphenyl-1-picrylhydrazyl
DQ	DOPAquinone
EC_{50}	Half maximal effective concentration
EDTA	Ethylenediaminetetraacetic acid
E_{NR}	Polarity
FRAP	Ferric ion reducing antioxidant power
GAE	Gallic acid equivalents
GC-MS	Gas chromatography-mass spectrometry
GSK	Glycogen synthase kinase
HAT	Hydrogen atom transfer

HBA	Hydrogen bond acceptor
HBD	Hydrogen bond donor
HE	Hydroethanolic
MAPK	Mitogen-activated protein kinase
MBC	Minimum bactericidal concentration
MCR	Melanocortin receptor
MED	Minimal erythemal dose
MHB	Mueller-Hinton broth
MI	Mechanical Impeller
MIC	Minimum inhibitory concentration
MITF	Microphthalmia-associated transcription factor
MSH	Melanocyte stimulating hormone
$\mathbf{n_D}$	Refractive index
PBS	Phosphate-buffered saline solution
PKA	Protein kinase A
POMC	Proopiomelanocortin
QE	Quercetin equivalents
ROS	Reactive oxygen species
SCF	Stem cell factor
SET	Single electron transfer
SPF	Sun protection factor
TE	Trolox equivalents
TFC	Total flavonoid content

TPC	Total phenolic content
TPTZ	2,4,6-Tripyridyl-s-triazine
Trolox	6-Hydroxy-2,5,7,8-tetramethylchroman-2-carboxylic acid
TSA	Tryptic soy agar
TSB	Tryptic soy broth
TYR	Tyrosinase
TYRP1	Tyrosinase-related protein 1
TYRP2	Tyrosinase-related protein 2
UV	Ultraviolet
UV-Vis	Ultraviolet-Visible
WNT	Wingless-related integration site
ZoI	Zone of inhibition
σ	Conductivity
ρ	Density
η	Viscosity

LIST OF FIGURES

Figure 1. Scheme of the stratum basale layer of the epidermis. Adapted from (D'Mello et al., 2016).. 1

Figure 2. Structure of mushroom tyrosinase isoform AbPPO4 (Agaricus bisporus polyphenol oxidase 4). Adapted from (Pretzler et al., 2017). 2

Figure 3. Melanogenesis catalyzed by TYR, TYRP1, and TYRP2. Adapted from (Pillaiyar et al., 2017). 3

Figure 4. Melanin biosynthesis signal pathway. Adapted from (Pillaiyar et al., 2017). 4

Figure 5. Hyperpigmentation (**A**) and hypopigmentation (**B**) cases. Adapted from (Silpa-archa et al., 2017; Thawabteh et al., 2023). 5

Figure 6. Chemical structure of synthetic tyrosinase inhibitors. Adapted from (Lee et al., 2016) using the ChemDraw software. 7

Figure 7. Topical brands used for the treatment of skin pigmentation **A)** Opzelura® **B)** Clobetasol Propionate **C)** Olivia quido® firming and fading I skin lightener cream **D)** Antipodes® Diem Vitamin C Pigment-Correcting Water Cream **E)** The Ordinary® Niacinamide 10% + Zinc 1% **F)** Bella Aurora® bio10 forte. 11

Figure 8. Chemical structures of thymol and carvacrol. The structures were obtained using the ChemDraw software. 15

Figure 9. Chemical structures of catechin and epicatechin. Adapted from (Ramalho et al., 2014) using the ChemDraw software. 16

Figure 10. Chemical structure of theobromine. The structure was obtained using the ChemDraw software. 17

Figure 11. Chemical structure of some HBAs and HBDs used in the formation of DES. Adapted from (Stephens & Smith, 2022) using the ChemDraw software. 21

Figure 12. Schematic representation of the Folin-Ciocalteu assay. Adapted from (Rangel et al., 2013). 24

Figure 13. Subclasses of flavonoids and corresponding structures. Adapted from (Das & Gezici, 2018) using the ChemDraw software. 25

Figure 14. Formation of the complex quercetin-aluminium chloride when using Aluminium Chloride assay. Adapted (Radulescu et al., 2019) from using the ChemDraw software. 26

Figure 15. DPPH assay: radical scavenging principle. Adapted from (Munteanu & Apetrei, 2021) using the ChemDraw software. 28

Figure 16. ABTS radical cation scavenging mechanism by an antioxidant molecule (AH). Adapted from (Munteanu & Apetrei, 2021) using the ChemDraw software. 29
Figure 17. FRAP reaction mechanism, where ArOH represents a phenolic antioxidant and $[ArOH]^{+}$ is an oxidised phenolic antioxidant. Adapted from (Bibi Sadeer et al., 2020) using the ChemDraw software. 30
Figure 18. Reaction between a phenolic compound and the ferrous ion (1) resulting in a decrease of the light purple color and reaction between ferrozine and the ferrous ion (2). Adapted from (J. S. Santos et al., 2017) using the ChemDraw software. 31
Figure 19. Schematic presentation of a typical GC-MS system. Adapted from (Skoog et al., 2017)... 35
Figure 20. Natural sources used for extraction **A)** Lavandula angustifolia **B)** Thymus vulgaris **C)** Corymbia citriodora **D)** Theobroma cacao **E)** Quercus suber L. Images adapted from (Identify, Explore and Share Your Observations of Wild Plants). 37
Figure 21. Procedure workflow for determination of total phenolic content following the Folin-Ciocalteu assay (the images were obtained using the BioRender software). 43
Figure 22. Procedure workflow for determination of the total flavonoid content following the aluminium chloride assay (the images were obtained using the BioRender software). 44
Figure 23. Procedure workflow for determination of the antioxidant activity following the DPPH radical scavenging activity assay (the images were obtained using the BioRender software). 45
Figure 24. Procedure workflow for determination of the antioxidant activity following the ABTS radical scavenging activity assay (the images were obtained using the BioRender software). 46
Figure 25. Procedure workflow for determination of the antioxidant activity following the ferric ion reducing antioxidant power assay (the images were obtained using the BioRender software). 47
Figure 26. Procedure workflow for determination of the antioxidant activity following the ferric chelating activity assay (the images were obtained using the BioRender software). 48
Figure 27. Schematic workflow for determination of minimum inhibitory concentration (MIC) (the images were obtained using the BioRender software) **1)** Serial dilutions of the extract are made in Mueller-Hinton broth (MHB) medium in a 96-well plate **2)** Bacterial inoculum is prepared and added to the 96-well plate **3)** The plate is incubated for 24 hours and the MIC value is determined. 50
Figure 28. Schematic workflow for determination of minimum bactericidal concentration (MBC) (the images were obtained using the BioRender software) **4)** After serial dilutions of the wells selected after MIC determination, aliquots from these wells are inoculated onto the surface of tryptic soy agar (TSA) plates. The plates are incubated for 24 hours and the MBC value is determined. 50

Figure 29. Procedure workflow for determination of zone of inhibition (ZoI) (the images were obtained using the BioRender software) **1)** Each bacteria strain is incorporated into tryptic soy agar (TSA) plates and incubated for 24 hours **2)** The sample is placed on wells cut into the surface of the agar **3)** After the plates are incubated for 24 hours, the zones of inhibition are measured. 51

Figure 30. Procedure workflow for determination of sun protection factor of extracts (the images were obtained using the BioRender software). 53

Figure 31. Chromatographic column employed in the purification of eutectic extracts before GC-MS characterization. 53

Figure 32. Procedure workflow for determination of tyrosinase inhibition (the images were obtained using the BioRender software)..... 55

Figure 33. Extraction yield (g extract/g starting material) obtained after extraction with a mechanical impeller (MI) for 30 and 90 minutes and a planetary mixer using **a)** HE (EtOH:H_2O) 50:50 solvent **b)** HE (EtOH:H_2O) 30:70 solvent **c)** deep eutectic solvent (DES) 1 **d)** DES 2 **e)** DES 3. 59

Figure 34. Total phenolic content (TPC) in the extracts presented as gallic acid equivalents (GAE) **a)** extracts obtained by extraction with HE (EtOH:H_2O) 50:50 solvent **b)** HE (EtOH:H_2O) 30:70 solvent **c)** deep eutectic solvent (DES) 1 **d)** DES 2 **e)** DES 3. Data is expressed as mean ± SD. 61

Figure 35. Total flavonoid content (TFC) in the extracts presented as quercetin equivalents (QE) **a)** extracts obtained by extraction with HE (EtOH:H_2O) 50:50 solvent **b)** HE (EtOH:H_2O) 30:70 solvent **c)** deep eutectic solvent (DES) 1 **d)** DES 2 **e)** DES 3. Data is expressed as mean ± SD. 63

Figure 36. The EC_{50} values of all natural extracts extracted with a mechanical impeller (MI) for 30 and 90 minutes and a planetary mixer using HE (EtOH:H_2O) 50:50 and 30:70, and deep eutectic solvents (DES) 1, 2 and 3, by DPPH assay. Trolox was used as reference and the samples containing only the solvents were evaluated to infer the role of the matrix. Data is expressed as mean ± SD. 66

Figure 37. The EC_{50} values of all natural extracts extracted with a mechanical impeller (MI) for 30 and 90 minutes and a planetary mixer using HE (EtOH:H_2O) 50:50 and 30:70, and deep eutectic solvents (DES) 1, 2 and 3, by ABTS assay. Trolox was used as reference and the samples containing only the solvents were evaluated to infer the role of the matrix. Data is expressed as mean ± SD. 68

Figure 38. Ferric ion reducing antioxidant power (FRAP) of all natural extracts extracted with a mechanical impeller (MI) for 30 and 90 minutes and a planetary mixer using HE (EtOH:H_2O) 50:50 and 30:70 solvent, and deep eutectic solvents (DES) 1, 2 and 3. Trolox was used as reference and the samples

containing only the solvents were evaluated to infer the role of the matric. Data is expressed as mean ± SD..... 69

Figure 39. The EC_{50} values of all natural extracts extracted with a mechanical impeller (MI) for 30 and 90 minutes and a planetary mixer using HE (EtOH:H_2O) 50:50 and 30:70, and deep eutectic solvents (DES) 1,2 and 3, by ferric chelating activity assay. EDTA was used as reference and the samples containing only the solvents were evaluated to infer the role of the matrix. Data is expressed as mean ± SD..... 71

Figure 40. Sun protection factor (SPF) values of all natural extracts extracted with a mechanical impeller (MI) for 30 and 90 minutes and a planetary mixer using HE (EtOH:H_2O) 50:50 and 30:70, and deep eutectic solvent (DES) 1,2 and 3. Sunscreen lotion Darphin® Soleil SPF 50 was used as standard and the samples containing only the solvents were evaluated to infer the role of the matrix. Data is expressed as mean ± SD..... 75

Figure 41. Gas chromatography-mass spectroscopy (GC-MS) analysis of the extracts obtained using method 2. 77

Figure 42. Gas chromatography-mass spectroscopy (GC-MS) analysis of the extracts obtained using method 11. 78

Figure 43. Curves of percentage of tyrosinase inhibition versus concentration for the lavender extracts **a)** HE (EtOH:H_2O) 50:50 solvent **b)** HE (EtOH:H_2O) 30:70 solvent **c)** deep eutectic solvent (DES) 1 **d)** DES 2 **e)** DES 3. 80

Figure 44. Curves of percentage of tyrosinase inhibition versus concentration for the thyme extracts **a)** HE (EtOH:H_2O) 50:50 solvent **b)** HE (EtOH:H_2O) 30:70 solvent **c)** deep eutectic solvent (DES) 1 **d)** DES 2 **e)** DES 3..... 81

Figure 45. Curves of percentage of tyrosinase inhibition versus concentration for the eucalyptus extracts **a)** HE (EtOH:H_2O) 50:50 solvent **b)** HE (EtOH:H_2O) 30:70 solvent **c)** deep eutectic solvent (DES) 1 **d)** DES 2 **e)** DES 3. 82

Figure 46. Curves of percentage of tyrosinase inhibition versus concentration for the cork extracts **a)** HE (EtOH:H_2O) 50:50 solvent **b)** HE (EtOH:H_2O) 30:70 solvent **c)** deep eutectic solvent (DES) 1 **d)** DES 2 **e)** DES 3..... 83

Figure 47. Curves of percentage of tyrosinase inhibition versus concentration for the cocoa extracts **a)** HE (EtOH:H_2O) 50:50 solvent **b)** HE (EtOH:H_2O) 30:70 solvent **c)** deep eutectic solvent (DES) 1 **d)** DES 2 **e)** DES 3..... 84

LIST OF TABLES

Table 1. Effects of natural chemical compounds on tyrosinase regulation, melanogenesis, and on other parameters. 7

Table 2. Effects of plant extracts on tyrosinase regulation, melanogenesis, and other parameters. 9

Table 3. Cosmetic applications of natural extracts. 12

Table 4. Chemical structures of most prevalent bioactives in lavender. The structures were obtained using the ChemDraw software. 13

Table 5. Chemical structures of the most abundant bioactives in eucalyptus. The structures were obtained using the ChemDraw software. 15

Table 6. Chemical structures of major phenolic acids in cork. The structures were obtained using the ChemDraw software. 17

Table 7. Various advanced methods for extraction of active compounds from plant materials. 19

Table 8. Basic structural skeletons of phenolic compounds and examples of important subfamilies of each class. Adapted from (Amawi et al., 2017) using the ChemDraw software. 23

Table 9. Antioxidant assays based on the reaction mechanism. Adapted from (Gulcin, 2020; Munteanu & Apetrei, 2021). 27

Table 10. Examples of plant extracts with antibacterial activity. 32

Table 11. Examples of plant extracts with photoprotective properties. 33

Table 12. Composition of the DES used as extraction solvents. 38

Table 13. Extraction conditions applied when using a mechanical impeller and a planetary mixer. 41

Table 14. The different extraction methodologies tested in this study. 41

Table 15. EE $\lambda \times I$ λ values of each of the wavelengths used to determine the SPF. 52

Table 16. Physicochemical properties of the extraction solvents: polarity (ENR), pH, viscosity (η), density (ρ), refraction index (n_D), and conductivity (σ). 56

Table 17. Minimum inhibitory concentrations (MICs) and Minimum bactericidal concentrations (MBCs) (mg/mL) of selected hydroethanolic extracts against Gram-positive and Gram-negative bacteria. 72

Table 18. Zones of inhibition (mm) of selected extracts against Gram-positive and Gram-negative bacteria. 73

Table 19. Optimized operational conditions for each extract tested and corresponding physicochemical properties. 86

1. INTRODUCTION

1.1 MELANIN

Melanin is the main compound responsible for hair, eye and skin pigmentation in humans and plays an important role in the photoprotection of skin cells against ultraviolet (UV) radiation and the scavenging of free radicals. There are two types of melanin: eumelanin, which is brownish black, and pheomelanin, which is reddish yellow. Eumelanin is the predominant type in individuals with dark skin and hair and is most effective against the harmful effects of UV radiation and reactive oxygen species (ROS). Pheomelanin is predominantly found in individuals with red hair and certain skin phototypes in which skin tumors are more common since this pigment is less effective in shielding the skin from UV damage. The specific type and amount of melanin produced in an individual depends on a variety of factors, including genetics and environmental factors such as UV radiation exposure (Castellano-Pellicena et al., 2021; Pahari et al., 2020; Slominski et al., 2022; Solano, 2020).

Melanin is mostly found in the *basal* layer (or *stratum basale*) of the human epidermis, where it is produced by melanocytes and accepted by surrounding keratinocytes (**Figure 1**) (Cichorek et al., 2013; Solano, 2020).

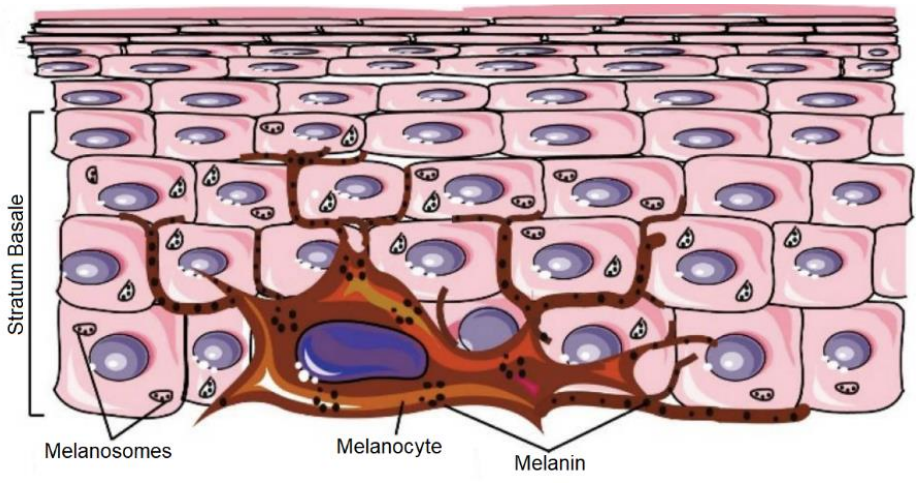


Figure 1. Scheme of the *stratum basale* layer of the epidermis. Adapted from (D'Mello et al., 2016).

However, the presence of melanocytes in the human body is not limited to the epidermis, they are also found in the hair and iris, where they contribute to the color of these structures, as well as the inner ear, nervous system, and heart. Melanocytes, which resemble dendritic cells, have specialized organelles called melanosomes that are used to produce and store melanin. The elongated dendrites of melanocytes

allow for the transmission of melanosomes from melanocytes to nearby keratinocytes. In the cytosol of keratinocytes, the melanosomes accumulate as perinuclear caps that are thought to shield DNA from UV rays (Cichorek et al., 2013; Solano, 2020). Other cells, such as adipocytes, certain neurons, and the pigmented epithelium of the retina, as well as melanocytes, have the capacity to create melanin (Cichorek et al., 2013).

1.1.1 Synthesis of melanin

Melanin is produced through a process called melanogenesis and is catalyzed by tyrosinase (TYR) and other proteins such as tyrosinase-related protein 1 (TYRP1, also known as gp75 glycoprotein or gp75) and tyrosinase-related protein 2 (TYRP2, also known as dopachrome tautomerase). Even though all three of these enzymes are part of the melanogenesis pathway, only tyrosinase is specifically required for melanogenesis (Boo, 2020).

Tyrosinase (EC 1.14.18.1) is a copper-containing enzyme located in the membrane of the melanosome with an inner melanosomal domain that contains the catalytic region, followed by a short transmembrane domain and a cytoplasmic domain (**Figure 2**) (Cichorek et al., 2013; Niu & Aisa, 2017; Sánchez-Ferrer et al., 1995).



Figure 2. Structure of mushroom tyrosinase isoform *Ab*PPO4 (*Agaricus bisporus* polyphenol oxidase 4). Adapted from (Pretzler et al., 2017).

The structure of tyrosinase consists of a single polypeptide chain that undergoes post-translational modifications to form an active enzyme. Tyrosinase is synthesized on the endoplasmic reticulum's ribosomes and then transported to the Golgi complex, where it is glycosylated, a process necessary for

its normal structure and function. It contains two copper atoms at its active site, each surrounded by three histidines, which are essential for its catalytic activity. Tyrosinase has two distinct forms: the inactive monomeric form and the oligomeric form, which is active and responsible for the synthesis of melanin. Apart from its role in melanin biosynthesis, tyrosinase has been found to have other functions as well such as wound healing, immune response, defence against pathogens, and browning of fruits and vegetables during ripening (Cichorek et al., 2013; Niu & Aisa, 2017; Sánchez-Ferrer et al., 1995).

Tyrosinase kickstarts the melanogenesis pathway by catalyzing the hydroxylation of L-tyrosine to L-DOPA and the following oxidation to DOPAquinone (DQ), which will act as a substrate for the synthesis of eumelanin and pheomelanin (**Figure 3**). The formation of DQ is the only rate-limiting step in melanin synthesis. In the presence of thiol compounds, such as cysteine or glutathione, DQ reacts with it to form 2- or 5-S-cysteinylDOPA. Subsequent oxidation gives benzothiazine intermediates and finally produces pheomelanin. In the absence of thiol compounds, eumelanin is produced. DQ undergoes intramolecular cyclization to produce leukodopachrome. The redox exchange between leukodopachrome and DQ gives rise to DOPAchrome. DOPAchrome can spontaneously lose carbon dioxide to form 5,6-dihydroxyindole (DHI) or, by the action of TYRP2, form 5,6-dihydroindole-2-carboxylic acid (DHICA). Polymerization of DHI and DHICA and their quinones ultimately leads to eumelanin production (Boo, 2020; Pahari et al., 2020).

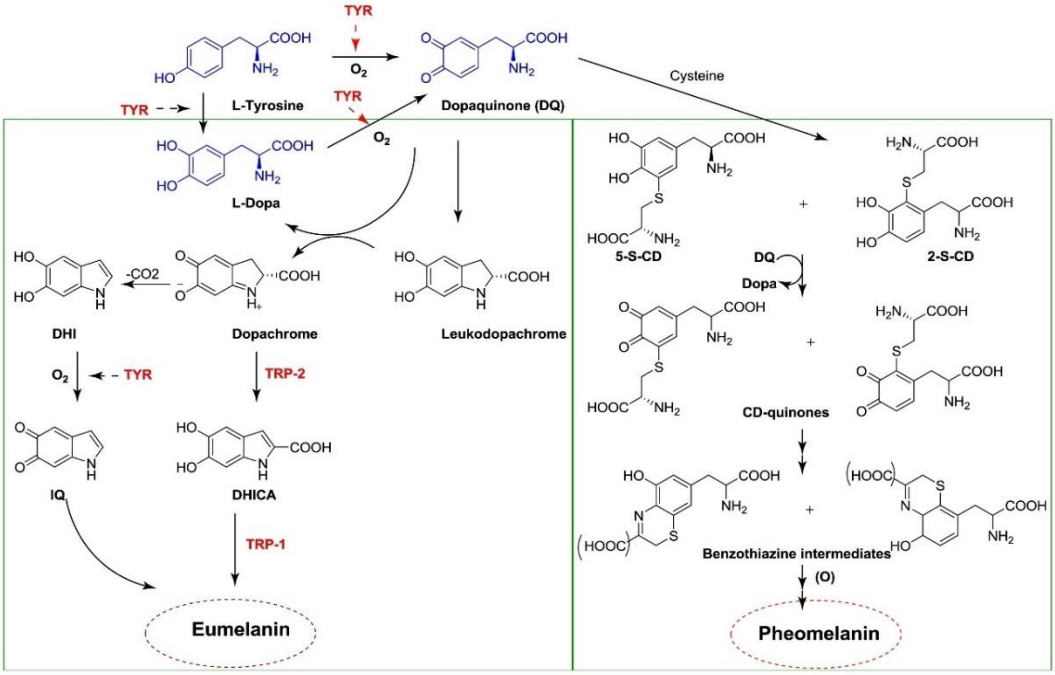


Figure 3. Melanogenesis catalyzed by TYR, TYRP1, and TYRP2. Adapted from (Pillaiyar et al., 2017).

1.1.2 Melanin biosynthesis signal pathways

Melanin synthesis is affected by diverse factors including genetics, hormones, and environmental conditions, and is regulated by several signalling pathways that ensure the synthesis, transport, and distribution of melanin (**Figure 4**) (Boo, 2020). Cyclic adenosine monophosphate (cAMP)/protein kinase A (PKA) signalling pathway is one of the most important signalling pathways (Fu et al., 2020).

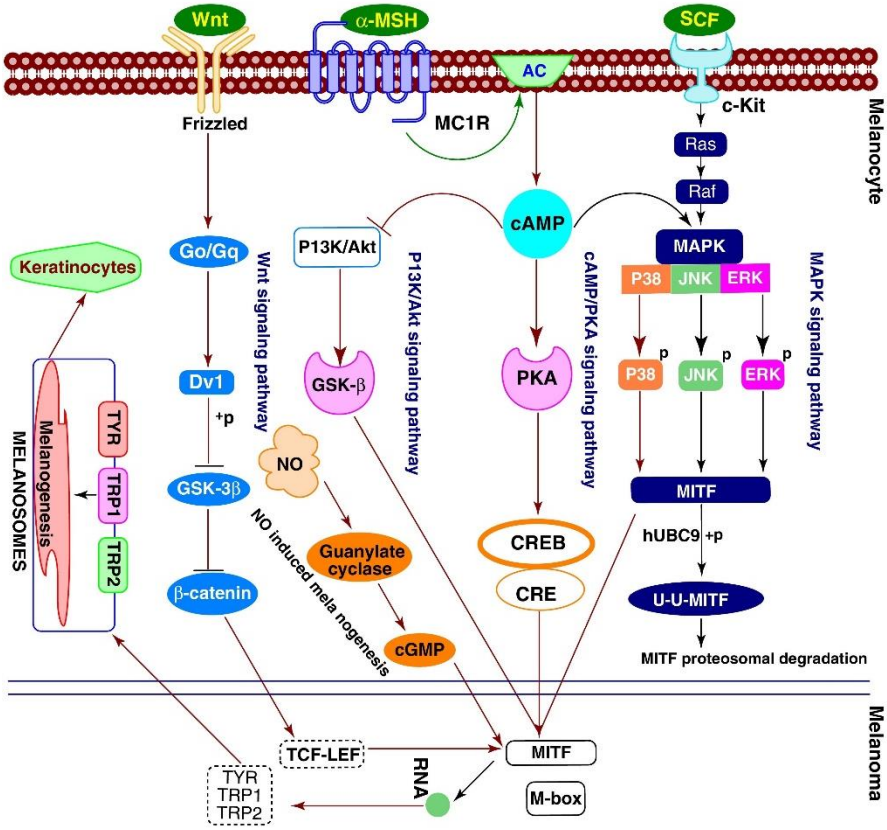


Figure 4. Melanin biosynthesis signal pathway. Adapted from (Pillaiyar et al., 2017).

Melanocortins are a group of peptide hormones derived from proopiomelanocortin (POMC) that include adrenocorticotrophic hormone (ACTH), α-melanocyte stimulating hormone (MSH), and β-MSH, and play a vital role in melanin control by inducing the expression of many key enzymes, such as TYR. These hormones have varying binding affinities for each of the five melanocortin receptors (MC1R-MC5R), expressed in various tissues (Boo, 2020). ACTH, α-MSH, and β-MSH act as agonists on melanocortin receptors (MC1R) present on the surface of melanocytes. The binding of α-MSH to MC1R initiates a signaling cascade, activating adenylate cyclase (AC) and cAMP. cAMP activates PKA, which phosphorylates and activates cAMP response element-binding protein (CREB). Phospho-CREB binds to the cAMP response element (CRE) on the promoter of microphthalmia-associated transcription factor

(MITF) in DNA and stimulates MITF mRNA expression in the nucleus (Boo, 2020; D'Mello et al., 2016; Fu et al., 2020). Activation of MITF results in the upregulation of the expression of melanogenic enzyme genes such as TYR, TYRP1, and TYRP2. In addition, MITF regulates melanocyte function including melanocyte differentiation, pigmentation, proliferation, and cell survival (Niu & Aisa, 2017).

Along with the α-MSH/MC1R pathway, other signaling pathways such as the stem cell factor (SCF)/receptor tyrosine kinase protein c-Kit /mitogen-activated protein kinases (MAPK) pathway and the wingless-related integration site (WNT)/frizzled/glycogen synthase kinase (GSK) pathway can also activate MITF expression (Boo, 2020; D'Mello et al., 2016).

1.1.3 Pigmentation disorders

Melanogenesis is a complex and highly regulated process. When melanogenesis is disrupted, defects in skin pigmentation happen. These can be congenital or acquired, temporary or permanent, and hypo- or hyperpigmented. When melanin synthesis is abnormally elevated, hyperpigmentary dermatological conditions such as melasma, senile lentigines, or freckles, result (**Figure 5A**). Dermatological diseases, hormones, age, hereditary factors, skin injuries or inflammation, acne, and, most importantly, sun exposure, can all boost melanin synthesis (Boo, 2020; Thawabteh et al., 2023). On the other hand, hypopigmentary conditions are brought on by the abnormal lack of melanin synthesis (**Figure 5B**). Prior skin trauma, including blisters, infections, burns, exposure to chemicals, and other wounds, is the most prevalent cause of low melanin content. Genetic diseases such as albinism, pityriasis versicolor and vitiligo can also result in hypopigmentation (Boo, 2020; Thawabteh et al., 2023). Hence the regulation of melanogenesis and tyrosinase activity is crucial for treating these disorders.

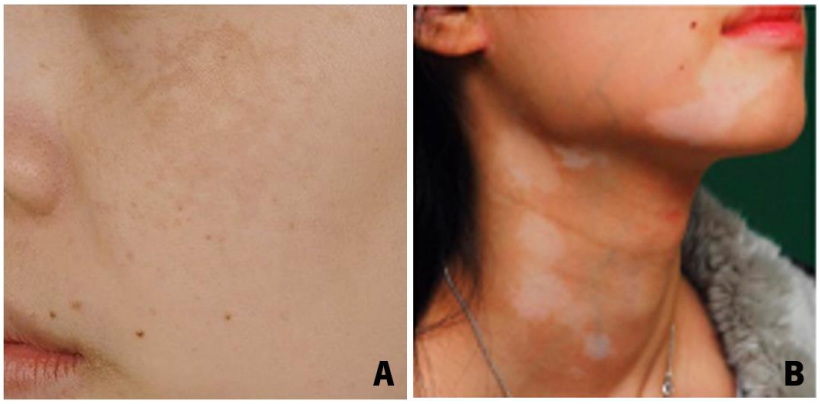


Figure 5. Hyperpigmentation (**A**) and hypopigmentation (**B**) cases. Adapted from (Silpa-archa et al., 2017; Thawabteh et al., 2023).

1.1.4 Melanogenesis inhibitors and stimulators from different sources

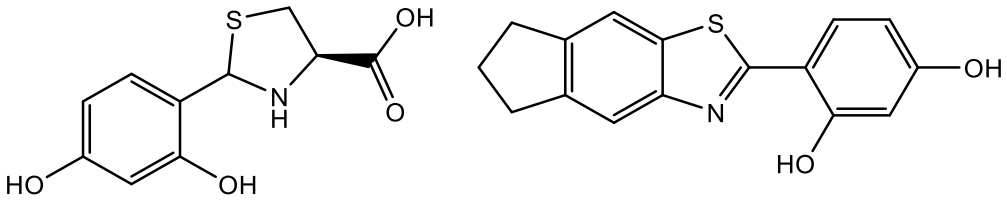
Tyrosinase is the rate-limiting enzyme of melanin production and, accordingly, most of the strategies for treating hyper- and hypopigmentary disorders are based on the inhibition and stimulation of tyrosinase activity, respectively. There is an ongoing effort to research compounds with high efficacy and less adverse side effects capable of treating these diseases (Lee et al., 2016; Masum et al., 2019).

Some of the inhibitors/stimulators found have synthetic origin, while others have been identified from small molecules of natural origin (single compounds) or plant extracts (mixtures).

1.1.4.1 Synthetic compounds for tyrosinase regulation

Throughout the years, numerous studies have been conducted to investigate the development of new synthetic tyrosinase inhibitors/stimulators based on previously studied natural compounds. Technology allowed to rationally design efficient synthetic analogues based on natural structural motifs, while also overcoming issues related to chemical stability, effectiveness, and isolated yield. Synthetic inhibitors such as N-hydroxy-N′-phenylthiourea, N-cyclopentyl-N-nitrosohydroxylamine, sildenafil methyl ether, oxazolones, tetraketones, triazolothiadiazoles, 4-hydroxybenzaldehyde derivatives, rhodanine derivatives are some of the reported (Lee et al., 2016; Masum et al., 2019).

Some synthetic tyrosinase inhibitors show better efficacy than kojic acid, a well-known tyrosinase inhibitor, in terms of IC_{50} value. Han and collaborators (Han et al., 2012), for example, synthesized (4R)-2-(2,4-dihydroxyphenyl)thiazolidine-4-carboxylic acid (MHY384) as a tyrosinase inhibitor (**Figure 6**). MHY384 suppressed tyrosinase activity in α-MSH-induced B16F10 melanoma cells and showed 30-fold more effectiveness than kojic acid in a mushroom tyrosinase inhibition assay. Similarly, Park and collaborators (J. W. Park et al., 2013) designed 4-(6,7-dihydro-5H-indeno[5,6-d]thiazol-2-yl)benzene-1,3-diol (MHY1556) (**Figure 6**), which inhibited mushroom tyrosinase with 100-fold higher activity than kojic acid, revealing that the 2,4-dihydroxyl substitution on the phenyl ring plays a major role in binding to tyrosinase. Furthermore, MHY1556 inhibited melanin content in a dose-dependent manner while exhibiting no substantial cytotoxicity in α-MSH-induced B16F10 melanoma cells (Lee et al., 2016).



MHY384 MHY1556

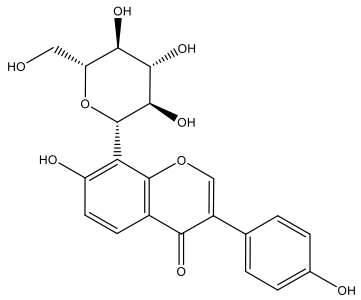
Figure 6. Chemical structure of synthetic tyrosinase inhibitors. Adapted from (Lee et al., 2016) using the ChemDraw software.

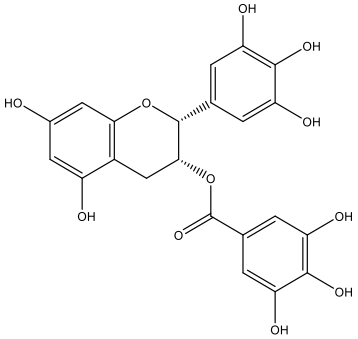
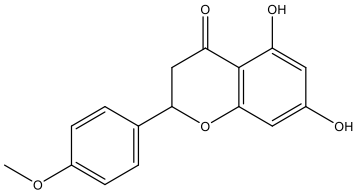
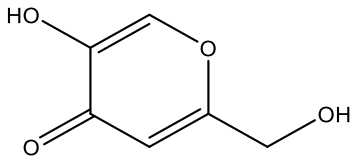
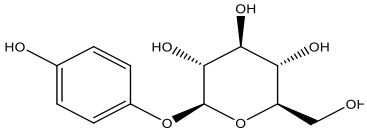
Although numerous synthetic inhibitors demonstrate excellent mushroom tyrosinase inhibition efficacy, only a few of them inhibit melanogenesis in cells or skin models. Additionally, their use still raises certain safety issues related to toxicity and allergenicity. Thus, the fundamental goal of recently discovered synthetic tyrosinase inhibitors is to achieve safe and adequate inhibitory efficacy in cell-based assays (Lee et al., 2016; Masum et al., 2019).

1.1.4.2 Naturally occurring compounds for tyrosinase regulation

The search for tyrosinase inhibitors/stimulators from natural sources is ongoing since they are a rich supply of bioactive molecules and typically exhibit lower toxicity and better bioavailability, especially for food, cosmetics, and medicinal applications. Mycological metabolites, plants, and aquatic algae are some of the natural sources studied (Masum et al., 2019; Zolghadri et al., 2019). **Table 1** lists selected research on the impact of various natural chemical substances on tyrosinase activity, melanogenesis, and other relevant parameters.

Table 1. Effects of natural chemical compounds on tyrosinase regulation, melanogenesis, and on other parameters.

Chemical substance	Results	Ref.
Puerarin 	*Pueraria thunbergiana* extract and its main bioactive puerarin stimulated the melanogenesis via cAMP/MITF-M signalling pathway *in vitro* and prevented the follicular depigmentation and vitiligo by stimulating melanin synthesis.	(W.-S. Park et al., 2014)

Epigallocatechin-3-gallate 	Epigallocatechin-3-gallate delayed the time of depigmentation, reduced the prevalence of depigmentation and decreased the area of depigmentation by reducing excessive inflammatory responses, especially infiltration of CD8+ T cells and inhibiting the levels of inflammatory mediators.	(Zhu et al., 2014)
Isosakuranetin 	Propolis component isosakuranetin has been shown to induce melanogenesis in B16 melanoma cells by up-regulating MITF. Furthermore, it inhibited the ERK1/2 and PI3K/AKT signalling pathways, which activated MITF and resulted in the production of TYR, TYRP1, and TYRP2.	(Drira & Sakamoto, 2015)
Kojic acid 	Kojic acid inhibits tyrosinase slowly and effectively, preventing melanin synthesis, and plays a crucial role in cellular melanin formation. It has been reported that kojic acid prevents melanosis by interfering with the oxygen intake required for enzymatic browning.	(Phasha et al., 2022)
Arbutin 	Arbutin inhibits TYR activity in human melanocytes in a dose-dependent manner while maintaining cell viability. Arbutin suppresses melanin formation in cells by reducing the catalytic activity of previously expressed TYR or inactivating it irreversibly.	(Boo, 2021)

Plant extracts are a rich source of bioactive chemicals and have long been utilized for both aesthetic and medicinal reasons due to their ability to produce a variety of biological and pharmacological effects (Fiocco et al., 2011). **Table 2** lists selected research on the impact of several natural extracts on tyrosinase activity, melanogenesis, and other relevant parameters.

Table 2. Effects of plant extracts on tyrosinase regulation, melanogenesis, and other parameters.

Plant material	Bioactive compounds	Results	Ref.
Lavender	Linalool, linalyl acetate, 1,8-cineole, terpinen-4-ol, camphor	Inhibitory effect on tyrosinase activity, serving as a mixed-type inhibitor. Reduced the affinity of the substrate for tyrosinase, yet did not bind to the active site, the dissociation of the enzyme–substrate complex was prevented.	(Hsu et al., 2007)
Thyme	Thymol, carvacrol	Thymol has inhibitory effects on melanogenesis due to the inhibition of the redox reaction between dopaquinone and leukodopachrome. Carvacrol has been shown to possess inhibitory effects on the synthesis of CREB protein and tyrosinase and TYRP1 expression. Additionally, it reduces MITF protein expression.	(Jeon et al., 2018; Satooka & Kubo, 2011)
Eucalyptus	1,8-Cineole, α- and β-pinene, and terpineol	Eucalyptus suppresses tyrosinase activity and depletes melanin in B16F10 mouse melanoma cells. This study indicated that the depigmenting effect occurs due to the eucalyptus antioxidant properties, and by the downregulation of both mitogen-activated protein kinases (MAPK) and protein kinase A (PKA).	(Moreira et al., 2022; Sugimoto et al., 2009)
Cocoa	Catechin, epicatechin and theobromine	Catechin derivatives have been shown to directly inhibit tyrosinase activity and down-regulate tyrosinase expression of B16 melanoma cells.	(Liu, 2022; Sato & Toriyama, 2009; Zhao et al., 2022)

		Theobromine has been reported to stimulate tyrosinase activity and, therefore, enhance the production of melanin in melanocytes.	
Cork	Phenolic acids (e.g., protocatechuic acid, gallic acid, caffeic acid, ellagic acid), flavonoids, phenolic aldehydes, and coumarins	Several cork components, such as flavanols and phenolic acids, are known tyrosinase inhibitors. *In vivo* and *in vitro* studies show that they have effect on melanocytes as inhibitors or alternative substrates of tyrosinase. Ellagitannins and ellagic acid inhibit the activity of tyrosinase. This phenolic acid inhibits the proliferation of melanocytes and melanin synthesis. Another study concluded that protocatechuic aldehyde has a potent tyrosinase inhibitory effect, acting as a competitive or alternative substrate.	(Carriço et al., 2018)

1.2 COSMETIC FORMULATIONS

Topical creams are the most often used therapy for skin discolouration. They have the ability to lighten or darken the skin and are applied directly to the afflicted region. The major advantage of topical creams is that they are less costly and easier to administer than oral therapies. Current re-pigmentation therapies include the use of topical steroids. Randomized controlled trials using ruxolitinib 1.5% (Opzelura®) (**Figure 7A**) cream for treating vitiligo in various patients revealed clinically excellent re-pigmentation of all body areas. A study performed by Lepe *et al.* used 0.05% clobetasol proprionate (**Figure 7B**) for the treatment of vitiligo in children and showed a re-pigmentation rate of 49.3%. Despite its effectiveness, topical steroids have been linked to a slew of local and systemic side effects (Lepe et al., 2003; Thawabteh et al., 2023).

There are much gentle cosmetics available on the market, especially for hyperpigmentation, that contain key ingredients essential in the treatment of pigmentary disorders. *Olivia quido® firming and fading I* skin lightener cream (**Figure 7C**) contains hydrocortisone, hydroquinone, and tretinoin and is used to gradually lighten hyperpigmented skin. Higher concentrations of hydroquinone suppress melanin formation by blocking sulfhydryl groups and functioning as a substrate for tyrosinase (OLIVIA QUIDO FIRM & FADE I Skin Lightener Cream – O SKIN Pharmaceutical; Sarkar et al., 2013). *Antipodes® Diem Vitamin C Pigment-Correcting Water Cream* (**Figure 7D**) is a formulation primed with peptides that helps to prevent and reduce the signs of hyperpigmentation. It is rich in vitamin C, which inhibits tyrosinase by binding to copper and suppresses the oxidative polymerization of melanin precursors, preventing melanin formation (Diem Vitamin C Pigment-Correcting Water Cream 60ml; Sarkar et al., 2013). *The Ordinary® Niacinamide 10% + Zinc 1%* (**Figure 7E**) contains a high concentration of niacinamide which is a vitamin B found in face creams and masks to reduce the look of enlarged pores, fine lines, and dullness. Niacinamide inhibits melanogenesis through interfering with the interaction of keratinocytes and melanocytes (Niacinamide 10% + Zinc 1% | The Ordinary; Sarkar et al., 2013). *Bella Aurora® bio10 forte* (**Figure 7F**) is a depigmenting treatment for dark spots caused by sun exposure or age spots and is a combination of active substances such as kojic acid, vitamin C, sclareolide, and marine exopolysaccharide (Bio10 Forte L-Tigo. Intensive Depigmenting Treatment).



Figure 7. Topical brands used for the treatment of skin pigmentation **A)** Opzelura® **B)** Clobetasol Propionate **C)** Olivia quido® firming and fading I skin lightener cream **D)** Antipodes® Diem Vitamin C Pigment-Correcting Water Cream **E)** The Ordinary® Niacinamide 10% + Zinc 1% **F)** Bella Aurora® bio10 forte.

In recent years, there has been an increasing interest in the development of new natural environmentally friendly cosmetic products. Some plants, fruits, and herbs have been used for centuries

in oriental and traditional medicine to treat a variety of diseases. These natural extracts have the capacity to calm, regenerate, heal, and protect the skin, making them great cosmetic components. Furthermore, due to their high concentration of bioactive components (e.g., phenolic acids, flavonoids, steroids, carotenoids, etc.), natural extracts provide several health advantages such as photoprotection, antiaging, anti-inflammatory, antibacterial, antiviral, and anticancer characteristics (Dini & Laneri, 2021; Hernandez et al., 2021). Natural extracts integrated into cosmetic formulations have emerged as an attractive choice for consumers looking for safer and more environmentally friendly cosmetics. **Table 3** presents a selection of studies on natural extracts utilized in cosmetic formulations.

Table 3. Cosmetic applications of natural extracts.

Plant material	Bioactive compounds	Cosmetic application	Ref.
Theobroma cacao	Catechin, epicatechin, and theobromine	Regulates collagen I, III, and IV and glycosaminoglycan production. Cocoa extract included into microemulsion is used in formulations.	(Dini & Laneri, 2021; Garcia et al., 2021; Singh et al., 2020)
Coffea arabica	Proanthocyanidins, quinic acid, caffeic acid, and chlorogenic acid	Skin-lightening agent, decreases reactive oxygen species formation and tyrosinase synthesis.	(Dini & Laneri, 2021; Farris, 2007; Ndiaye et al., 2011)
Prunus dulcis	Triterpenoids, catechin, flavonol glycosides, phenolic acids, phytosterols, fatty acids, and lipid-soluble vitamins	Almond extract can treat eczema and pimples. Almond oil nourishes, softens, and strengthens the hair.	(Dini & Laneri, 2021; Rao & Lakshmi, 2012)
Glycine max	Isoflavones	Soybean extract can reduce ultraviolet induced oxidative DNA damage and skin photodamage.	(Dini & Laneri, 2021; Mazière et al., 2000)

1.3 NATURAL SOURCES

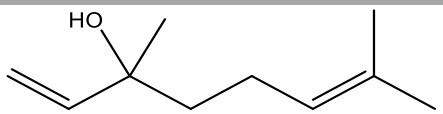
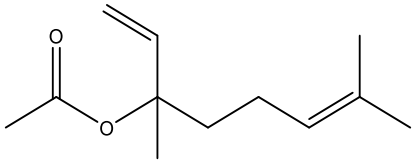
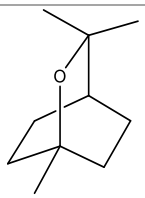
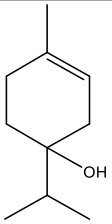
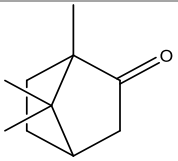
In this study, lavender, thyme, eucalyptus, cocoa, and cork extracts will be characterized and examined for their tyrosinase activity.

1.3.1 Lavender

Lavender (*Lavandula* sp.) is often used in aromatherapy, food, or incorporated into cosmetics and perfumes. Due to its numerous therapeutic properties, lavender is also used in traditional medicine to treat a variety of diseases (Dobros et al., 2022).

The primary bioactives in lavender are linalool, linalyl acetate, 1,8-cineole, terpinen-4-ol, and camphor (**Table 4**).

Table 4. Chemical structures of most prevalent bioactives in lavender. The structures were obtained using the ChemDraw software.

Compound	Structure
Linalool	
Linalyl acetate	
1,8-Cineole	
Terpinen-4-ol	
Camphor	

One of the main bioactives in lavender is linalool, a naturally occurring terpene alcohol that gives lavender its characteristic scent. Linalool has been shown to have relaxing and sedative effects on the central nervous system, making it a popular ingredient to reduce stress, anxiety, and promote better sleep. Studies have also suggested that linalool may have anti-inflammatory properties, and it has been studied for its potential in managing various conditions such as pain, inflammation, and neurodegenerative diseases (Batiha et al., 2023). Another bioactive compound found in lavender is linalyl acetate, the acetate ester of linalool that also contributes to the aroma of lavender. Linalyl acetate has been shown to have sedative, anaesthetic, and antispasmodic actions (Lesage-Meessen et al., 2015). In addition, lavender also contains 1,8-cineole, terpinene-4-ol, and camphor, which have been studied for their potential health benefits. 1,8-Cineole, also known as eucalyptol, is a monoterpenoid commonly used in respiratory health products (Surbhi et al., 2021). Terpinene-4-ol has been shown to have antimicrobial and anti-inflammatory properties (Ezzat et al., 2021). Camphor is commonly used in aromatherapy and phytotherapy and has also been shown to have antimicrobial activity (Habán et al., 2023; Lesage-Meessen et al., 2015).

1.3.2 Thyme

Thyme (*Thymus vulgaris*) is a popular herb and medicinal plant recognized for its potential health benefits related to the presence of bioactive compounds that contribute to its medicinal properties, including antioxidant, anti-inflammatory, antimicrobial, and antiviral activities (Nieto, 2020).

One of the key bioactive compounds in thyme is thymol (**Figure 8**), which is a natural monoterpene phenol responsible for thyme's characteristic aroma and has been extensively studied for its antioxidant, antimicrobial, antihypertensive, immunomodulatory and anticancer properties (Nieto, 2020; Rathod et al., 2021).

Another main constituent of thyme is carvacrol (**Figure 8**), which is an isomer of thymol. Carvacrol exhibits antibacterial and antifungal, antiviral, anti-inflammatory, and antioxidant activities. It has also been investigated for its potential anticancer properties (Nieto, 2020; Rathod et al., 2021; Sharifi-Rad et al., 2018). Besides monoterpene phenols, thyme is also a source of phenolic acids, biphenyl compounds, flavonoids, and essential oils (Nieto, 2020).

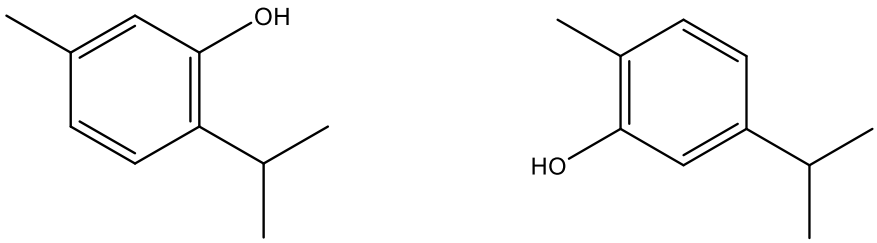
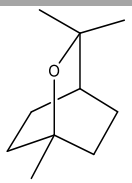
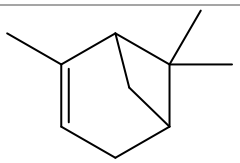
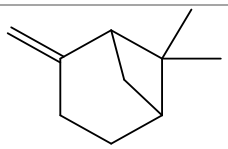
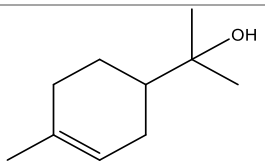


Figure 8. Chemical structures of thymol and carvacrol. The structures were obtained using the ChemDraw software.

1.3.3 Eucalyptus

Eucalyptus (*Eucalyptus* spp.) is known for its distinct aroma and various therapeutic properties, such as anti-diabetic, anti-bacterial, anti-inflammatory, and antioxidant. It is rich in bioactive compounds such as 1,8-cineole, α- and β-pinene, and terpineol (**Table 5**) (Surbhi et al., 2021).

Table 5. Chemical structures of the most abundant bioactives in eucalyptus. The structures were obtained using the ChemDraw software.

Compound	Structure
1,8-Cineole	
α-Pinene	
β-Pinene	
Terpineol	

1,8-Cineole, also known as eucalyptol, has been studied for its numerous biological activities, including anti-inflammatory, antimicrobial, antihelminthic, and respiratory benefits (Surbhi et al., 2021). Another bioactive compound found is pinene, a monoterpene hydrocarbon with two isomeric forms: alpha-

pinene and beta-pinene, the former being more abundant in different species of eucalyptus. Both have been studied for their various biological activities, including antimicrobial and antioxidant properties. Alpha-pinene has also been linked to eucalyptus' anticancer properties (Surbhi et al., 2021).

Terpineol is a natural mono-terpenoid alcohol with a wide range of properties including antibacterial, antihypertensive, anti-inflammatory as well as anticancer effects (Khaleel et al., 2018; Surbhi et al., 2021).

1.3.4 Cocoa

Cocoa, also known as *Theobroma cacao*, has been extensively studied for its bioactive compounds that offer a plethora of health-promoting properties. From a decrease in the risk of chronic diseases, such as cardiovascular diseases and cancer, to positive effects on the nervous system, visual function, and skin, cocoa consumption offers numerous benefits for health and disease (Martin & Ramos, 2021).

One of the key bioactives found in cocoa is flavonoids, mainly flavanols, with epicatechin and catechin being the most abundant (**Figure 9**). Flavanols have been shown to have numerous health benefits, including antioxidant activity and beneficial effects on endothelial function (Katz et al., 2011; Martin & Ramos, 2021).

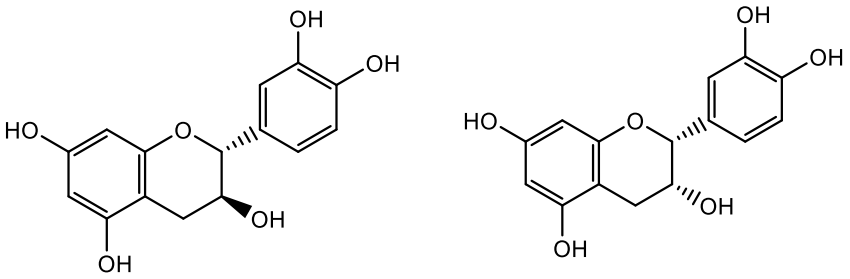


Figure 9. Chemical structures of catechin and epicatechin. Adapted from (Ramalho et al., 2014) using the ChemDraw software.

Another bioactive compound found in cocoa is theobromine (**Figure 10**), a natural alkaloid that belongs to the xanthine family. Theobromine is a mild stimulant that can provide a gentle energy boost and has been found to have positive effects on mood and mental alertness (Katz et al., 2011; Martin & Ramos, 2021).

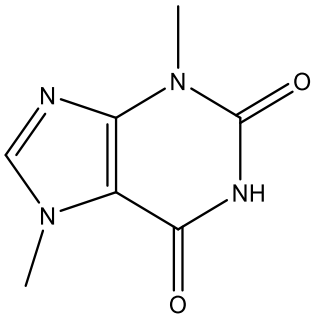


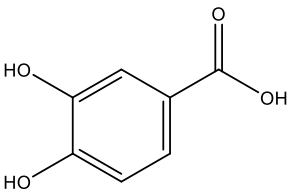
Figure 10. Chemical structure of theobromine. The structure was obtained using the ChemDraw software.

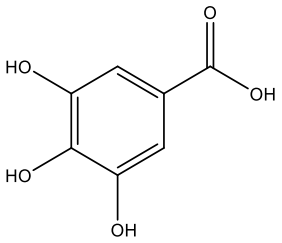
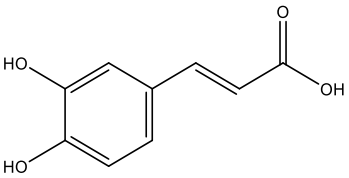
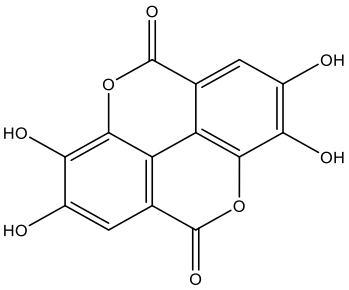
1.3.5 Cork

Cork, derived from the bark of the cork oak tree (*Quercus suber*), is a natural and sustainable material that has been used for various commercial purposes. Apart from its functional properties, cork also contains bioactive compounds that deserve attention due to their potential health benefits (Azevedo et al., 2022; Freitas et al., 2022).

Cork has a wide range of extractable components that are not covalently linked to the cell wall's structural components and therefore can be easily extracted. These components include phenolic acids (e.g., protocatechuic acid, gallic acid, caffeic acid), with ellagic acid being the most abundant (**Table 6**). Flavonoids, phenolic aldehydes, and coumarins are also present in cork. All these classes of compounds are known for their antioxidant and anti-inflammatory, among other properties (Carriço et al., 2018; S. A. O. Santos et al., 2013). Cork is particularly rich in hydrolyzable tannins, namely ellagitannins, which have been shown to have antioxidant, anti-inflammatory, and anticancer activities (Fernandes et al., 2009; S. A. O. Santos et al., 2013).

Table 6. Chemical structures of major phenolic acids in cork. The structures were obtained using the ChemDraw software.

Compound	Structure
Protocatechuic acid	

Gallic acid	
Caffeic acid	
Ellagic acid	

1.4 Extraction Methods

Natural products possess diverse chemical structures and biological activities, making them valuable for applications in medicine, food, cosmetics, and more. Plants' active compounds are usually contained inside the plant matrices, so appropriate extraction methods are needed to facilitate the separation and isolation of the desired compounds. The most conventional extraction methods include maceration, percolation, hydrodistillation, and Soxhlet extraction. Although easy to operate, these methods consume large quantities of solvent and require a longer extraction time (Chuo et al., 2022; Zhang et al., 2018).

Many modern or greener extraction methods such as ultrasound-assisted extraction, microwave-assisted extraction, and supercritical fluid extraction have been used in natural products extraction (Zhang et al., 2018). **Table 7** presents some advantages and limitations as well as some recent works regarding the extraction of active compounds using these methods.

Table 7. Various advanced methods for extraction of active compounds from plant materials.

	Ultrasound-assisted extraction	Microwave-assisted extraction	Supercritical fluid extraction
Principle	Employs high-frequency ultrasound waves which lead to the formation, growth, and collapse of microbubbles within the extraction solvent. During the collapse phase, high temperatures and pressures are generated locally, causing mass transfer, disruption of cell walls, and the release of target compounds (Chuo et al., 2022; Zhang et al., 2018).	Microwaves generate heat by the interaction between the polar molecules in the solvent and the electromagnetic field produced by microwaves. The alternating electromagnetic field causes the polar molecules to rotate rapidly, generating heat through molecular friction (Chuo et al., 2022; Zhang et al., 2018).	Employs a supercritical fluid, typically carbon dioxide (CO_2), as the solvent. Supercritical fluids can permeate easily into plant materials, solubilize active compounds and transfer them to bulk solvent (Chuo et al., 2022; Zhang et al., 2018).
Advantages	It decreases extraction time and improves extraction efficiency. Utilizes less energy and solvent consumption and preserves thermally sensitive compounds (Chuo et al., 2022; Zhang et al., 2018).	It decreases extraction time and improves extraction efficiency, reduces the usage of organic solvent and energy, and is more reproducible (Chuo et al., 2022; Zhang et al., 2018).	Allows the extraction of specific compounds by adjusting the pressure and temperature, providing high selectivity; no solvent residue in the extracted product, CO_2 used is non-toxic, non-flammable, and readily available (Chuo et al., 2022; Zhang et al., 2018).
Limitations	Prolonged exposure to ultrasound waves may cause degradation of certain compounds (Chuo et al., 2022).	Some heat-sensitive compounds may degrade under microwave radiation, requiring optimization of extraction conditions to minimize	It is most effective for non-polar and moderately polar compounds, while polar compounds may require co-solvents (Chuo et al., 2022).

		potential losses (Chuo et al., 2022).	
Plant material	*Eucalyptus globulus* (56% ethanol as solvent; 1:10 solid-to-solvent ratio; 40 kHz; 90 min) (Gullón et al., 2019).	*Eucalyptus globulus* (56% ethanol as solvent; 1:10 solid-to-solvent ratio; 7 min) (Gullón et al., 2019).	*Cannabis sativa* (33 MPa; 80 °C; 0.55 kg solvent/h, 4 h; 5% ethanol as co-solvent) (Rovetto & Aieta, 2017).
	Thymus serpyllum L. (50% ethanol as solvent; 1:30 solid-to-solvent ratio; 20 kHz; 0.3 mm particle size; 15 min) (Jovanović et al., 2017).	*Thymus fontanesii* (50% ethanol as solvent; 1:15 solid-to-solvent ratio; 150 °C; 9.5 min) (Nabet et al., 2019).	*Lippia graveolens* (35 MPa; 60 °C; 0.29 kg CO_2/h; 75 min) (Soto-Armenta et al., 2019).

Choosing the right solvent for extraction is a critical step in successfully extracting the target chemicals. The nature of the target chemicals, the source material, the desired selectivity, and the extraction method used all influence the solvent selection. Alcohols, such as EtOH and MeOH, are widely used solvents for active chemical extraction (Chuo et al., 2022; Zhang et al., 2018).

Organic solvents such as ethyl acetate or alkyl alcohols such as methanol or ethanol are commonly used in extraction procedures. While organic solvents have several advantages in extraction procedures, it is critical to evaluate their possible environmental implications. These solvents have been linked to atmospheric accumulation (due to their low boiling temperatures), flammability, and severe toxicity (Ruesgas-Ramón et al., 2017). As a result, new alternative green solvents are being investigated.

Supercritical fluids, like CO_2 or water, or biomass-derived solvents, such as EtOH, could be an option but their versatility and solvation properties are rather restricted. Another alternative is ionic liquids, which consist of an association between an organic cation and a coordinating anion. They possess low vapor pressure, non-inflammability, and are stable at high temperatures. However, because of their high cost, high toxicity, difficulty in purifying, and poor biocompatibility and biodegradability, they are not the best green alternative (Chemat et al., 2019; Ruesgas-Ramón et al., 2017).

Since its introduction by Abbott *et al.* in 2003, deep eutectic solvents (DES) have emerged as green and sustainable solvents for the effective extraction of bioactive compounds from plant material. DES are

becoming a better alternative to conventional organic solvents due to their low toxicity and cost, availability, and environmentally friendly nature (Duan et al., 2016). DES are composed of a mixture of a hydrogen bond acceptor (HBA) and a hydrogen bond donor (HBD). The HBA is typically a halide salt while the HBD is an organic compound such as urea, ethylene glycol, and glycerol. **Figure 11** depicts the structure of some HBAs and HBDs used in the formation of DES.

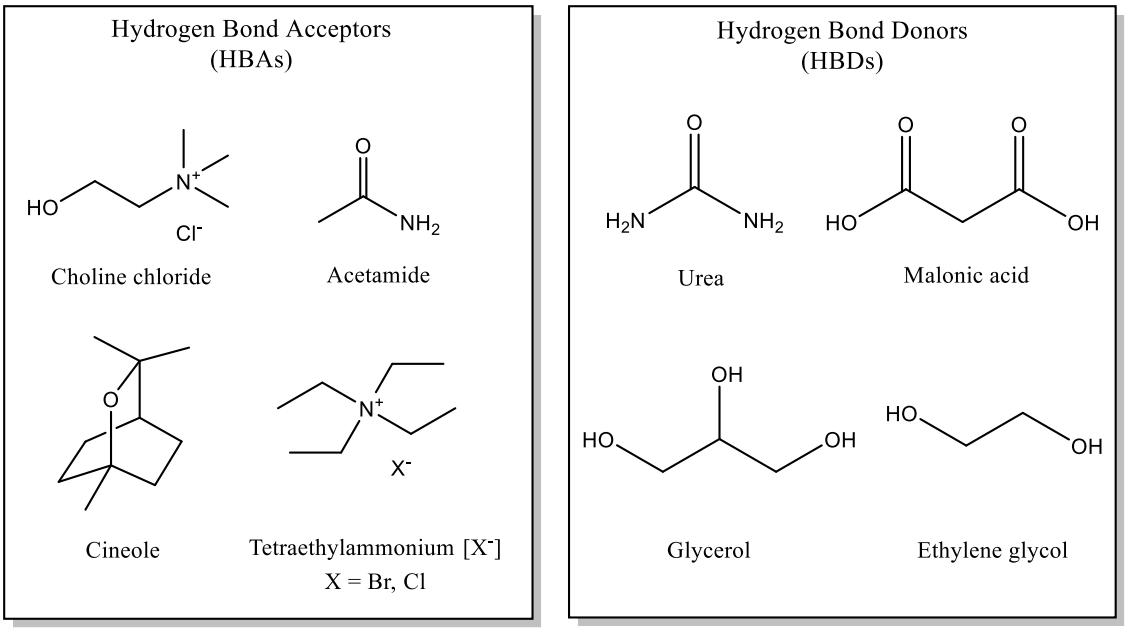


Figure 11. Chemical structure of some HBAs and HBDs used in the formation of DES. Adapted from (Stephens & Smith, 2022) using the ChemDraw software.

When these components are mixed in an appropriate ratio, a eutectic mixture is formed, resulting in a liquid with a considerably lower melting point compared to its individual components, due to the formation of intermolecular hydrogen bonds (Pena-Pereira & Namieśnik, 2014; Ruesgas-Ramón et al., 2017). Moreover, DES are characterized by their ease of preparation, which requires mixing and agitation of the respective components under moderate warming conditions (80-100 °C), with no need for purification because the purity of resulting DES is determined by the purity of individual elements. Because of their hydrogen bonding capability, DES are typically hydrophilic and quickly dissolved in aqueous solution (Pena-Pereira & De La Calle, 2018).

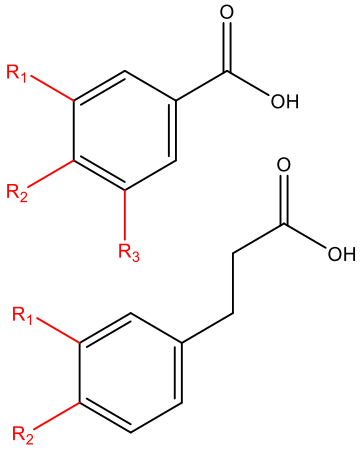
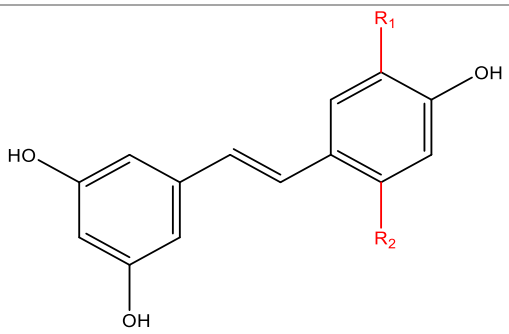
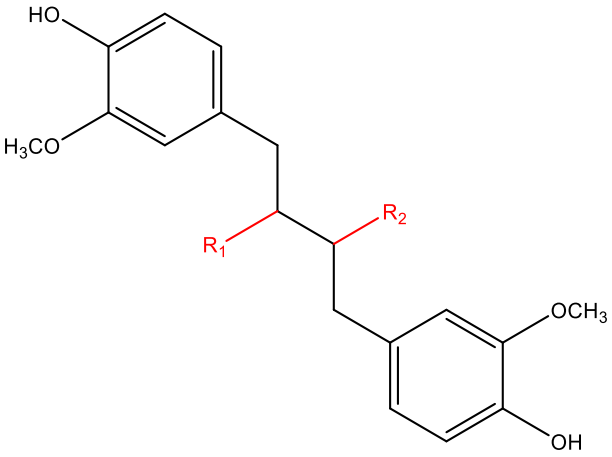
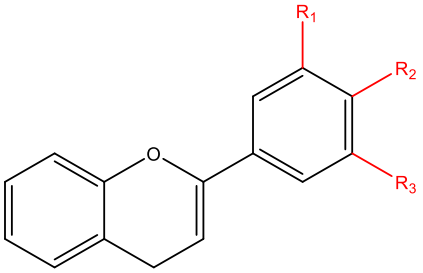
1.5 CHARACTERIZATION OF NATURAL EXTRACTS

The characterization of natural extracts is an essential step in understanding their chemical composition, bioactivity, and potential applications in various fields, including food, pharmaceuticals, and cosmetics. In this work, the physic-chemical characterization of the extracts will be carried out including assessment of phenolic and flavonoid content, antioxidant activity, antimicrobial properties, sun protection factor, gas chromatography-mass spectrometry analysis, and tyrosinase inhibition.

1.5.1 Total phenolic content

Phenolic compounds, one of the main classes of secondary metabolites, have antioxidant properties and play important roles in human health due to their potential beneficial effects, such as anti-inflammatory and anti-cancer properties. These compounds are characterized by the presence of at least one aromatic ring with one or more hydroxyl groups (-OH) attached. Depending on the number and arrangement of their carbon atoms, they can be divided into several major classes including phenolic acids, stilbenes, lignans, and flavonoids (**Table 8**) (Amawi et al., 2017; Crozier et al., 2009; Garcia-Salas et al., 2010). Many phenolic compounds have been found to directly inhibit tyrosinase activity by binding to the active site of the enzyme. Moreover, they can disrupt melanogenesis by influencing tyrosinase gene expression, regulating melanosome transfer, and decreasing tyrosinase transcription by inhibiting the upstream MAPK signalling pathway (Mapoung et al., 2021).

Table 8. Basic structural skeletons of phenolic compounds and examples of important subfamilies of each class. Adapted from (Amawi et al., 2017) using the ChemDraw software.

Classification	Basic structure	Main subclasses
Phenolic acids		Benzoic acid Cinnamic acid
Stilbenes		Resveratrol
Lignans		Secoisolariciresinol Matairesinol
Flavonoids		Flavones Anthocyanidins Flavanols Flavanones Isoflavones Flavonols

The **Folin-Ciocalteu test** is a widely used method for the determination of the total phenolic content (TPC). This assay is based on the reaction between the Folin-Ciocalteu reagent and the phenolic compounds present in the sample, in alkaline medium. Under these conditions, the dissociation of a phenolic proton leads to the formation of a phenolate ion. The Folin-Ciocalteu reagent, which consists of a complex of phosphomolybdic-phosphotungstic acid, is reduced (the central molybdenum ion Mo^{6+} to Mo^{5+}), resulting in a blue color that can be measured spectrophotometrically at around 750 nm (**Figure 12**). The intensity of the color is proportional to the phenolic content present in the extract. TPC is measured using a calibration curve based on a reference phenolic standard, such as gallic acid (Blainski et al., 2013; Munteanu & Apetrei, 2021; Rangel et al., 2013). However, it is important to note the non-specificity of the Folin-Ciocalteu assay, which might result on the quantification of other compounds present in the solution, like reducing sugars, that can also reduce the Folin reagent, leading to overestimated results (Bibi Sadeer et al., 2020).

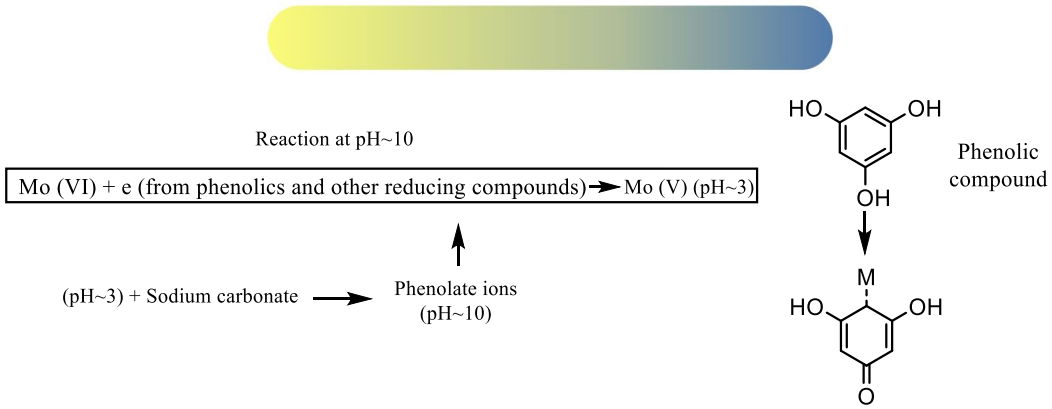


Figure 12. Schematic representation of the Folin-Ciocalteu assay. Adapted from (Rangel et al., 2013).

The Folin-Ciocalteu test is frequently used due to its simplicity, low cost, and accuracy. It is also a popular choice due to its reproducibility and robustness (Munteanu & Apetrei, 2021).

1.5.2 Total flavonoid content

Flavonoids are a class of polyphenols that have a basic structure consisting of a 15-carbon skeleton arranged in two aromatic rings connected by a three-carbon bridge forming an oxygenated heterocyclic ring. Modifications of the various functional groups to the basic flavone skeleton lead to various subclasses of flavonoids such as flavones, anthocyanidins, flavanols, flavanones, isoflavones, and flavonols (**Figure 13**) (Das & Gezici, 2018; Magalhães et al., 2012). One of the most important health benefits of flavonoids

is their antioxidant activity. They can neutralize harmful free radicals in the body which are linked to a variety of diseases. Flavonoids also have anti-inflammatory and antimicrobial properties (Das & Gezici, 2018; Magalhães et al., 2012). Similar to other phenolic compounds, flavonoids have been studied for their potential effects on tyrosinase activity and melanin production. Studies show that some flavonoids can directly bind to TYR's catalytic pocket, leading to the inhibition of the enzyme. Additionally, they can affect tyrosinase activity by modulating its expression via the regulation of cAMP, MITF, or various signalling pathways (El-Nashar et al., 2021).

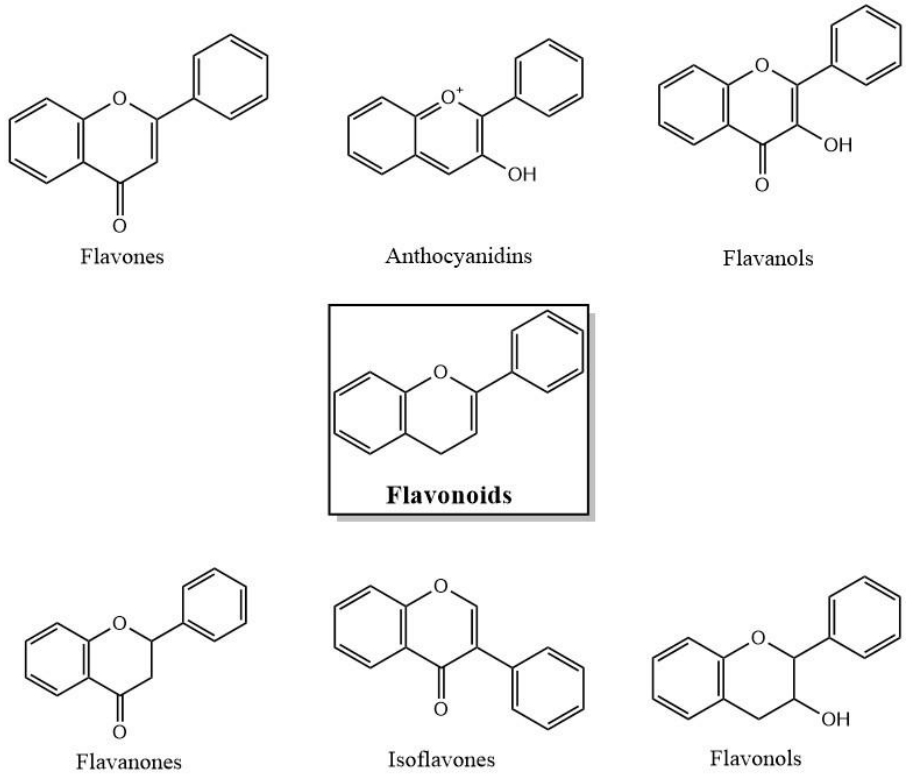
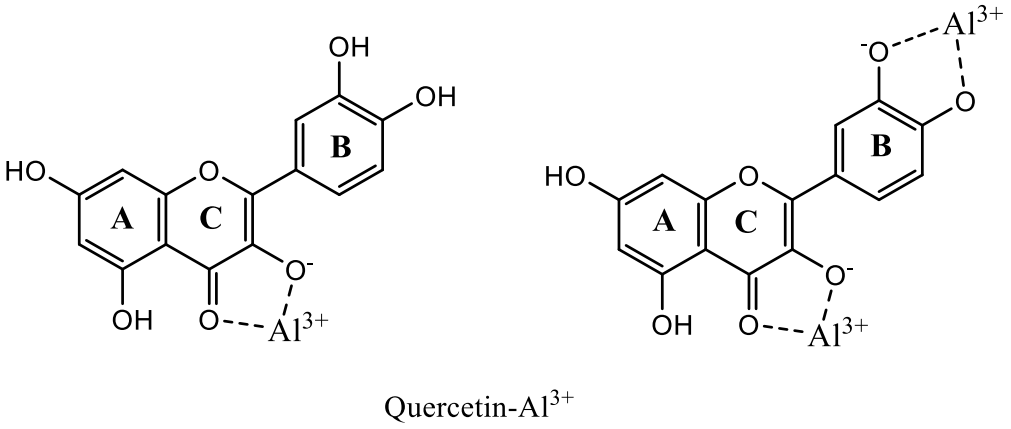


Figure 13. Subclasses of flavonoids and corresponding structures. Adapted from (Das & Gezici, 2018) using the ChemDraw software.

The **Aluminium chloride assay** is a widely used method for the quantification of the total flavonoid content (TFC). This method is based on the formation of a colored complex between Al^{3+} and the keto groups at C-4 and the hydroxyl groups at C-3 or C-5 of flavonoids. This complex absorbs light in the visible region, resulting in a yellow color that can be measured spectrophotometrically at about 500 nm (Ilmi et al., 2020; Shraim et al., 2021). The intensity of the color is proportional to the concentration of flavonoids present in the extract. TFC is measured using a calibration curve based on a reference flavonoid standard. Quercetin, catechin, and rutin are a few of the flavonoid standards that are most frequently employed. **Figure 14** demonstrates the complex formation between Al^{3+} and flavonoids, using quercetin as an

example. The aluminium chloride test is a simple and rapid since method requiring only few readily available reagents (Shraim et al., 2021).



Quercetin-Al^{3+}

Figure 14. Formation of the complex quercetin-aluminium chloride when using Aluminium Chloride assay. Adapted (Radulescu et al., 2019) from using the ChemDraw software.

1.5.3 Antioxidant activity

In recent years, antioxidants have gained attention due to their potential health benefits. These compounds act by neutralizing free radicals, which are highly reactive and harmful molecules that are a result of normal metabolic processes, such as digestion and respiration. Antioxidants can donate an electron to the free radical and stabilize it, which prevents it from causing damage to cells and tissues. Antioxidants can thereby reduce oxidative stress caused by the existence of free radicals, which is linked to conditions like diabetes, high blood pressure, Alzheimer's, and Parkinson's (Gulcin, 2020; Munteanu & Apetrei, 2021). Additionally, it has been shown that tyrosinase activity can be altered by the presence of ROS since the enzyme favours superoxide anion radicals, leading to an increase in melanin synthesis. Antioxidants can then counteract the harmful effects of ROS, such as DNA damage and melanocyte proliferation, by reducing oxidative stress and inhibiting tyrosinase activity indirectly (Muddathir et al., 2017).

The different methods for antioxidant assessment can be classified into three categories according to the chemical reactions that may be involved, as presented in **Table 9**.

Table 9. Antioxidant assays based on the reaction mechanism. Adapted from (Gulcin, 2020; Munteanu & Apetrei, 2021).

Antioxidant Assay	Principle	Examples
Hydrogen atom transfer (HAT)	Measures the capacity of an antioxidant to remove free radicals by hydrogen donation.	**ORAC -** Oxygen radical absorbance capacity **TRAP -** Total radical trapping antioxidant parameter **TOSC -** Total radical scavenging capacity
Single electron transfer (SET)	Measures the capacity of an antioxidant to reduce compounds such as metals, carbonyls, and radicals by transferring an electron.	**CUPRAC -** Cupric ions (Cu^{2+}) reducing antioxidant power **FRAP -** Ferric ion reducing antioxidant power
Mixed mode tests (HAT/SET)	Uses both HAT and SET mechanisms and is usually based on the elimination of a stable chromophore.	**ABTS -** 2,2′-Azino-*bis*(3-ethylbenzothiazoline-6-sulfonic acid) radical scavenging assay **DPPH -** 2,2-Diphenyl-1-picrylhydrazyl radical scavenging assay

1.5.3.1 2,2-Diphenyl-1-picrylhydrazyl (DPPH) radical scavenging assay

The **DPPH (2,2-diphenyl-1-picrylhydrazyl) assay** is a widely used colorimetric method to evaluate the antioxidant activity of different samples. $DPPH^{\cdot}$ is a π-radical, present in its monomer form in a solid state and solution. It is characterized as a stable free radical due to the delocalization of the spare electron over the molecule as a whole, so that the molecule does not dimerize, as would be the case with most other free radicals (Gulcin, 2020).

This method is based on the ability of the antioxidants to donate electrons in order to stabilize the DPPH radical. It gives rise to the reduced form with the loss of the deep purple color. This change is measured at about 517 nm and discoloration acts as an indicator of antioxidant activity (**Figure 15**). The degree of discoloration is correlated with the antioxidant content of the sample. This is a simple, rapid, and low-cost technique that does not require special sample treatment and needs only a UV-Vis (ultraviolet-visible) spectrophotometer as equipment (Gulcin, 2020).

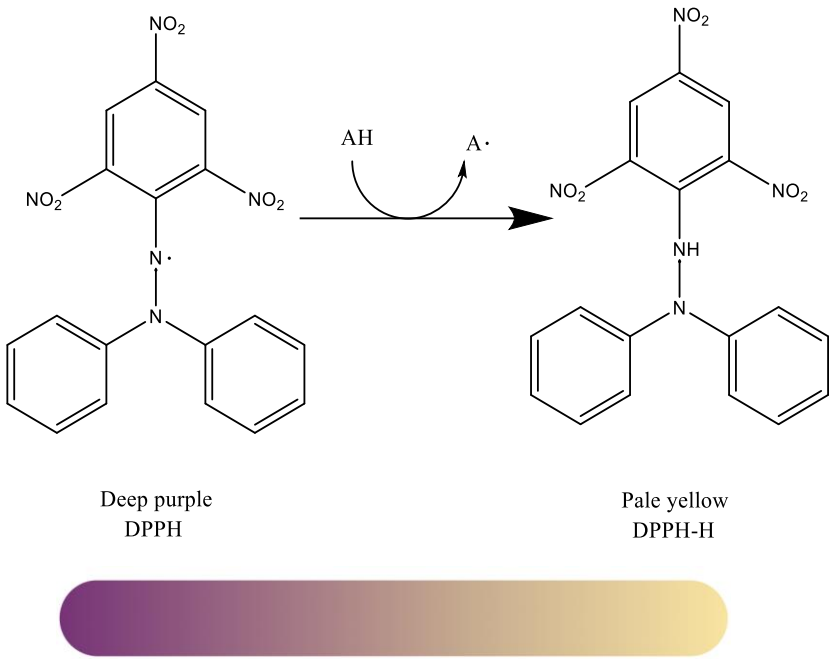


Figure 15. DPPH assay: radical scavenging principle. Adapted from (Munteanu & Apetrei, 2021) using the ChemDraw software.

1.5.3.2 2,2′-Azino-*bis*(3-ethylbenzothiazoline-6-sulfonic acid) (ABTS) radical scavenging assay

The **ABTS (2,2′-azino-*bis*(3-ethylbenzothiazoline-6-sulfonic acid)) assay** was first described in 1999 by Re *et al.* and has become a standard method for assessing the antioxidant activity of various substances. The test is performed by measuring the antioxidants' capacity to stabilize the $ABTS^{\cdot+}$ radical cation. $ABTS^{\cdot+}$ (blue-green) is generated from ABTS (colorless) in the presence of an oxidant agent such as potassium persulphate. In the presence of antioxidants, the radical loses its blue-green color, which translates into a decrease in absorbance at 734 nm (**Figure 16**). The degree of discoloration is correlated with the antioxidant content of the sample (Ilyasov et al., 2020; Munteanu & Apetrei, 2021; Stobiecka et al., 2022).

This simple and low-cost method enables the determination of antioxidant activity of a wide range of substances, since $ABTS^{\cdot+}$ radical reacts with both synthetic and natural molecules, and may be used over a wide pH range (Stobiecka et al., 2022).

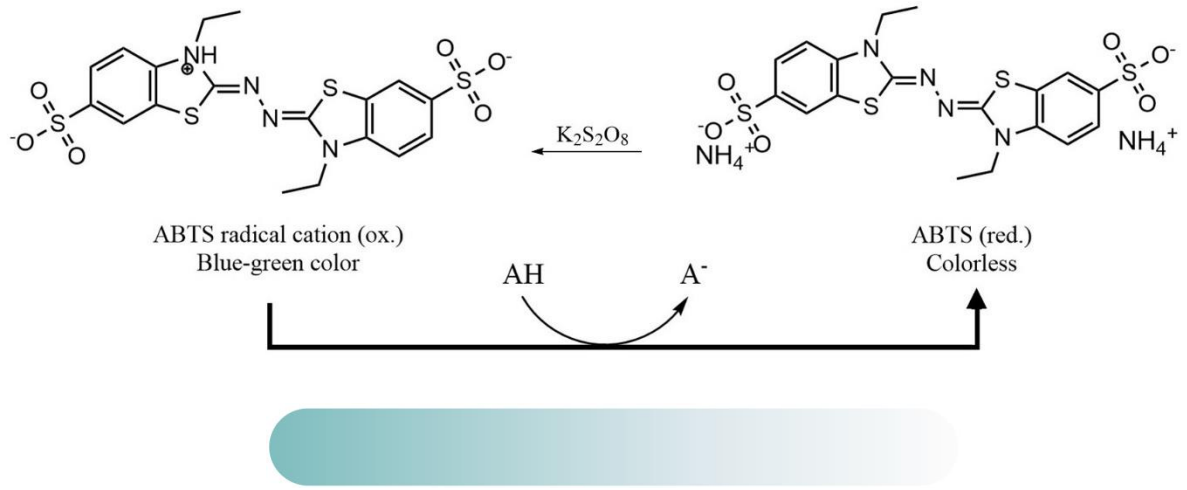


Figure 16. ABTS radical cation scavenging mechanism by an antioxidant molecule (AH). Adapted from (Munteanu & Apetrei, 2021) using the ChemDraw software.

1.5.3.3 Ferric ion reducing antioxidant power (FRAP) assay

The **ferric ion reducing antioxidant power (FRAP) assay**, first described in 1996 by Benzie and Strain, is a widely used test based on the ability of antioxidants to reduce the complex of ferric ions (Fe^{3+})-ligand to ferrous complex (Fe^{2+}), under acidic conditions. This reaction is monitored by the formation of a blue complex which can be detected by an increase in absorbance at 593 nm (**Figure 17**). This assay usually uses a ferric ion-containing reagent, such as TPTZ (2,4,6-tripyridyl-s-triazine), that yields ferrous ions upon reduction of the complex and forms the blue-colored complex. This simple, rapid, inexpensive, and highly reproducible method can be adapted for a variety of samples (Munteanu & Apetrei, 2021; Rumpf et al., 2023).

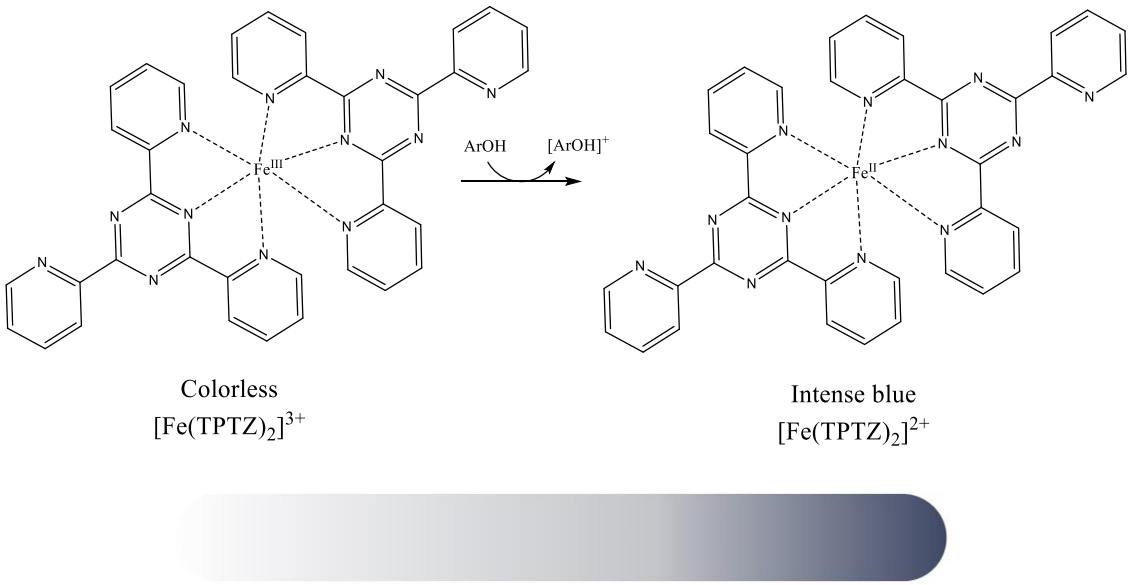


Figure 17. FRAP reaction mechanism, where ArOH represents a phenolic antioxidant and $[ArOH]^{\cdot}$ is an oxidised phenolic antioxidant. Adapted from (Bibi Sadeer et al., 2020) using the ChemDraw software.

1.5.3.4 Ferric chelating activity assay

The **ferric chelating activity assay** measures the capacity of antioxidants to chelate or bind to ferrous ions (Fe^{2+}). Species like Fe^{2+} are known to catalyze the production of ROS and stimulate lipid peroxidation through the Fenton reaction and by decomposing lipid hydroperoxides into more reactive peroxyl and alkoxyl radicals. By chelating iron ions, antioxidants can lower the availability of these ions and the oxidative damage produced by them (Gulcin, 2020; J. S. Santos et al., 2017).

This method uses ferrozine to assess the antioxidant activity of a wide range of samples. Under mild acid conditions (pH 6) ferrozine can generate a complex with a light purple colour by forming chelates with ferrous ions. However, in the presence of other chelating agents, this process is disrupted resulting in a decrease in the color of the ferrozine-Fe^{2+} complex (**Figure 18**). In this assay, the ability of the antioxidants to chelate the ferrous ions can be monitored by the loss of the purple color of the complex at 562 nm. The lower the absorbance, the lower the concentration of the ferrozine-Fe^{2+} complex and, consequently, the stronger the chelation of the sample (Gulcin, 2020; J. S. Santos et al., 2017). This is a simple, quick, and inexpensive method (Bibi Sadeer et al., 2020; J. S. Santos et al., 2017).

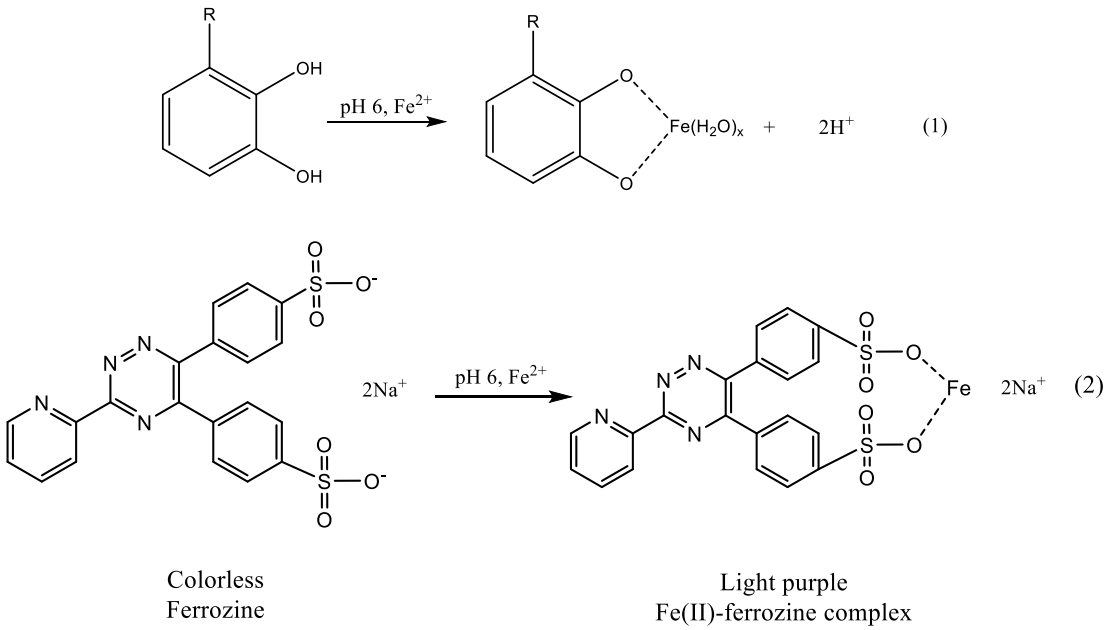


Figure 18. Reaction between a phenolic compound and the ferrous ion (1) resulting in a decrease of the light purple color and reaction between ferrozine and the ferrous ion (2). Adapted from (J. S. Santos et al., 2017) using the ChemDraw software.

1.5.4 Antimicrobial Activity

Plants have been used for medicine purposes for centuries in many cultures around the world, and the rise of antibiotic resistance, as well as the need for alternatives to synthetic food preservatives, has made the search for novel natural antimicrobials with lower toxicity and side effects more important than ever (Allami et al., 2020; Nascimento et al., 2000; Sakkas & Papadopoulou, 2017).

Many plants have been studied for their antibacterial characteristics related to compounds synthesized in the plant's secondary metabolism. **Table 10** lists some plant extracts with antimicrobial properties. The presence of a great number of alkaloids, tannins, phenols, flavonoids, and other bioactives, makes plant extracts extremely active against a wide variety of microorganisms. Resistance to plant ingredients is less likely since plant extracts' antimicrobial action can be associated with a number of routes due to their different functional groups (Allami et al., 2020; Nascimento et al., 2000; Sakkas & Papadopoulou, 2017).

Table 10. Examples of plant extracts with antibacterial activity.

Plant material	Bacteria	Mechanism of action	Ref.
Cocoa (*Theobroma Cacao* L.)	*E. coli* *Klebsiella pneumoniae*	Cell membrane rupture	(Nayim et al., 2018)
Chinese cork oak (*Quercus variabilis* Blume)	*S. aureus*	Cell membrane rupture and metabolism disruption	(Zhou et al., 2019)
Bean (*Phaseolus vulgaris* L.)	*E. coli*	Cell membrane rupture	(Nayim et al., 2018)
Pomegranate (*Punic granatum* L.)	*S. aureus*	Cell membrane rupture	(Álvarez-Martínez, Rodríguez, et al., 2021)

Polyphenols, such as flavonoids and tannins, alkaloids, and terpenoids, are among the plant components that have received the most attention in recent years for their antibacterial action (Álvarez-Martínez, Barrajón-Catalán, et al., 2021). The antibacterial activity of tannins is attributed to their ability to disrupt bacterial cell membranes by reacting with their surface proteins to form stable water-insoluble components. The antibacterial effect of alkaloids is due to their ability to intercalate with the DNA of both Gram-positive and Gram-negative bacteria, interfering with cell division and protein biosynthesis, as well as cell wall and membrane rupture. Both flavonoids and terpenes have been associated with disruption of the cell membrane and disturbance in protein and DNA metabolism (Álvarez-Martínez, Barrajón-Catalán, et al., 2021; Hemeg et al., 2020).

These substances appear to be more effective against Gram-positive bacteria like *S. aureus* than Gram-negative bacteria like *E. coli*, which is due to the different architectures of Gram-positive and Gram-negative bacteria's cell walls (Álvarez-Martínez, Barrajón-Catalán, et al., 2021). Gram-positive bacteria have a thick cell wall consisting of peptidoglycan surrounding a single plasma membrane. The structure of the cell wall allows hydrophobic molecules to easily penetrate the cells and act on both the cell wall and within the cytoplasm. Gram-negative bacteria have a much thinner cell wall consisting of a single layer of peptidoglycan and an additional outer membrane, containing lipopolysaccharides. This outer

membrane acts as an additional barrier and provides protection against compounds with antimicrobial activity (Nazzaro et al., 2013).

1.5.5 Sun Protection Factor

Solar ultraviolet radiation can be classified into three categories UVC (200-280 nm), UVB (280-320 nm), and UVA (320-400 nm). The negative consequences of UV radiation, such as a deficiency in the skin's immune system and abnormalities in the DNA, are primarily caused by UVB. The production of ROS promotes oxidative stress, which can lead to skin defects known as photoaging. Natural extracts are gaining popularity as a safe and effective alternative to chemical sunscreens since they have fewer side effects than chemical sunscreens that absorb UVB rays with synthetic ingredients. Natural compounds can be considered as possible sources due to their UV absorption and antioxidant activity, which gives them the potential to be used in the treatment and prevention of UV-induced diseases. **Table 11** lists some plant extracts with photoprotective properties (Cefali et al., 2019; Hidayah et al., 2023; Pachuau & Chhakchhuak, 2013).

Table 11. Examples of plant extracts with photoprotective properties.

Plant material	Main effects	Ref.
Reed grass (*Calamagrostis effuse*)	UV absorber, antioxidant activity; UVA– UVB absorption coefficient	(Mejía-Giraldo et al., 2016)
Yarrow (*Achillea millefolium* L.)	Antioxidant activity, tyrosinase inhibitory activity, SPF (14.04)	(Gaweł-Bęben et al., 2020)
Morning glory (*Ipomoea mauritiana*)	Antioxidant, SPF (11.3)	(Napagoda et al., 2016)
Walnut (*Juglans regia* L.)	Antioxidant, anti-inflammatory, photoprotective, SPF (8.8), UVB absorber	(Muzaffer et al., 2018)

Phenolic compounds are the most studied components with photoprotective properties. Flavonoids have significant UV absorption capabilities in the range of 200-400 nm due to the presence of double bonds in aromatic rings in their molecular structure (Li et al., 2023). High concentrations of flavonoids

such as rutin and quercetin are believed to be capable of preventing or, at least, reducing the damage of the harmful effects of UV light (Ebrahimzadeh et al., 2014; Li et al., 2023). Phenolic acids are thought to be capable of inhibiting DNA damage by acting in redox-sensitive signalling cascades and preventing UV-induced oxygen-free radical production and lipid peroxidation (Ebrahimzadeh et al., 2014). Monomeric anthocyanin pigment, ellagitannins, and catechin are also thought to be powerful antioxidants that protect against UV-induced free radical damage (Li et al., 2023).

1.5.6 Identification of extracts' volatile compounds by gas chromatography-mass spectrometry

Gas chromatography coupled to mass spectrometry (GC-MS) is an analytical technique used to identify and quantify volatile compounds in a mixture. GC-MS combines gas chromatography (GC) which separates the mixture into its individual components and mass spectrometry (MS) which identifies the components by their mass and chemical structure (Braithwaite & Smith, 1999; Skoog et al., 2017).

The vaporized sample is first injected into the head of a chromatographic column. GC separates the sample components based on the differential distribution between a mobile gaseous phase and a liquid or solid stationary phase held in the column. According to their boiling points, polarity, and other physical properties, the components separate and move through the column at different rates. The gaseous mobile phase, also known as the carrier gas, moves the sample components through the column. After separation, the molecules elute into the mass spectrometer (Skoog et al., 2017).

In the MS the components go through the ionization source where they are ionized and fragmented. The different fragments, in the ion form, are introduced into the mass analyser which separates them based on their mass-to-charge ratio (m/z). The mass spectrum generated by the mass spectrometer provides information about the chemical structure of the separated compounds. Each compound has a unique mass spectrum, which can be used to identify it. The mass spectrum can also be used to quantify the amount of each compound present in the sample. A scheme of a typical GC-MS system is shown in **Figure 19** (Skoog et al., 2017).

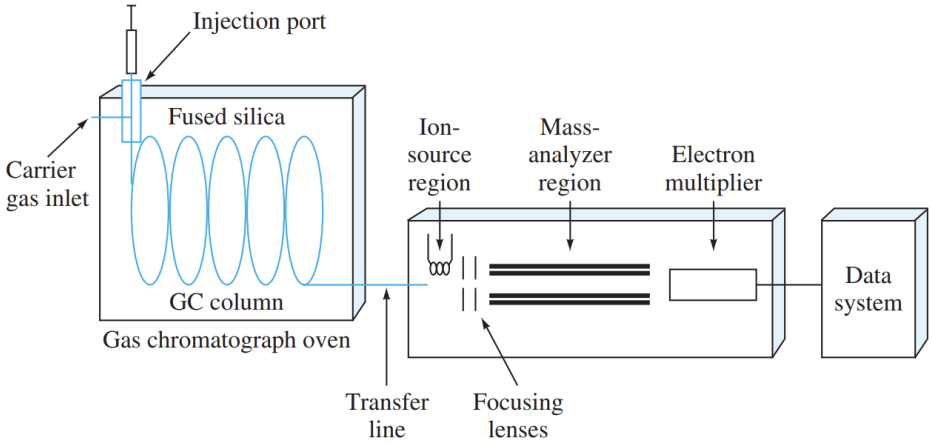


Figure 19. Schematic presentation of a typical GC-MS system. Adapted from (Skoog et al., 2017).

GC-MS technique has several advantages since it is highly sensitive, allowing for the detection and quantification of compounds at very low concentrations. It is also highly selective, allowing individual compounds in complex mixtures to be identified, through comparison with compound libraries (Skoog et al., 2017).

2. MOTIVATION AND AIMS OF THIS WORK

Melanogenesis is a complex and highly regulated process. When melanogenesis is disrupted, defects in skin pigmentation, known as hypo- and hyperpigmentation, occur (Boo, 2020; Thawabteh et al., 2023). Although there are treatments on the market to treat these ailments, research on substances that can treat these conditions with great effectiveness and fewer bad side effects is ongoing. Natural sources provide a wide range of health advantages due to their richness of bioactive compounds with photoprotective, antiaging, and antibacterial properties. As a result, natural extracts integrated into cosmetic formulations have emerged as an appealing choice for people looking for safer and more environmentally friendly cosmetics for the treatment of skin problems (Dini & Laneri, 2021; Hernandez et al., 2021).

Because active chemicals in plants are often restricted inside plant matrix, proper extraction procedures are required to assist the separation and isolation of the desired molecules. To replace the present extraction processes, simpler, cheaper, and less wasteful extraction technologies must be developed (Chuo et al., 2022; Zhang et al., 2018).

Aside from choosing on an extraction process, selecting the suitable solvent for extraction is also an important step in successfully getting the necessary chemicals. Organic solvents, which have a number of negative environmental effects, are commonly used in extraction processes. Due to their low toxicity and cost, availability, and ecologically benign character, deep eutectic solvents (DES) have emerged as green and sustainable solvents and a superior option to traditional organic solvents (Duan et al., 2016).

Considering this, the main aims of this work are:

- Investigate the use of simpler and less wasteful extraction methods to extract bioactive compounds from natural sources;
- Investigate the use of newer greener solvents in the extraction process;
- Characterize various natural extracts in terms of their physicochemical properties for use in the cosmetic field.

3. MATERIALS AND METHODS

3.1 MATERIALS AND CHEMICALS

The natural sources used in this study are represented in **Figure 20**. The lavender (*Lavandula angustifolia*), thyme (*Thymus vulgaris*), and eucalyptus (*Corymbia citriodora*) leaves were purchased from Cantinho das Aromáticas, Portugal. The cocoa (*Theobroma cacao*) beans were purchased from Chocolataria Equador, Portugal. The cork (*Quercus suber* L.) powder was supplied by Cork Supply, Portugal.



Figure 20. Natural sources used for extraction **A)** *Lavandula angustifolia* **B)** *Thymus vulgaris* **C)** *Corymbia citriodora* **D)** *Theobroma cacao* **E)** *Quercus suber* L. Images adapted from (Identify, Explore and Share Your Observations of Wild Plants).

DL-Lactic acid (80.0%), glycerol (99.0%), Folin-Ciocalteu reagent, gallic acid (97.5-102.5%), quercetin, DPPH (2,2-diphenyl-1-picrylhydrazyl), trolox (6-hydroxy-2,5,7,8-tetramethylchroman-2-carboxylic acid) (97.0%), potassium persulfate (99.99%), pyridine, potassium phosphate (99.0%), ferric chloride (97.0%), and chloroform (99.8%) were purchased from Sigma-Aldrich, Germany. Sodium carbonate (99.8%), aluminium chloride, and sodium hydroxide (98.0%) were purchased from Riedel-de Haën (Germany), Acros Organics (USA), and Labkem (Spain), respectively. ABTS (2,2′-azino-*bis*(3-ethylbenzothiazoline-6-sulfonic acid)) (98.0%) and L-tyrosine (98.0%) were purchased from Alfa Aesar, USA. Citric acid,

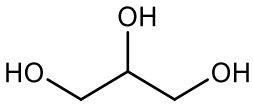
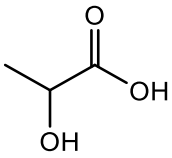
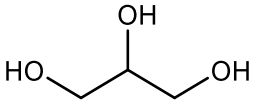
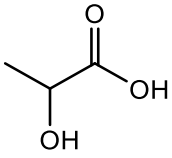
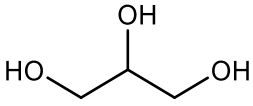
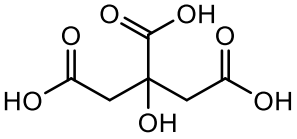
hydrochloric acid, ferrous chloride (97.0%), ferrozine (97.0%), and ethanol (99.8%) were purchased from Fisher Scientific, USA. Nile red, EDTA (ethylenediaminetetraacetic acid) (98.0%), and N,O-*Bis*(trimethylsilyl)trifluoroacetamide (BSTFA + TMCS, 99:1) were purchased from TCI Chemicals, Japan. Ammonia solution (25%) was purchased from Panreac, Spain. All chemicals were used without further purification. The commercial sunscreen lotion Darphin® Soleil SPF 50 was purchased from a pharmacy.

3.2 EXTRACTION SOLVENTS DEVELOPMENT AND CHARACTERIZATION

3.2.1 Extraction solvents production

The extraction solvents used in this work were two hydroethanolic (HE) mixtures and three deep eutectic solvents (DES). The HE (EtOH:H_2O) 50:50 mixture was prepared by combining equal volumes of ethanol and distilled water. The HE (EtOH:H_2O) 30:70 solvent was prepared by combining volumes of ethanol and distilled water in the ratio of 30:70, respectively. The eutectic mixtures used in this work (**Table 12)** were produced by vigorously stirring the raw constituents at temperatures ranging from 25 to 100 °C. After 1 hour, a clear solution was formed, and the mixture was stored at room temperature for future use. For their accurate characterization, the DES mixtures were subjected to a lyophilization process to remove water.

Table 12. Composition of the DES used as extraction solvents.

DES	HBA	HBD	Molar ratio
DES 1	Glycerol (GLY) 	Lactic acid (LA) 	1:1
DES 2	Glycerol (GLY) 	Lactic acid (LA) 	4:1
DES 3	Glycerol (GLY) 	Citric Acid (CA) 	1:1

3.2.2 Characterization of the extraction solvents

3.2.2.1 Polarity

Nile red (NR) was used as a solvatochromatic probe to estimate the extraction solvents polarity in the form of molar transition energy (E_{NR}). The dye solution was dissolved in the extraction solvent to obtain a concentration of 10^{-5} M and the dye absorption spectrum (λ_{max}) was read on a UV-Vis spectrophotometer (BioTek Synergy H1 microplate reader). All the measurements were performed at atmospheric pressure at 25 °C. Distilled water and ethanol were also measured for reference. E_{NR} (kcal/mol) was determined using the following **Equation (1)**:

$$E_{NR} = \frac{hcNA}{\lambda_{max}} = \frac{28591}{\lambda_{max}} \quad \textbf{(1)}$$

Where h is Planck's constant; c is the speed of light in a vacuum; NA is the Avogadro constant.

3.2.2.2 pH measurement

The pH of the extraction solvents was evaluated using a pH bench meter (VSTAR83, probe 8157BNUMD, Thermo Scientific).

3.2.2.3 Viscosity

To determine the viscosity (η) of the DES, two approaches were followed. For DES 1 and 2 the viscosity was assessed using a Brookfield DV-II+Pro viscometer (spindle 27, 50 rpm at room temperature for 4 h, with 30 s time points, torque 3.0×10^{-6} N m). For DES 3 the viscosity was assessed using a Discovery HR-1 Rheometer (TA Instruments), using a 40 mm parallel plate, at 25 °C. The flow method was as follows: 1. Flow ramp 25 °C; 120.0s; 0.1 to final 300.0 1/s; 2. Flow ramp 25 °C; 120.0s; 300.0 to final 300.0 1/s ; 3. Flow ramp 25 °C; 120.0s; 0.1 to final 300.0 1/s. The results were expressed as Pa s.

3.2.2.4 Density

The density (ρ) of the extraction solvents was measured in triplicate by weighting 25 mL of each solvent inside a 25.00 ± 0.01 mL pycnometer. The final density value was calculated using the quotient between the mass and the volume of the solvent.

3.2.2.5 Refraction index

The indices of refraction (n_D) of the extraction solvents were measured using an Atago RX-9000α refractometer. All the measurements were performed at atmospheric pressure at 25 °C.

3.2.2.6 Conductivity

The conductivity (σ) of the extraction solvents was measured using a Thermo Scientific Benchtop Meter (Orion Versa Star Pro). All the measurements were performed at atmospheric pressure at 25 °C.

3.3 EXTRACTION OF BIOACTIVE COMPOUNDS FROM NATURAL SOURCES

Lavender (*Lavandula angustifolia*), thyme (*Thymus vulgaris*), eucalyptus (*Corymbia citriodora*), cork (*Quercus suber* L.), and cocoa (*Theobroma cacao*) were the chosen natural sources of this study. The samples were first ground into a fine powder using a coffee grinder (KUNFT KCG5414). Extraction of bioactive compounds from all powdered natural sources was carried out using two hydroethanolic mixtures (HE (EtOH:H_2O) 50:50 and 30:70) and three natural eutectic mixtures (**Table 12**).

Extraction was accomplished following two equipments: a mechanical impeller (MI) (Heidolph) and a planetary mixer (THINKY ARE-250). The conditions applied when using these equipments are shown in **Table 13**.

Table 13. Extraction conditions applied when using a mechanical impeller and a planetary mixer.

Conditions	MI	Planetary mixer
Ratio natural source:solvent	10 g: 50 mL	5 g: 50 mL
Program	-30 minutes; 5000 rpm -90 minutes; 5000 rpm	3 cycles: 1) 5 min., 1000 rpm; 2) 5 min., 2000 rpm; 3) 5 min., 2000 rpm; 4) 5 min., 2000 rpm; 5) 5 min., 1000 rpm; total time: 75 min Defoaming at the end of each step: 1 min., 2200 rpm
Temperature	EtOH:H_2O: Room temperature Eutectic solvents: 70 °C	50 °C

The extraction process was followed by filtration of the powder. For the extractions with the hyroethanolic mixtures, the filtrated liquid was transferred to a rotary evaporator (Heidolph) to be concentrated at 40 °C. After being concentrated, the samples were subjected to a lyophilization process to remove the water and later be characterized. For the extractions with the eutectic mixtures, the filtrated liquid was kept and later lyophilized and characterized. The solid was collected, dried in the oven, and weighed. The extraction yields (g extract/g starting material) were calculated following **Equation (2)**:

$$\text{Extraction yield} = \frac{W_1 - W_2}{W_1} \quad \textbf{(2)}$$

Where W_1 is the initial powdered sample weight in grams; W_2 is the weight at the end of the extraction procedure in grams.

From this point forward, the different extraction methodologies used in this work will follow **Table 14** nomenclature for simplicity of understanding.

Table 14. The different extraction methodologies tested in this study.

Method	Conditions
Method 1	MI for 30 minutes with HE (EtOH:H_2O) 50:50
Method 2	MI for 90 minutes with HE (EtOH:H_2O) 50:50
Method 3	Planetary mixer with HE (EtOH:H_2O) 50:50
Method 4	MI for 30 minutes with HE (EtOH:H_2O) 30:70
Method 5	MI for 90 minutes with HE (EtOH:H_2O) 30:70

Method 6	Planetary mixer with HE (EtOH:H_2O) 30:70
Method 7	MI for 30 minutes with DES 1
Method 8	MI for 90 minutes with DES 1
Method 9	Planetary mixer with DES 1
Method 10	MI for 30 minutes with DES 2
Method 11	MI for 90 minutes with DES 2
Method 12	Planetary mixer with DES 2
Method 13	MI for 30 minutes with DES 3
Method 14	MI for 90 minutes with DES 3
Method 15	Planetary mixer with DES 3

3.4 CHARACTERIZATION OF THE EXTRACTS

3.4.1 Determination of total phenolic content (TPC)

The total phenolic content of the extracts was determined using the Folin-Ciocalteu method, as described by Singleton & Rossi (1965) (**Figure 21**). Extracts were dissolved in dimethyl sulfoxide (DMSO) to obtain concentrations of 10 mg/mL for extracts obtained by hydroethanolic extraction and 100 mg/mL for extracts obtained by eutectic extraction. In a 96-well microplate, 2 µL of sample were mixed with 10 µL of Folin-Ciocalteu reagent and 120 µL of distilled water. After mixing, 40 µL of 15% sodium carbonate (Na_2CO_3) and 28 µL of distilled water were subsequently added to the mixture. The microplate was kept in the dark for 2 hours at room temperature, following which the absorbance was measured at 750 nm (BioTek Synergy H1 microplate reader), taking DMSO as a blank. The calibration curve was obtained from a series of standard solutions of gallic acid with the following concentrations: 0.0015, 0.015, 0.15, 0.45, 0.9, 1.5, 2.5, and 5 mg/mL. The results were expressed as milligrams of gallic acid equivalents (GAE) per gram of dry weight of the sample (mg/g). All determinations were performed in duplicate. The total phenolic content was determined using the following **Equation (3)**:

$$C = C_1 \times \frac{V}{m} \quad \textbf{(3)}$$

Where C_1 is the concentration of gallic acid established from the calibration curve in mg/mL; V is the volume of extract in mL; m is the mass of the plant extract in grams.

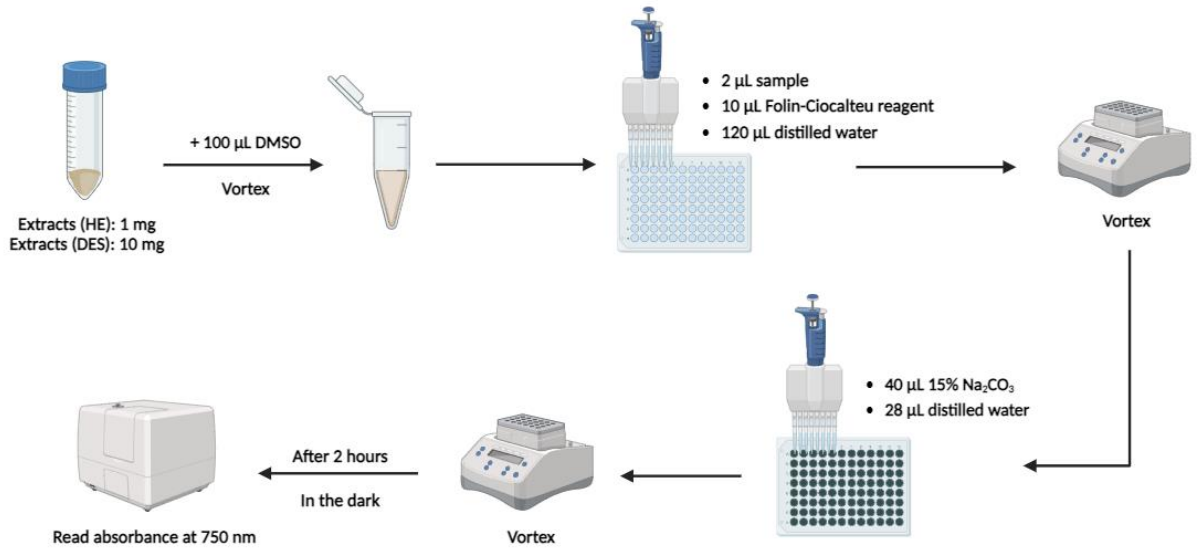


Figure 21. Procedure workflow for determination of total phenolic content following the Folin-Ciocalteu assay (the images were obtained using the BioRender software).

3.4.2 Determination of total flavonoid content (TFC)

The total flavonoid content of the extracts was determined using the aluminium chloride assay, as described by Zhishen *et al.* (1999) (**Figure 22**). Extracts were dissolved in DMSO to obtain concentrations of 10 mg/mL for extracts obtained by hydroethanolic extraction and 100 mg/mL for extracts obtained by eutectic extraction. In a 96-well microplate, 17.5 µL of sample were mixed with 140 µL of distilled water and 5.25 µL of 10% sodium nitrite ($NaNO_2$). After 5 minutes, 5.25 µL of 20% aluminium chloride ($AlCl_3$), 70 µL of 1M sodium hydroxide (NaOH), and 112 µL of distilled water were subsequently added to the mixture. The absorbance was measured at 510 nm (BioTek Synergy H1 microplate reader) at room temperature, taking DMSO as a blank. The calibration curve was obtained from a series of standard solutions of quercetin with the following concentrations: 0.1, 0.5, 1, 2, 3, 4, 6, 8, and 10 mg/mL. The results were expressed as milligrams of quercetin equivalents (QE) per gram of dry weight of the sample (mg/g). All determinations were performed in duplicate. The total flavonoid content was determined using the following **Equation (4)**:

$$C = C_1 \times \frac{V}{m} \quad \textbf{(4)}$$

Where C_1 is the concentration of quercetin established from the calibration curve in mg/mL; V is the volume of extract in mL; m is the mass of the plant extract in grams.

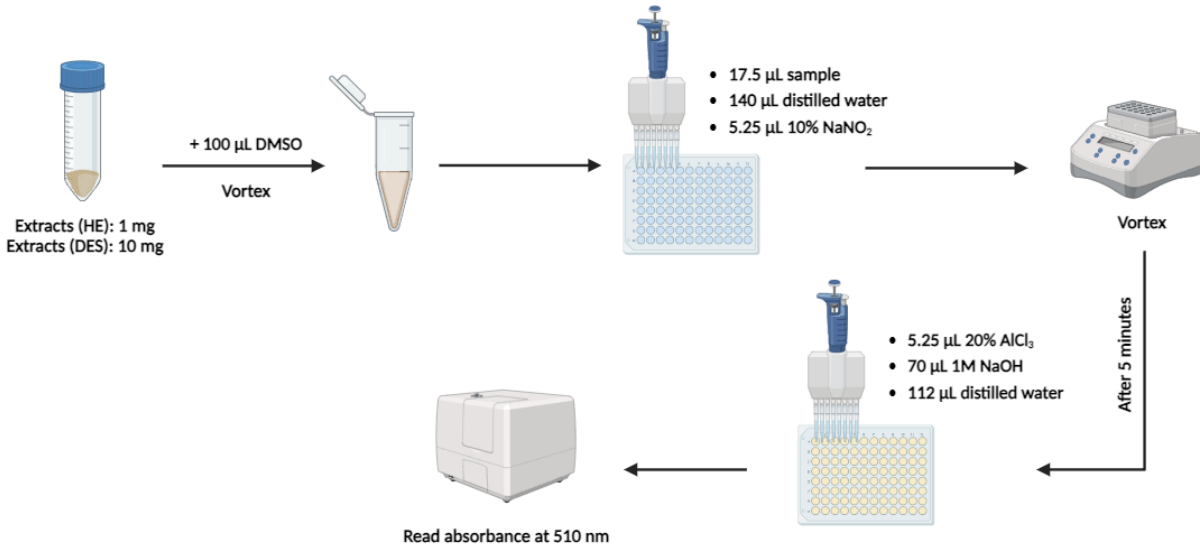


Figure 22. Procedure workflow for determination of the total flavonoid content following the aluminium chloride assay (the images were obtained using the BioRender software).

3.4.3 Determination of antioxidant activity

From the various analytical methods available for evaluation of the antioxidant activity of a sample, the colorimetry-based assays were chosen since they are the most accessible and widely used methods for evaluating the antioxidant activity of biological samples.

3.4.3.1 DPPH radical scavenging activity assay

The antioxidant activity evaluated by the DPPH assay followed the method described by Brand-Williams *et al.* (1995) (**Figure 23**). DPPH solution (200 µM, 99.8% ethanol) was prepared daily and stored at 4 °C and protected from light when not in use between analyses. Except for the eucalyptus extract, which was dissolved in 99.8% ethanol because it is insoluble in water, the extracts were dissolved in distilled water to achieve the following concentrations: 0.005, 0.01, 0.05, 0.1, 0.15, 0.2, and 0.5 mg/mL. In a 96-well microplate, 10 µL of sample were mixed with 140 µL of DPPH solution. The absorbance was monitored continuously for 1 hour at 515 nm (BioTek Synergy H1 microplate reader) at room temperature. Trolox (6-hydroxy-2,5,7,8-tetramethylchroman-2-carboxylic acid) was used as a standard to perform the calibration curve of DPPH reduction. All determinations were performed in

triplicate. The percentage of reduced DPPH at steady state (% $DPPH_r$) was calculated following **Equation (5)**:

$$DPPH_r\ (\%) = \frac{(A_i - A_r)}{A_i} \times 100 \qquad \textbf{(5)}$$

Where A_r is the absorbance registered at steady state; A_i is the initial absorbance registered at time zero.

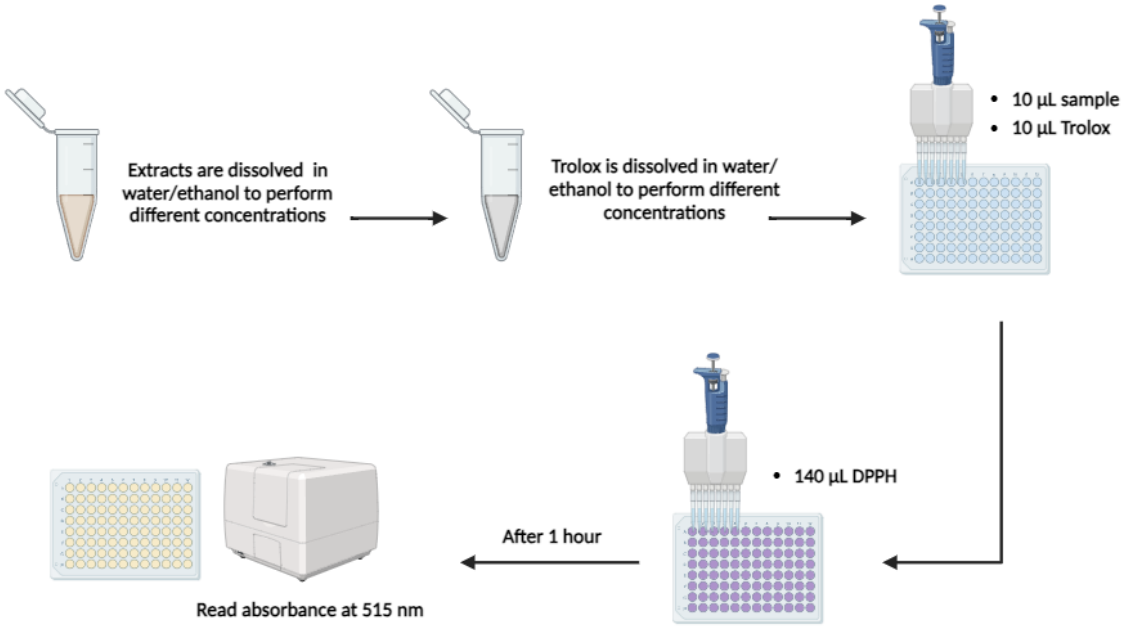


Figure 23. Procedure workflow for determination of the antioxidant activity following the DPPH radical scavenging activity assay (the images were obtained using the BioRender software).

The EC_{50} was obtained from the percentage of reduced DPPH curve and represents the concentration yielding 50% scavenging of DPPH. The antioxidant activity of the extracts was expressed as Trolox equivalents (TE) per 1 g of dry weight sample (mg TE/ g extract), as the following **Equation (6)**:

$$TE = \frac{EC_{50}\ \text{Trolox}}{EC_{50}\ \text{extract}} \qquad \textbf{(6)}$$

3.4.3.2 ABTS radical scavenging activity assay

The antioxidant activity evaluated by the ABTS assay followed the method described by Re *et al.* (1999) (**Figure 24**). The ABTS radical solution was prepared by mixing 5 mL of 7.4 mM ABTS solution with 88 µL of 2.6 mM potassium persulfate ($K_2S_2O_8$) solution and allowing them to react for 16 h at room

temperature in the dark. The $ABTS^{\cdot+}$ mixture was then diluted with the amount of 99.8% ethanol necessary to reach an absorbance of 0.7 ± 0.1 at 734 nm. With the exception of the eucalyptus extract, which was dissolved in 99.8% ethanol because it is insoluble in water, the extracts were dissolved in distilled water to achieve the following concentrations: 0.0005, 0.002, 0.01, 0.03, 0.125, and 0.5 mg/mL. In a 96-well microplate, 10 µL of sample were mixed with 140 µL of ABTS radical solution. The microplate was kept in the dark for 6 minutes at room temperature, following which the absorbance was measured at 734 nm (BioTek Synergy H1 microplate reader), taking water or ethanol as a blank. Trolox was used as a standard. All determinations were performed in duplicate. The percentage of antioxidant activity (% AA) was calculated following **Equation (7)**:

$$AA\ (\%) = \frac{(Abs_{control} - Abs_{sample})}{Abs_{control}} \times 100 \quad \textbf{(7)}$$

Where $Abs_{control}$ is the absorbance of ABTS radical + water/ethanol; Abs_{sample} is the absorbance of ABTS radical + sample/standard.

The EC_{50} was obtained from the percentage of antioxidant activity curve and represents the concentration yielding 50% scavenging of ABTS. The antioxidant activity of the extracts was expressed as Trolox equivalents (TE) per 1 g of dry weight sample (mg TE/ g extract), as shown in **Equation (6)**.

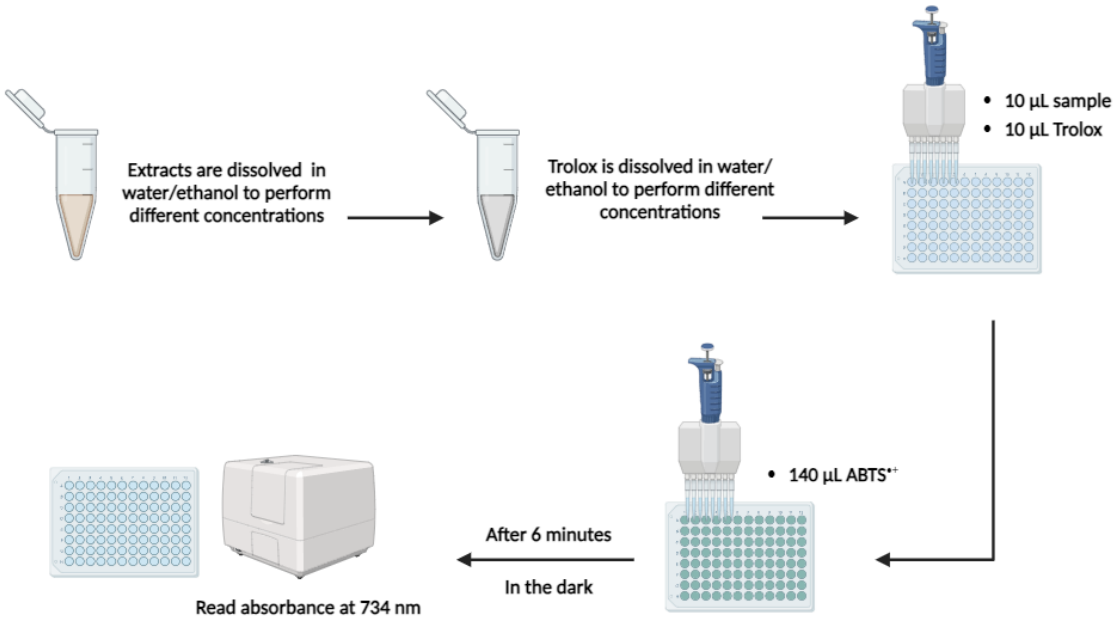


Figure 24. Procedure workflow for determination of the antioxidant activity following the ABTS radical scavenging activity assay (the images were obtained using the BioRender software).

3.4.3.3 Ferric ion reducing antioxidant power (FRAP) assay

The antioxidant activity evaluated by the FRAP assay followed the method described by Benzie & Strain (1996) (**Figure 25**). The FRAP reagent was prepared by mixing 300 mM acetate buffer (pH 3.6) with 10 mM TPTZ (2,4,6-tripyridyl-s-triazine) solution in 40 mM hydrochloric acid (HCl) and 20 mM ferric chloride ($FeCl_3$) solution in a 10:1:1 (v/v/v) ratio. Except for the eucalyptus extract, which was dissolved in 99.8% ethanol because it is insoluble in water, the extracts were dissolved in distilled water to achieve the following concentrations: 0.5, 0.7, 0.8, 1, 1.3, 1.6, and 2 mg/mL. In a 96-well microplate, 5 µL of sample were mixed with 145 µL of FRAP reagent. The microplate was incubated for 10 minutes at 37 °C, following which the absorbance was measured at 593 nm (BioTek Synergy H1 microplate reader), taking water or ethanol as a blank. Trolox was used as a standard. All determinations were performed in duplicate. The percentage of antioxidant activity (% AA) was calculated following **Equation (8)**:

$$AA\ (\%) = \frac{(Abs_{sample} - Abs_{control})}{Abs_{sample}} \times 100 \qquad \textbf{(8)}$$

Where Abs_{sample} is the absorbance of FRAP reagent + sample/standard; $Abs_{control}$ is the absorbance of FRAP reagent + water/ethanol.

The EC_{50} was obtained from the percentage of antioxidant activity curve and represents the concentration needed to reduce the Fe^{3+}-TPTZ complex by 50%. The antioxidant activity of the extracts was expressed as Trolox equivalents (TE) per 1 g of dry weight sample (mg TE/ g extract), as shown in **Equation (6)**.

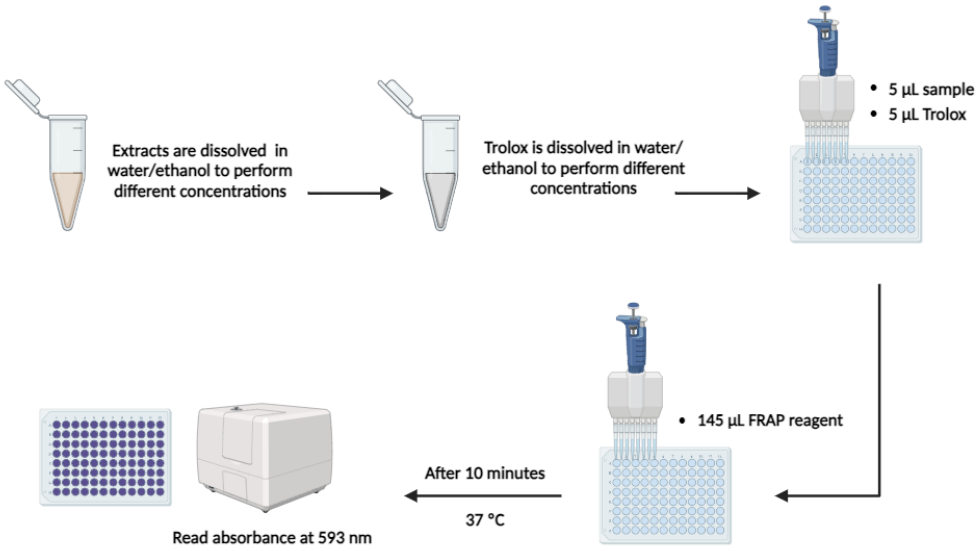


Figure 25. Procedure workflow for determination of the antioxidant activity following the ferric ion reducing antioxidant power assay (the images were obtained using the BioRender software).

3.4.3.4 Ferric chelating activity assay

The antioxidant activity evaluated by the ferric chelating activity assay followed the ferrous iron-ferrozine complex method described by Dinis *et al.* (1994) (**Figure 26**). The extracts were dissolved in 50% ethanol to achieve the following concentrations: 1, 2, 4, 8, and 10 mg/mL. In a 96-well microplate, 25 µL of sample were mixed with 12.5 µL of 2 mM ferrous chloride ($FeCl_2$) and 112.5 µL of distilled water. The microplate was incubated for 5 minutes at room temperature, following which 50 µL of 5 mM ferrozine were added. After 10 minutes, the absorbance was measured at 562 nm (BioTek Synergy H1 microplate reader), taking ethanol as a blank. EDTA (ethylenediaminetetraacetic acid) was used as a standard. All determinations were performed in duplicate. The ability of the sample to chelate ferrous ion was calculated following **Equation (9)**:

$$\text{Chelating activity (\%)} = \frac{(Abs_{control} - Abs_{sample})}{Abs_{control}} \times 100 \quad \textbf{(9)}$$

Where $Abs_{control}$ is the absorbance of the ferrozine-ferrous iron complex + ethanol; Abs_{sample} is the absorbance of ferrozine-ferrous ion complex + sample/standard.

The EC_{50} was obtained from the percentage of chelating activity curve and represents the concentration needed to chelate 50% of the ferrous ion. The antioxidant activity of the extracts was expressed as EDTA equivalents per 1 g of dry weight sample (mg EDTA equivalents/ g extract), as shown in **Equation (10)**:

$$\text{EDTA equivalents} = \frac{EC_{50}\ \text{EDTA}}{EC_{50}\ \text{extract}} \quad \textbf{(10)}$$

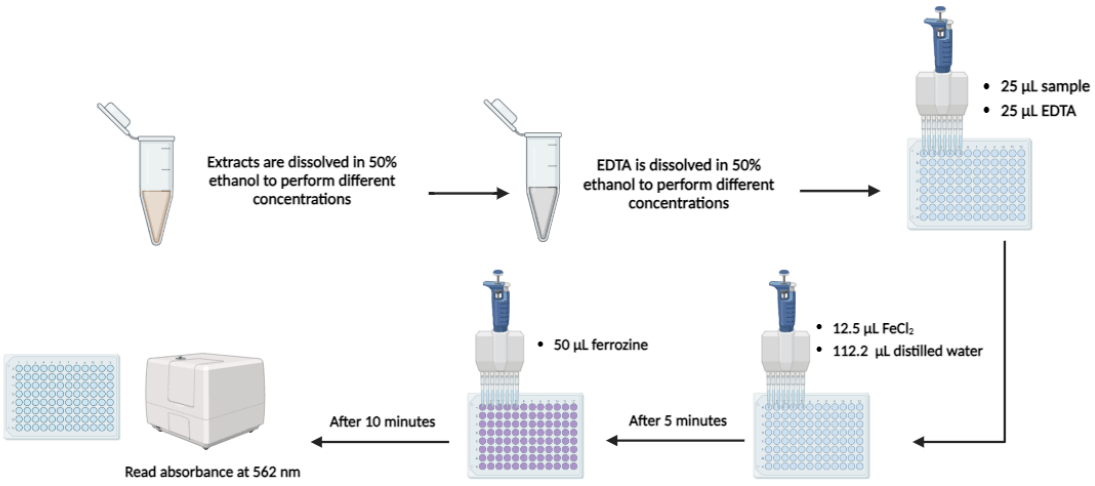


Figure 26. Procedure workflow for determination of the antioxidant activity following the ferric chelating activity assay (the images were obtained using the BioRender software).

3.4.4 Determination of antimicrobial activity

The antimicrobial activity was determined using two methodologies: i) broth microdilution method, to obtain the minimum inhibitory and bactericidal concentrations (MICs, MBCs), and ii) agar-well diffusion method.

3.4.4.1 Broth microdilution method (MICs and MBCs determination)

The antimicrobial activity out of the extracts was carried out on the samples produced using method 1. The antimicrobial activity of these extracts was evaluated against Gram-positive, *Staphylococcus aureus (S. aureus)* and *Staphylococcus epidermidis (S. epidermidis)* strains and Gram-negative, *Escherichia coli (E. coli)* and *Pseudomonas aeruginos*a *(P. aeruginosa)* strains bacteria. The minimum inhibitory and bactericidal concentrations (MICs, MBCs) of each sample against the bacteria were determined using the broth microdilution method described by Wiegand *et al.* (2008). Extracts were first dissolved in water to obtain concentrations of 20.48 mg/mL.

For MICs determination, a 96-well plate was prepared using 3 rows for each antimicrobial agent with 100 µL of Mueller-Hinton broth (MHB) in column 12 (sterility control) and 50 µL from columns 2 to 11. Two-fold serial dilutions of the antimicrobial agent were then prepared from columns 1 to 10 (**Figure 27**). Afterwards, 50 µL of bacteria inoculum prepared at a concentration of 10×10^5 colony forming units (CFUs)/mL in MHB were added to each well from columns 1 to 11. Absorbance was measured at 600 nm before and after plate incubation for 24 hours at 37 °C and 100 rpm. The MIC value for each agent/bacteria was considered the lowest concentration of the antimicrobial agent that prevented the visible growth of bacteria and was confirmed by the differences in absorbance readings.

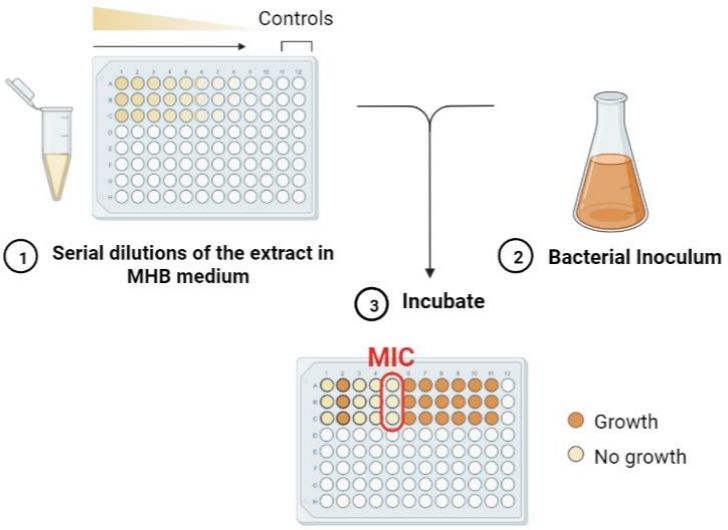


Figure 27. Schematic workflow for determination of minimum inhibitory concentration (MIC) (the images were obtained using the BioRender software) **1)** Serial dilutions of the extract are made in Mueller-Hinton broth (MHB) medium in a 96-well plate **2)** Bacterial inoculum is prepared and added to the 96-well plate **3)** The plate is incubated for 24 hours and the MIC value is determined.

For the determination of MBCs, a new 96-well plate was prepared with 180 µL of phosphate saline solution (PBS) from rows B to H and columns 1 to 9, leaving the first row (A) free. Then, 100 µL of the MIC well, the 2 wells before and after the MIC concentration, and well 11 (growth control) were transferred to row A of the new 96-well plate. 20 µL of the first row (A) were transferred to the second (B), and the second to the third until the H row. Afterwards, aliquots of 10 µL were removed from each well and were then inoculated onto the surface of TSA (tryptic soy agar) plates (**Figure 28**). One plate was used for each column. The plates were incubated for 24 hours at 37 °C and 100 rpm. The MBC value for each agent/bacteria was considered the lowest concentration of an antimicrobial agent at which no colonies formed under these conditions, indicating the concentration that effectively kills the microorganism.

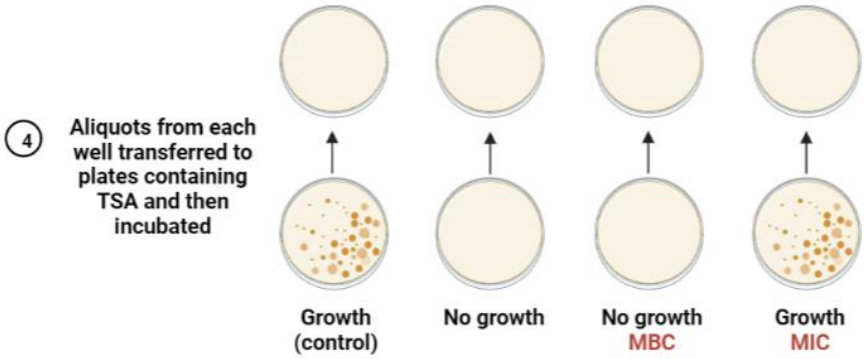


Figure 28. Schematic workflow for determination of minimum bactericidal concentration (MBC) (the images were obtained using the BioRender software) **4)** After serial dilutions of the wells selected after MIC determination, aliquots from these wells are inoculated onto the surface of tryptic soy agar (TSA) plates. The plates are incubated for 24 hours and the MBC value is determined.

3.4.4.2 Agar-well diffusion method

The antimicrobial activity of the extracts obtained using eutectic mixtures as solvents was carried out on samples produced using method 8 and 11. The antimicrobial activity of these extracts was evaluated against Gram-positive, *Staphylococcus aureus (S. aureus; ATCC 6538)* and *Staphylococcus epidermidis (S. epidermidis; ATCC 35984)* strains and Gram-negative, *Escherichia coli (E. coli; ATCC 25922)* strain bacteria. Each strain was incubated with TSB (tryptic soy broth) inoculum for 24 hours at 37 °C.

The zone of inhibition (ZoI) of each sample against the bacteria was determined using an adaptation of the test described by Kirby-Bauer (**Figure 29**). The size of the halo was used as a qualitative measure of sample activity. Initially, the cell suspension was diluted in TSB to a concentration of 1×10^7 CFUs/mL, and then 100 µL of this solution was incorporated into TSA plates. Afterwards, 50 µL of sample were placed on 6 mm diameter wells cut into the surface of the agar. Plates were incubated for 24 hours at 37 °C. After incubation, the halo (zone of transparent medium indicating no microorganism growth) formed around the sample was measured. All experiments were performed in triplicate for each sample and were repeated at least three times.

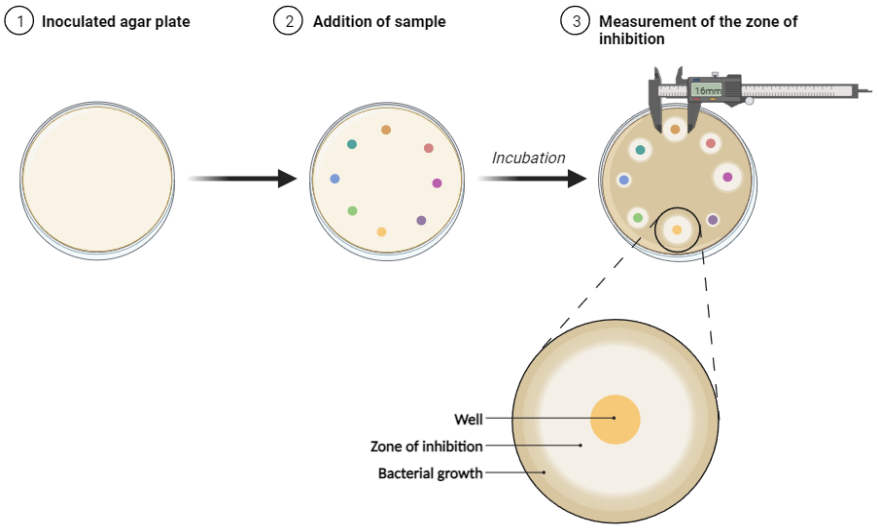


Figure 29. Procedure workflow for determination of zone of inhibition (ZoI) (the images were obtained using the BioRender software) **1)** Each bacteria strain is incorporated into tryptic soy agar (TSA) plates and incubated for 24 hours **2)** The sample is placed on wells cut into the surface of the agar **3)** After the plates are incubated for 24 hours, the zones of inhibition are measured.

3.4.5 Determination of sun protection factor (SPF)

The sun protection factor (SPF) of the extracts was obtained using a simple *in vitro* method described by Mansur *et al.* (1986) (**Figure 30**). SPF measures how well a product protects the skin from UVB radiation and is defined as the ratio of UV energy required to produce a minimal erythemal dose (MED) in protected skin to unprotected skin. Commercial sunscreen lotion Darphin® Soleil SPF 50 (as standard) and extracts were dissolved in 50% ethanol to obtain a concentration of 250 µg/mL. Absorbance was measured between 290-320 nm at an interval of 5 nm (BioTek Synergy H1 microplate reader) at room temperature, taking 50% ethanol as a blank. All determinations were done in duplicate. The SPF value was calculated using the following Mansur **Equation (11)**:

$$SPF_{sample} = CF \sum_{290}^{320} EE\ (\lambda) \times I\ (\lambda) \times A\ (\lambda) \qquad \textbf{(11)}$$

Where correction factor CF = 10; EE (λ) is the erythemogenic effect of radiation of wavelength λ; I (λ) is the intensity of solar light of wavelength λ; A (λ) is the spectrophotometric absorbance values at wavelength λ. The EE (λ)×I (λ) values are constant and were determined by Sayre *et al.* (1979) (**Table 15**).

Table 15. EE (λ)×I (λ) values of each of the wavelengths used to determine the SPF.

Wavelength (λ)	EE (λ)×I (λ)
290	0.0150
295	0.0817
300	0.2874
305	0.3278
310	0.1864
315	0.0837
320	0.0180

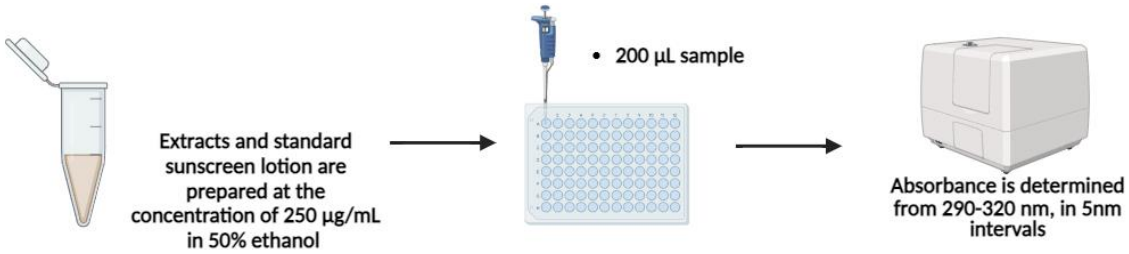


Figure 30. Procedure workflow for determination of sun protection factor of extracts (the images were obtained using the BioRender software).

3.4.6 Gas chromatography-mass spectroscopy (GC-MS) analysis

The extracts obtained using method 2 and 11, corresponding to the highest extraction yield samples were characterized by GC-MS. Before characterization by GC-MS, the extracts were purified in order to separate the components extracted from the eutectic solvents used and thus facilitate the analysis. Purification by chromatography (silica, height = 20 cm, diameter = 3 cm; chloroform:ethanol, 100:0 to 0:100; to finish ethanol:ammonia, 97:3) was carried out (**Figure 31**).

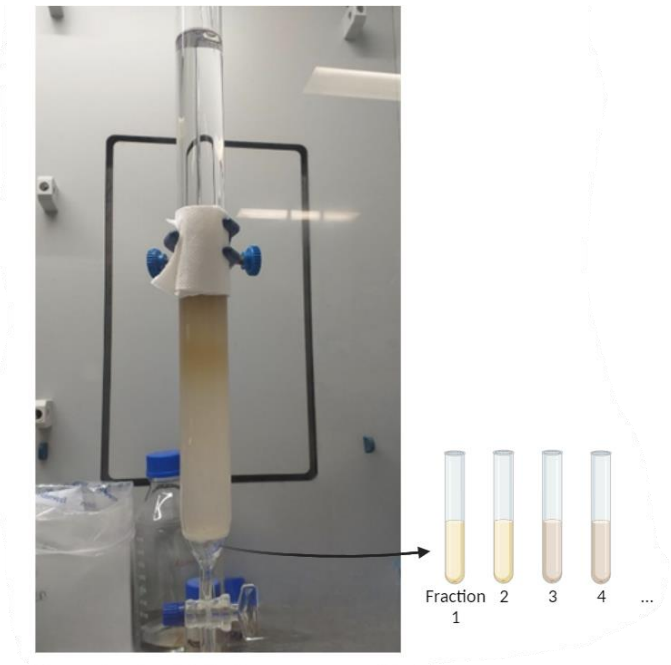


Figure 31. Chromatographic column employed in the purification of eutectic extracts before GC-MS characterization.

In the initial fractions, nonpolar chemical components such as steroids, oils, fatty acids, terpenoids, and aromatic compounds were eluted. In the intermediate fractions eluted with a high proportion of ethanol, natural deep eutectic solvent components and other polar molecules, such as alcohols and minor

acids, were found. In the final fractions, sugars and other polar molecules were recovered. Following that, the samples were derivatized through transesterification prior to GC-MS analysis. The extracts were first dissolved in pyridine to a concentration of 10 mg/mL. In a vial, 10 µL of each mixture were added to 90 µL of pyridine and 100 µL of N,O-*Bis*(trimethylsilyl)trifluoroacetamide (BSTFA). The reaction mixture was left to rest inside the oven at 60 °C for 20 minutes before being injected into the GC-MS equipment. GC-MS was carried out in a SCION SQ1/436 GC instrument (Bruker), using a Rxi-5Sil MS column (Restek; 30 m, internal diameter 0.25 mm, film thickness 0.25 µm) under the following conditions: oven temperature held at 70 °C for 1 min, followed by increments of 5.0 °C/min from 70 to 260 °C (5 min) and from 260 to 300 °C (0 min); injector and detector with temperatures of 280 and 270 °C, respectively; high purity helium C-60 (Gasin, Portugal) as the carrier gas at a constant flow rate of 1.0 mL/min; electron impact (EI) mode at 70 eV; data acquisition in full scan mode, and a 35–600 *m/z* mass range with a scan time of 250 ms. All determinations were carried out in triplicate. Identification was based on the interpretation of fragmentation patterns and supported by mass spectral data from Wiley, NIST 17 (John Wiley and Sons, Hoboken, NJ, USA) and NIST/EPA/NIH 2020 (National Institute of Standards and Technology, Gaithersburg, MD, USA) mass spectral libraries and by comparison with published spectra. The relative abundances of the compounds were calculated from the peak areas in the total ion gas chromatograms.

3.4.7 Tyrosinase inhibition assay

The tyrosinase inhibitory activity of the extracts was evaluated in this study (**Figure 32**). The extracts were first dissolved in DMSO to achieve the following concentrations: 0.005, 0.01, 0.02, 0.03, 0.04, 0.05, and 0.1 mg/mL. In a 96-well microplate, 70 µL of sample were mixed with 30 µL of tyrosinase enzyme solution (2450000 U/µL of enzyme). The microplate was incubated for 5 minutes at room temperature, following which 110 µL of 2 mM L-tyrosine solution in 50 mM potassium phosphate buffer (pH 6.5) were added. After 30 minutes, the absorbance was measured at 492 nm (BioTek Synergy H1 microplate reader). All determinations were performed in triplicate. The percentage of inhibition was calculated following **Equation (12)**:

$$\text{Inhibition } (\%) = \frac{(\text{Abs}_{\text{control}} - \text{Abs}_{\text{sample}})}{\text{Abs}_{\text{control}}} \times 100 \quad \textbf{(12)}$$

Where Abs_{sample} is the absorbance of tyrosinase enzyme solution + sample; $Abs_{control}$ is the absorbance of tyrosinase enzyme solution + DMSO.

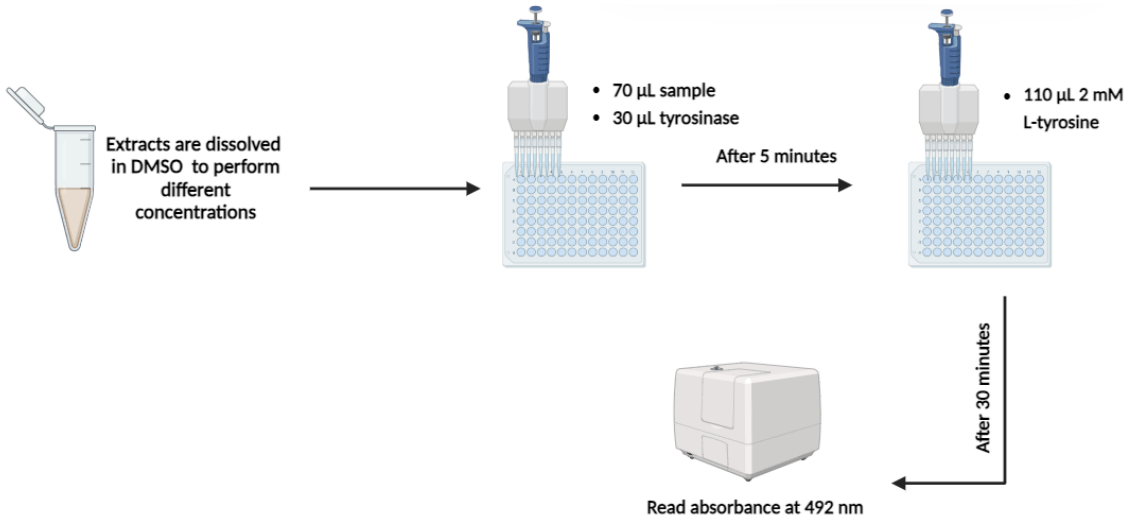


Figure 32. Procedure workflow for determination of tyrosinase inhibition (the images were obtained using the BioRender software).

4. RESULTS AND DISCUSSION

4.1 CHARACTERIZATION OF THE EXTRACTION SOLVENTS

The eutectic mixtures used in this work are presented in **Table 12**, showing the molecules acting as hydrogen bond acceptors in the first column and the hydrogen bond donors in the second column. The different combinations resulted in eutectic mixtures which are expected to work as solvents capable of extracting phenolics, terpenoids, and other compounds from the natural sources. DES offer many unique physicochemical properties such as chemical and thermal stability, no flammability, low toxicity, biodegradability, low cost, and simple preparation, which makes them interesting for applications in areas such as pharmaceuticals, foods, and cosmetics (Cunha & Fernandes, 2018; Dai et al., 2015; Duan et al., 2016).

Besides the eutectic mixtures mentioned, two hydroethanolic (HE) mixtures (HE (EtOH:H_2O) 50:50 and HE (EtOH:H_2O) 30:70) were also studied.

The physicochemical characterization of the HE and DES solvents has considered the following properties: polarity (E_{NR}), pH, viscosity (η), density (ρ), refraction index (n_D), and conductivity (σ) (**Table 16**).

Table 16. Physicochemical properties of the extraction solvents: polarity (E_{NR}), pH, viscosity (η), density (ρ), refraction index (n_D), and conductivity (σ).

Solvent	E_{NR} (kcal/mol) (λ, nm)	pH	η (Pa s)	ρ (g/cm^3)	n_D	σ (µS/cm)
HE (EtOH:H_2O) 50:50	49.98 (572)	5.82	-	0.93	1.35	2.83
HE (EtOH:H_2O) 30:70	49.64 (576)	6.26	-	0.96	1.34	1.39
DES 1 (GLY:LA 1:1)	48.54 (589)	0.90	1.01	1.24	1.46	0.90
DES 2 (GLY:LA 4:1)	74.55 (384)	1.48	1.17	1.23	1.46	0.32
DES 3 (GLY:CA 1:1)	47.73 (599)	0.15	18.19	1.44	1.48	2.78

Polarity (E_{NR}) is the ability of a solvent to dissolve chemical compounds and was determined using Nile red as a solvochromatic probe (Freitas et al., 2022). Although the solvents have high polarity values, they are very similar, except the DES 2. DES 3 is the most polar of the eutectic mixtures followed by DES

1, and DES 2. Regarding the HE solvents, HE (EtOH:H_2O) 30:70 is more polar than HE (EtOH:H_2O) 50:50. Both HES and DES 1 have polarities between ethanol (51.984 kcal/mol) and water (48.214 kcal/mol).

The pH values are in line with what was expected. DES 1 and 2 are acidic since they are composed of lactic acid, an organic acid with a low pH value. However, because DES 2 contains a higher proportion of glycerol, which has a neutral pH when compared to lactic acid, the pH of this eutectic will be higher than that of DES 1, which contains the same proportion of glycerol and lactic acid. DES 3 is the most acidic of the eutectic since it is composed of citric acid, which is a stronger acid than lactic acid.

All the DES tested present high viscosity (η) values, with DES 3 being the most viscous solvent out of the three eutectic mixtures, followed by DES 2 and, finally, DES 1. The high viscosity of these solvents is typically attributed to the presence of substantial hydrogen-bonding interactions between the components (Dai et al., 2015). This characteristic of DES can be disadvantageous because the higher the viscosity, the slower the fluid moves, reducing the efficiency of DES as extraction solvents. However, it is possible to overcome this drawback by using external forces (like stirring), diluting the solvent with water, or using higher temperatures during extraction (Dai et al., 2015).

Density (ρ) is related to the mass concentration for a given volume. All the DES tested show density values higher than water (1 g/mL) (Freitas et al., 2022). The densities of the eutectic mixtures range from 1.24 to 1.44 g/mL, with DES 3 being the densest and DES 2 the least dense. Both HES show density lower than water, which is in accordance with what was expected.

The refractive index (n_D) is generally used to identify the degree of purity of a given liquid or the concentration of certain species in a mixture. This physical parameter can vary depending on the proportion of the solvent mixture and on the temperature at which the measurement is performed (Freitas et al., 2022). Regarding the HES solvents, both showed very similar refraction indexes. Among the DES mixtures, DES 3 is the one with the highest n_D. All extraction solvents used have a refractive index higher than water (n_D = 1.333) at 25 °C (Freitas et al., 2022).

Conductivity (σ) measures the facility of an electrical charge to pass through a given material. A material is conductive when it has a very low resistance to the flow of an electric current, allowing the electrical charge to be transferred without loss of energy (Freitas et al., 2022). HE (EtOH:H_2O) 50:50 is more conductive than HE (EtOH:H_2O) 30:70. Generally, DES with higher viscosity present lower conductivity (Cunha & Fernandes, 2018). The first two eutectics show that DES 2, which is more viscous than DES 1, is less conductive than DES 1. Nevertheless, DES 3 is the most viscous eutectic and it has the highest conductivity. The conductivities of DES can increase significantly as temperature rises due to a decrease in DES viscosity.

The physicochemical properties of solvents must be studied since they vary depending on the solvent's composition, altering its use and ability to extract bioactive chemicals.

4.2 Extraction of bioactive compounds from natural sources

The extraction of bioactive compounds from natural sources was carried out using five different solvents (HE (EtOH:H_2O) 50:50, HE (EtOH:H_2O) 30:70, DES 1, DES 2, and DES 3) and three extraction procedures (mechanical impeller (MI) for 30 minutes, mechanical impeller (MI) for 90 minutes, and planetary mixer for 90 minutes). The dried plants were ground into a powder before extraction to increase the contact surface area between the plant matrix and the solvent, which may boost the extract's yield and concentration of bioactive compounds through better segregation (Awad et al., 2021). The effect of extraction techniques and solvents on extraction efficiency was assessed (**Figure 33**).

For the three procedures tested, the extraction yields obtained using hydroethanolic (HE) solvents were all quite similar. Except for cork, using HE (EtOH:H_2O) 50:50 as a solvent promoted a higher extraction yield than when using HE (EtOH:H_2O) 30:70 solvent. The highest extraction yield was obtained for the cocoa extract using method 3 (0.53 g extract/g starting material) (**Figure 33a**). The HE solvent may improve extraction efficiency by speeding mass transfer promoting the diffusion of extractable components through plant tissues. Organic solvents, as previously mentioned, are commonly utilized for bioactive extraction but are frequently very flammable and poisonous. As a result, greener solvents like DES are being utilized to replace harmful solvents. The results obtained confirm previous study reporting DES as good replacers of conventional organic solvents (Radošević et al., 2016). In general, regardless of the technique used, extraction with DES results in similar or greater yields than extraction with HE solvents. For all sources, at least one DES outperformed the HE solvents in terms of extraction yield. Because DES can give and take protons and electrons, it can create hydrogen bonds between phenolic compounds, for example, and DES molecules, enhancing their dissolving capacity and consequently extraction efficiency (Radošević et al., 2016).

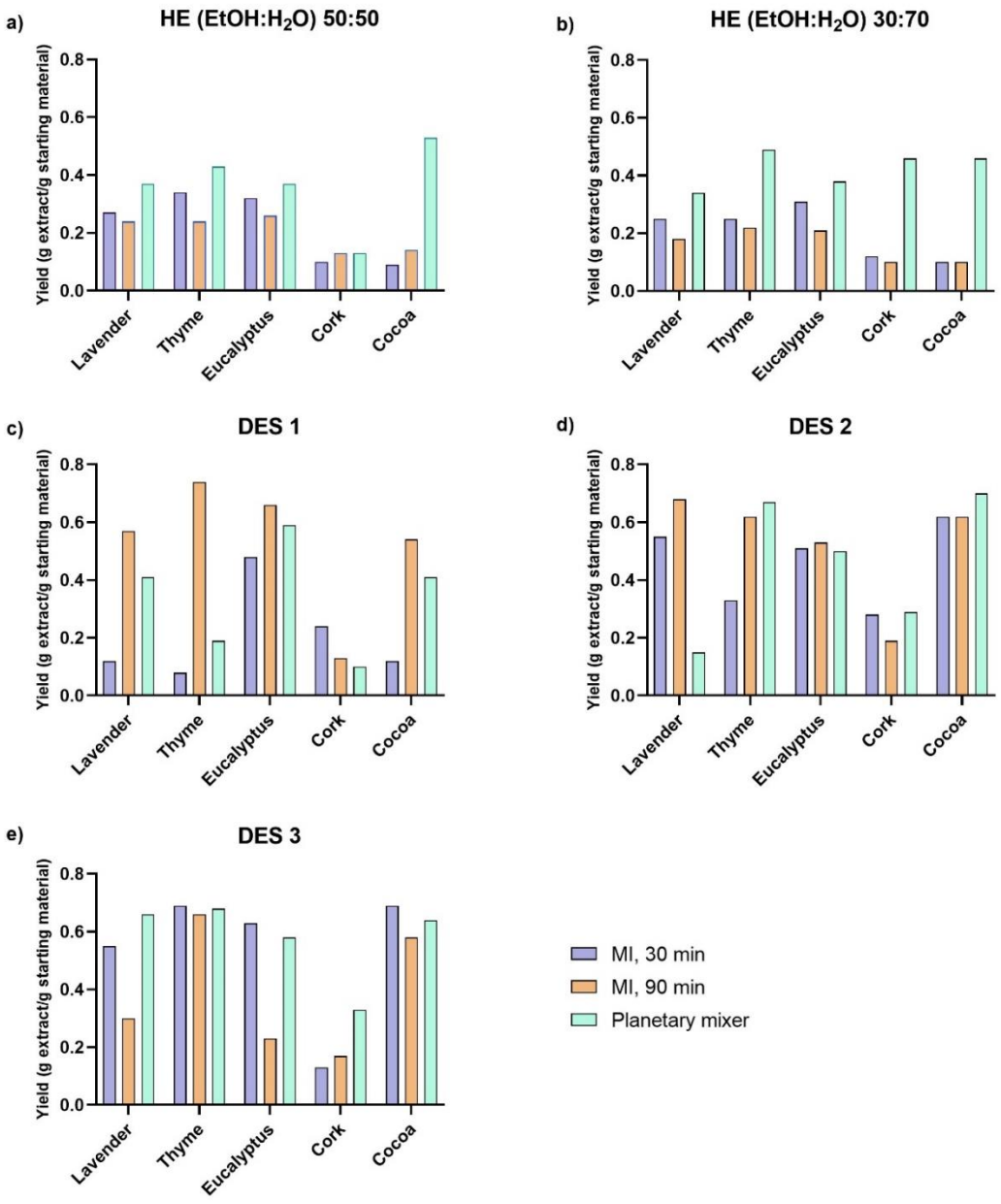


Figure 33. Extraction yield (g extract/g starting material) obtained after extraction with a mechanical impeller (MI) for 30 and 90 minutes and a planetary mixer using **a)** HE (EtOH:H_2O) 50:50 solvent **b)** HE (EtOH:H_2O) 30:70 solvent **c)** deep eutectic solvent (DES) 1 **d)** DES 2 **e)** DES 3.

DES 3 as a solvent shows, in many cases, superior extraction ability compared to DES 1 and DES 2. Although the three DES are viscous, this may not affect extraction capacity because the procedures involved the use of high temperatures (70 °C for MI and 50 °C for planetary mixer), which speeds up the dissolution process and has been shown to be an efficient way to reduce solvent viscosity (Dai et al., 2015).

Analysing the efficacy of the extraction methods tested, the higher extraction levels were obtained when using the planetary mixer for 90 minutes, followed by the MI for 90 minutes and, finally, by the MI

for 30 minutes. The planetary mixer uses planetary rotation, in which the vial rotates around its own axes while also orbiting around a central point. This movement generates high forces within the sample material, allowing bioactive compounds to be released. The planetary mixer offers the advantages of employing less quantity of natural sources, having a short extraction duration, and being versatile and simple to use. When using the MI for extraction, the results reveal that longer periods of incubation display the higher extraction yields.

Considering all the natural sources tested, the highest extraction yield was obtained for thyme, using method 8 (0.74 g extract/g starting material) (**Figure 33c**). Regardless the solvent or the extraction procedure, and contrarily to reported by Freitas *et al.* (2022), cork was the source which displayed the lowest extraction yield (0.10 g extract/g starting material). We believe that this data resulted from errors made during the extraction procedure.

4.3 CHARACTERIZATION OF NATURAL EXTRACTS

4.3.1. Total phenolic content (TPC)

Phenolic compounds are a wide class of secondary metabolites renowned for their antioxidant properties. The extracts' total phenolic content was determined in gallic acid equivalents (GAE) and is presented in **Figure 34**.

The results reveal that the TPC varied significantly depending on the solvent used for the extraction. The TPC measured is significantly low on extracts obtained using eutectic solvents when compared to extracts when hydroethanolic solvents were used in the extraction process. It is important to note that since the eutectic solvent was not taken out, it is still present in the extracts produced using these solvents. This means that part of the extract is eutectic, while other is sample. From the results it is inferred that these extracts have a TPC that is 10 times smaller because there is 10 times less sample in them than in HE extracts.

TPC values from extracts obtained using HE solvents range from 41.90 ± 3.49 to 362.10 ± 19.75 mg GAE/g extract for the HE (EtOH:H_2O) 50:50 solvent and 54.98 ± 0.09 to 345.24 ± 2.91 mg GAE/g extract for the HE (EtOH:H_2O) 30:70 solvent. The lowest total phenolic content was obtained for lavender using method 3 (41.90 ± 3.49 mg GAE/g extract) (**Figure 34a**), while the highest TPC appeared in cork with method 1 (362.10 ± 19.75 mg GAE/g extract) (**Figure 34a**). This is in line with other studies

reporting that the TPC in various extracts of Portuguese *Quercus suber* L. was 200-350 mg GAE/g extract (S. A. O. Santos et al., 2010).

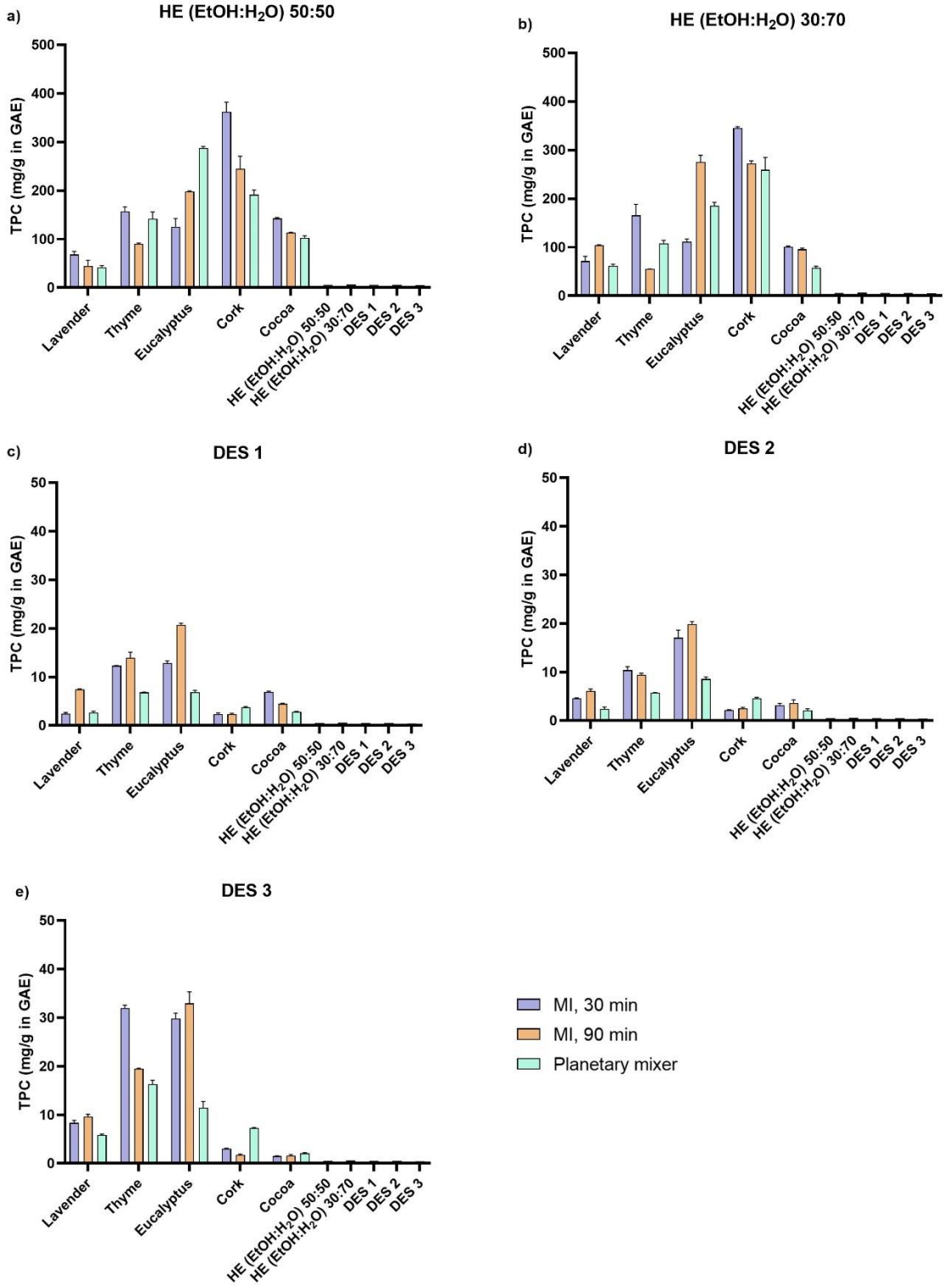


Figure 34. Total phenolic content (TPC) in the extracts presented as gallic acid equivalents (GAE) **a)** extracts obtained by extraction with HE (EtOH:H_2O) 50:50 solvent **b)** HE (EtOH:H_2O) 30:70 solvent **c)** deep eutectic solvent (DES) 1 **d)** DES 2 **e)** DES 3. Data is expressed as mean ± SD.

Analysing the role of the eutectic mixtures as extraction solvents, TPC values range from 2.41 ± 0.23 to 20.81 ± 0.33 mg GAE/g extract for samples extracted with DES 1, 2.05 ± 0.35 to 19.88 ± 0.53 mg GAE/g extract for samples extracted with DES 2, and 1.51 ± 0.06 to 33.36 ± 1.68 mg GAE/g extract for samples extracted with DES 3. The lowest total phenolic content was obtained for cocoa extracted with method 13 (1.51 ± 0.06 mg GAE/g extract) (**Figure 34e**), while the highest TPC appeared in eucalyptus extracted with method 14 (33.36 ± 1.68 mg GAE/g extract)(**Figure 34e**). In general, eucalyptus and thyme showed high phenolic content. These values are lower than those previously reported of 58.1 mg GAE/g extract for *Eucalyptus citriodora* (Idris et al., 2021).

The dissolution of bioactive compounds is strongly related to the polarity of the solvent used. Phenolic compounds are generally polar, making the use of more polar solvents the most efficient way to proceed for their extraction. Water has been used along with ethanol to create a more polar mixture, increasing the interactions and hydrogen bonding with polar functional groups, resulting in higher extraction yields of polar compounds (Kaur & Ubeyitogullari, 2023).

The lower TPC obtained could also be due to an insufficient amount of the Folin-Ciocalteu reagent in the reaction medium. Additionally, the eutectic solvents have a very low pH value, whereas the Folin-Ciocalteu method makes use of a reaction that happens in an alkaline medium. The reaction of dissociation of a phenolic proton that results in the formation of phenolate ion, which is responsible for reducing the Folin-Ciocalteu reagent, may not be fully maximized due to the excessive acidity of the solvents, and as a result, the blue color does not fully develop. To overcome this issue, the eutectic samples should be alkalinized before the application of the method.

Regarding the extraction methods tested, extracts obtained using the MI for 30 and 90 minutes showed the highest TPC values in most cases.

The Folin-Ciocalteu assay is a well-known, simple, and rapid method but presents the limitation of not being specific to phenolics, which can lead to biased results.

4.3.2 Total flavonoid content (TFC)

Flavonoids are one of the major types of polyphenols with powerful antioxidant, anti-inflammatory, and antimicrobial properties. The total flavonoid content on extracts obtained using the different extraction solvents was determined and presented as quercetin equivalents (QE) (**Figure 35**).

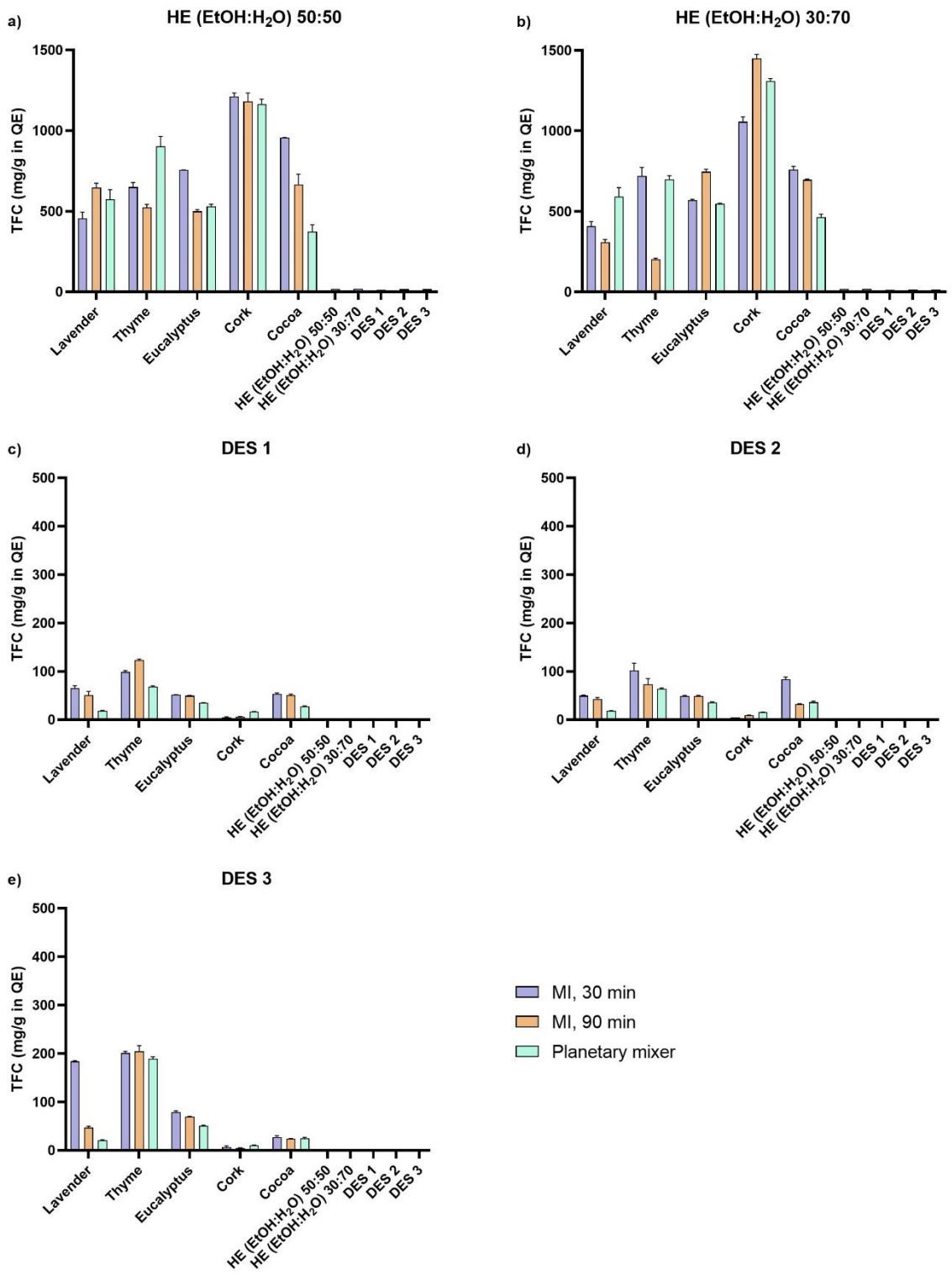


Figure 35. Total flavonoid content (TFC) in the extracts presented as quercetin equivalents (QE) **a)** extracts obtained by extraction with HE (EtOH:H_2O) 50:50 solvent **b)** HE (EtOH:H_2O) 30:70 solvent **c)** deep eutectic solvent (DES) 1 **d)** DES 2 **e)** DES 3. Data is expressed as mean ± SD.

The results show that, similarly to the TPC, the TFC differed significantly depending on the extraction solvent. The TFC measured on the extracts extracted with eutectic solvents was significantly low when

compared with extracts obtained using HE solvents. Alike what happened in the TPC assessments, the eutectic solvent was not taken out, it is still present in the extracts produced using these solvents. This means that part of the extract is eutectic, while other is sample. From the results it is inferred that these extracts have a TFC that is 10 times smaller because there is 10 times less sample in them than in HE extracts.

TFC values from extracts obtained with HE solvents range from 371.78 ± 44.46 to 1214.21 ± 28.74 mg QE/g extract using HE (EtOH:H_2O) 50:50 solvent and 203.44 ± 5.51 to 1481.5 ± 55.60 mg QE/g extract using HE (EtOH:H_2O) 30:70 solvent. The lowest total flavonoid content was obtained for thyme extracted with method 5 (203.44 ± 5.51 mg QE/g extract) (**Figure 35b**), while the highest TFC appeared in cork extracted with method 5 (1481.5 ± 55.60 mg QE/g extract) (**Figure 35b**). In fact, the cork extracted with the HE solvents stood out for its flavonoid content. These TFC values are substantially higher than those reported, where the total flavonoid content obtained for Algerian *Quercus suber* L. extracted with methanol:water solvent was 49.00 ± 2.00 mg QE/g extract (Touati et al., 2015).

Regarding the role of eutectic mixtures as solvents, TFC values range from 5.89 ± 0.82 to 123.22 ± 1.72 mg QE/g extract using DES 1, 5.36 ± 0.11 to 101.67 ± 15.33 mg QE/g extract using DES 2, and 4.81 ± 1.12 to 203.97 ± 11.74 mg QE/g extract using DES 3. The lowest total flavonoid content was obtained for cork extracted with method 13 (4.81 ± 1.12 mg QE/g extract) (**Figure 35e**), while the highest TFC was seen for thyme extracted with method 14 (203.97 ± 11.74 mg QE/g extract) (**Figure 35e**). Even though the eutectic extracts present lower TFC when compared to the hydroethanolic, these TFC values for thyme are substantially higher than those that have been reported, in which the TFC of the methanolic extract of Iranian *Thymus vulgaris* L. was 3.87 mg QE/g extract (Mokhtari et al., 2023).

Additionally, the eutectic solvents have a very low pH value and, similarly to what happened in the TPC assay, because of their extreme acidity, the reaction efficiency might not be maximized, and the color is not fully developed.

Regarding the extraction methods tested, extracts obtained using the MI for 30 minutes showed the highest TFC values in most cases, followed by the MI for 90 minutes, and the planetary mixer, following the same tendency as the TPC content.

It is possible to note that the content of total flavonoids is higher than the content of total phenolics. This may be due to lower extractability of some phenolic compounds, for example, phenolic acids. It is also possible that the natural sources have been stored for some time and some phenolic compounds that otherwise would have contributed to the TPC have been lost or transformed (Sasikumar et al., 2020).

The aluminium chloride assay is a rapid, simple, and cheap method to assess flavonoid content.

4.3.3 Antioxidant activity

The antioxidant activity of the extracts is a key factor to consider when assessing its potential application in cosmetic products. Because there is no uniform approach, a sample's antioxidant capacity should be evaluated using more than one type of antioxidant assay. As a result, the antioxidant activities of the various extracts in this study were assessed using four tests.

4.3.3.1 DPPH radical scavenging assay

The antioxidant activity of the extracts was determined using the DPPH radical scavenging assay (**Figure 36**). The results are expressed as EC_{50} (mg/mL) which is the concentration of the sample required to capture 50% of DPPH radicals. The lower the EC_{50} value, the stronger the scavenging activity. Trolox is used herein as a standard.

It has been demonstrated that there is a strong correlation between antioxidant capacity and total phenolic content of a sample, implying that extracts with the greatest TPC values have greater DPPH scavenging capabilities. The ability of phenolic compounds to serve as reducing agents, hydrogen donors, and/or singlet oxygen quenchers is related to their antioxidant capability (Sasikumar et al., 2020).

This correlation is consistent with the TPC results obtained from the HE extractions (**Figure 34**), in which eucalyptus and cork were the extracts that presented higher TPC and also the extracts that presented lower EC_{50} (EC_{50} values ranging from 0.55 ± 0.01 to 1.05 ± 0.06 mg/mL for eucalyptus and 0.35 ± 0.006 to 0.58 ± 0.009 mg/mL for cork) (**Figures 36c** and **36d**).

When using the eutectics as solvents, this tendency is less noted as the cocoa extracts displayed the highest DPPH scavenging activity (EC_{50} values ranging from 2.12 ± 0.14 to 3.81 ± 0.17 for DES 1 and 1.77 ± 0.07 to 1.91 ± 0.16 for DES 2) (**Figure 36e**) even though this extract did not show high phenolic content. Eucalyptus extracted with DES 3 showed the lowest EC_{50} (EC_{50} values ranging from 1.27 ± 0.054 to 3.03 ± 0.29) (**Figure 36c**), which goes in accordance with its high phenolic content in this solvent.

The antioxidant activity may not always be directly relatable with the content of phenolic compounds in the sample due to other compounds in the extracted mixture that can interfere with both quantification methods (Sasikumar et al., 2020). In this scenario, the eutectic solvent may be interfering with the quantification procedures because the correlation is weaker in these extracts.

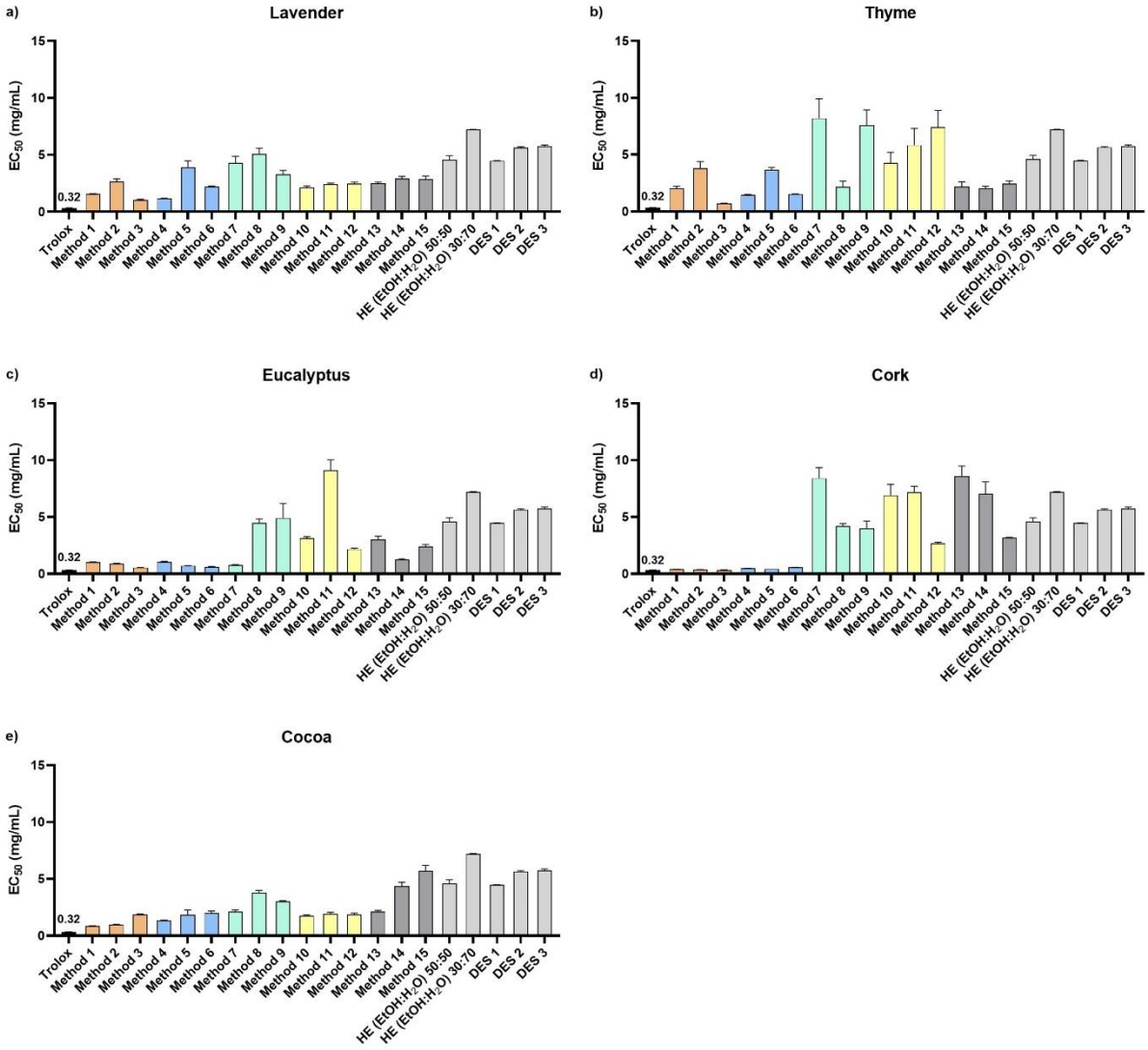


Figure 36. The EC_{50} values of all natural extracts extracted with a mechanical impeller (MI) for 30 and 90 minutes and a planetary mixer using HE (EtOH:H_2O) 50:50 and 30:70, and deep eutectic solvents (DES) 1, 2 and 3, by DPPH assay. Trolox was used as reference and the samples containing only the solvents were evaluated to infer the role of the matrix. Data is expressed as mean ± SD.

Regarding the extraction method, both the MI for 30 minutes and the planetary mixer for 90 minutes represent good methods for extracting bioactive compounds from natural sources. The lowest EC_{50} values were obtained when using the MI for 90 minutes as extraction procedure.

4.3.3.2 ABTS radical scavenging assay

The antioxidant activity of all extracts was determined using the ABTS radical scavenging assay (**Figure 37**). The results are expressed as EC_{50} (mg/mL) which is the concentration of extract required

to capture ABTS radicals in an extent of 50%. The lower the EC_{50} value, the stronger the scavenging activity. Trolox is used as a standard.

All extracts obtained using HE solvent exhibited very low EC_{50} values. The most active extracts were, similarly to DPPH results, eucalyptus and cork with EC_{50} values ranging from 33.93 ± 0.18 to 49.93 ± 0.003 mg/mL for eucalyptus and 28.84 ± 0.13 to 42.96 ± 0.46 mg/mL for cork (**Figures 37c** and **37d**). These extracts have an antioxidant activity quite similar to the Trolox standard in terms of EC_{50}.

As stated before, a strong relationship between antioxidant capability and the total phenolic content of the sample has been reported. These results go in accordance with the TPC results obtained for the HE extractions (**Figure 34**), in which cork and eucalyptus were the extracts that presented higher TPC and also the extracts that presented lower EC_{50}.

When eutectic solvents are used for extraction, eucalyptus presented once again the best antioxidant activity (EC_{50} values ranging from 155.84 ± 2.90 to 477.62 ± 31.02 mg/mL using DES 1, 125.41 ± 2.83 to 251.76 ± 14.76 mg/mL using DES 2, and 98.89 ± 1.66 to 381.37 ± 9.58 mg/mL using DES 3) (**Figure 37c**). These findings are consistent with the TPC data, where eucalyptus exhibited the greatest total phenolic content (TPC) among the eutectic extracts (**Figure 34**). Hence, the presence of phenolic components in plant extracts plays a substantial role in enhancing their antioxidant capacity. Regarding the extraction methods employed, it can be observed that the three methods yielded comparable outcomes, with no method exhibiting significant superiority over the others.

According to Zárate *et al.* (2020), the ABTS approach is regarded as more sensitive in comparison to the DPPH method due to its ability to neutralize the ABTS radical by the transfer of a hydrogen atom or an electron. Moreover, the ABTS assay exhibits reduced susceptibility to color interference arising from samples, which can be attributed to the utilization of a higher wavelength (734 nm) (Rumpf et al., 2023).

The ABTS scavenging assay is a cost-effective and straightforward technique. The ABTS test requires a longer duration compared to the DPPH assay due to the necessity of generating the ABTS radical, which may take up to 16 hours.

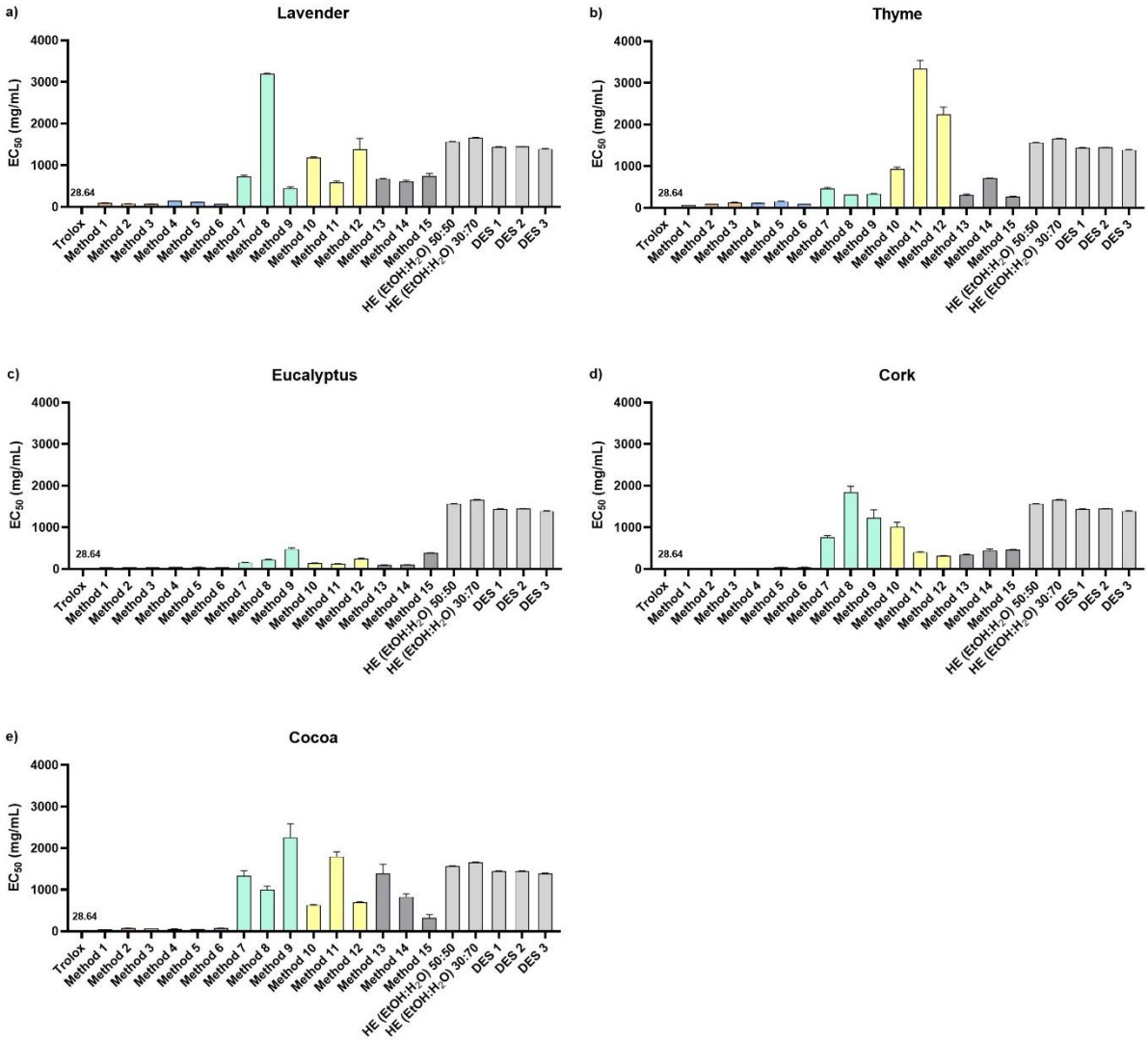


Figure 37. The EC_{50} values of all natural extracts extracted with a mechanical impeller (MI) for 30 and 90 minutes and a planetary mixer using HE (EtOH:H_2O) 50:50 and 30:70, and deep eutectic solvents (DES) 1, 2 and 3, by ABTS assay. Trolox was used as reference and the samples containing only the solvents were evaluated to infer the role of the matrix. Data is expressed as mean ± SD.

4.3.3.3 Ferric ion reducing antioxidant power (FRAP) assay

Antioxidants have the ability to stabilize free radicals through the process of electron donation. The method underlying this particular assay includes the utilization of transition metals, specifically iron, and relies on their reduction potential. The ferric ion reducing antioxidant power assay was employed to measure the antioxidant activity of all extracts (**Figure 38**). The findings are presented in terms of Trolox equivalents (TE) per gram of dry weight sample (mg TE/g extract).

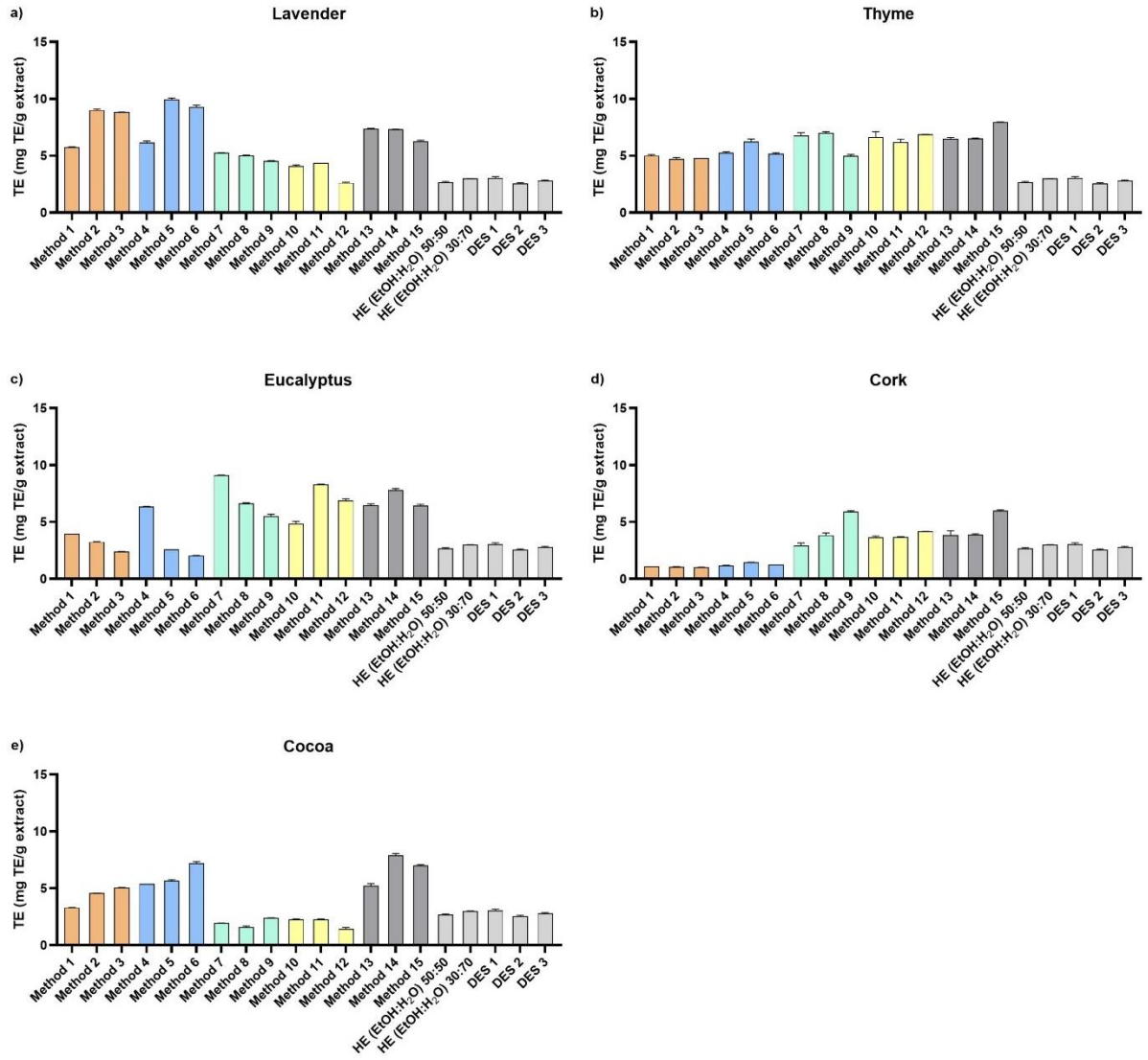


Figure 38. Ferric ion reducing antioxidant power (FRAP) of all natural extracts extracted with a mechanical impeller (MI) for 30 and 90 minutes and a planetary mixer using HE (EtOH:H_2O) 50:50 and 30:70 solvent, and deep eutectic solvents (DES) 1, 2 and 3. Trolox was used as reference and the samples containing only the solvents were evaluated to infer the role of the matric. Data is expressed as mean ± SD.

There exists a known association between the ferric reducing power and the total phenolic content of a given sample. Specifically, extracts with elevated total phenolic content values demonstrate correspondingly greater levels of ferric reducing activities. The phenolic compounds may exert their action due to the presence of hydroxyl groups that can serve as electron donors. Moreover, the reducing capacity of numerous substances has been directly correlated with their antioxidant capabilities (Sasikumar et al., 2020).

The extracts obtained using HE solvents presented variable values of TE. The most active extract was lavender with values ranging from 5.77 ± 0.014 to 9.00 ± 0.10 mg TE/g extract using HE (EtOH:H_2O) 50:50 and 6.15 ± 0.14 to 9.96 ± 0.11 mg TE/g extract using HE (EtOH:H_2O) 30:70 (**Figure 38a**).

Although lavender extract does not possess the highest phenolic content among the extracts studied, it has the highest ferric reducing power. Regarding the extractions using eutectic solvents, eucalyptus provided the strongest reducing capacity for DES 1 and 2 (values ranging from 5.52 ± 0.16 to 9.12 ± 0.013 mg TE/g extract for DES 1 and 4.88 ± 0.17 to 8.29 ± 0.04 mg TE/g extract for DES 2) (**Figure 38c**). The results indicate that lavender extract had the highest efficacy among the tested extracts with DES 3, with a range of 6.29 ± 0.07 to 7.37 ± 0.05 mg TE/g extract (**Figure 38a**). The findings related to eucalyptus align with the total phenolic content of the extract, as depicted in **Figure 34**. In general, DES 3 has been found to extract compounds that exhibit a high degree of reducing power. Additionally, it has been observed that DES 3 is the eutectic solvent with the highest ability to extract the highest TPC. Regarding the extraction methods employed, it can be observed that the three procedures yielded comparable outcomes, with no one method exhibiting superiority over the others.

The FRAP assay is a cost-effective and straightforward technique. Moreover, the process of preparing the working solution is time-consuming.

4.3.3.4 Ferric chelating activity assay

Transition metals, such as iron, have the ability to generate free radicals, which can lead to the development of diseases that are linked to oxidative stress. The process of chelation involving transition metals represents a potential mechanism by which antioxidants can effectively remove these deleterious substances. The chelating capacity of all extracts to Fe^{2+} was assessed using the ferrous iron-ferrozine complex technique (**Figure 39**). The outcomes are shown in terms of EC_{50} (mg/mL), which is the concentration of the sample needed to chelate 50% of the ferrous iron. A stronger antioxidant power is indicated by a lower EC_{50} value. EDTA serves as a commonly employed standard.

The extracts demonstrate a lack of substantial ferric chelating activity in comparison to the standard EDTA, despite the utilization of high quantities of the extract (10 mg/mL). The EC_{50} value for EDTA is 20.62 ± 0.17 mg/mL. The cocoa extract obtained by method 2 exhibited the lowest EC_{50} value (830.92 ± 103.52 mg/mL) (**Figure 39e**). This value was found to be more 40-fold greater than that of the EDTA standard. Although a correlation has been found between phenolic chemicals and ferric chelating activity, the extracts under investigation do not exhibit any ferric chelating activity.

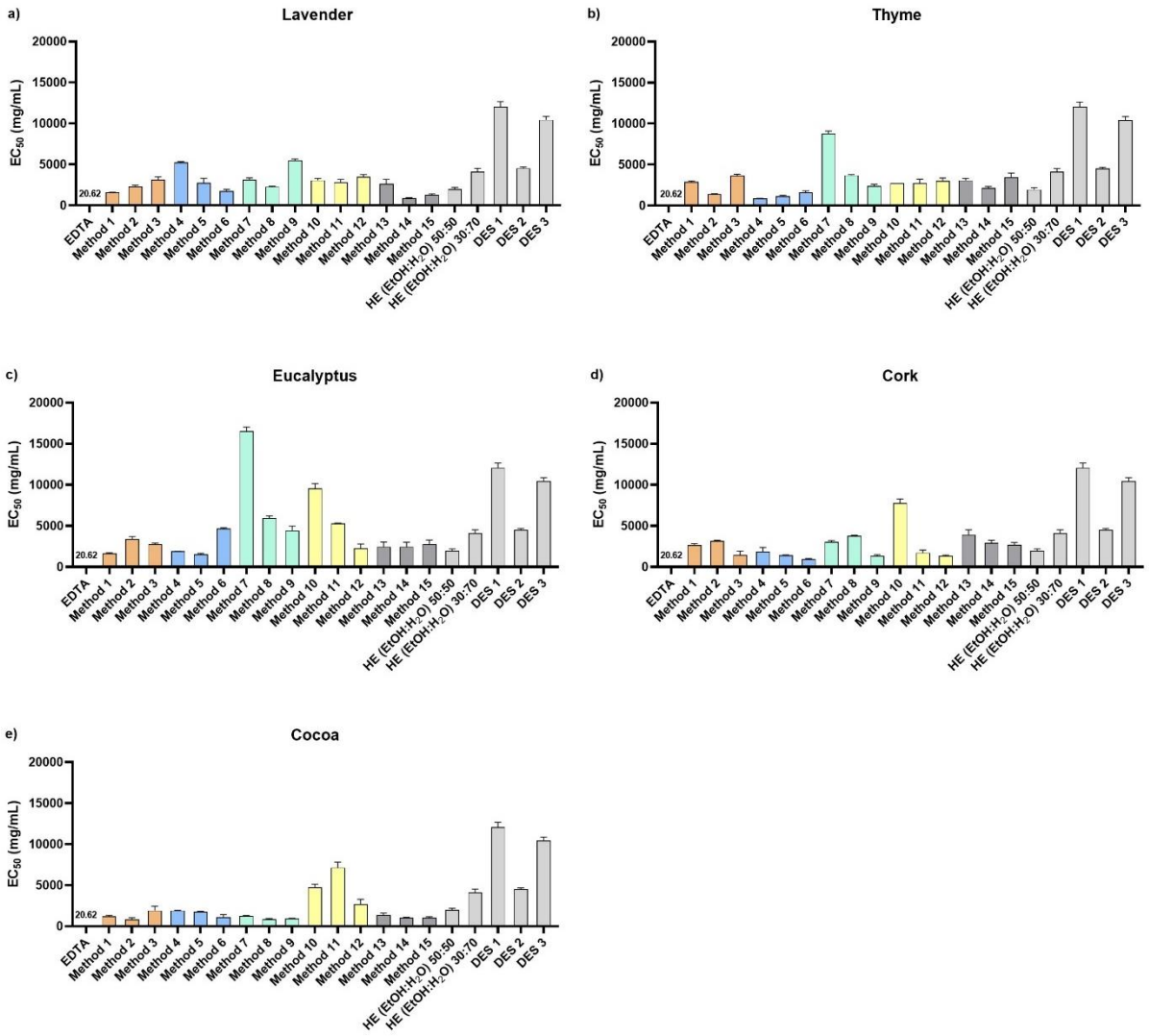


Figure 39. The EC_{50} values of all natural extracts extracted with a mechanical impeller (MI) for 30 and 90 minutes and a planetary mixer using HE (EtOH:H_2O) 50:50 and 30:70, and deep eutectic solvents (DES) 1,2 and 3, by ferric chelating activity assay. EDTA was used as reference and the samples containing only the solvents were evaluated to infer the role of the matrix. Data is expressed as mean ± SD.

The assessment of antioxidant capacity in a biological sample cannot be accurately determined by a single experiment due to the omission of various criteria. Potential interferences within reaction mixtures can lead to the potential for either underestimation or overestimation. Moreover, it has been observed that the outcomes of multiple assays conducted on a single extract can exhibit substantial variations. Hence, it is imperative to employ diverse methodologies for the assessment of overall antioxidant capability. The selection of a methodology will be contingent upon various aspects such as cost, reagent accessibility, complexity, and length of the procedure.

4.3.4 Determination of antimicrobial activity

4.3.4.1 Minimum inhibitory concentrations (MICs) and minimum bactericidal concentrations (MBCs)

Bioactive substances frequently exhibit antimicrobial properties, a characteristic of significant relevance in the field of cosmetics due to their potential to mitigate the occurrence of skin infections. The study investigated the antibacterial activity of extracts prepared using method 1. The strains of bacteria tested included Gram-positive bacteria such as *Staphylococcus aureus* and *Staphylococcus epidermidis*, as well as Gram-negative bacteria including *Escherichia coli* and *Pseudomonas aeruginosa*. **Table 17** displays the acquired minimum inhibitory concentrations (MICs) and minimum bactericidal concentrations (MBCs) of the chosen extracts for every bacterial strain.

Table 17. Minimum inhibitory concentrations (MICs) and Minimum bactericidal concentrations (MBCs) (mg/mL) of selected hydroethanolic extracts against Gram-positive and Gram-negative bacteria.

Bacteria	Lavender		Thyme		Eucalyptus		Cork		Cocoa	
	MIC (mg/mL)	MBC (mg/mL)	MIC	MBC	MIC	MBC	MIC	MBC	MIC	MBC
S. aureus	-	-	5.12	5.12	5.12	5.12	5.12	5.12	-	-
S. epidermidis	-	-	-	-	-	-	5.12	5.12	-	-
E. coli	-	-	-	-	-	-	-	-	-	-
P. aeruginosa	-	-	-	-	-	-	2.56	5.12	-	-

The lavender and cocoa extracts exhibited no activity against any of the bacterial strains. Among the bacteria that were subjected to testing, it was observed that *S. aureus* exhibited the highest susceptibility to the antimicrobial capabilities of the extracts derived from thyme, eucalyptus, and cork, as evidenced by the manifestation of both MIC and MBC effects. The observed phenomenon can be attributed to the distinctive composition of the cell wall of Gram-positive bacteria, which facilitates the efficient infiltration of hydrophobic molecules into the cellular interior, enabling their interaction with both the cell wall and the cytoplasm (Nazzaro et al., 2013). Nevertheless, this observation appears to be of minor significance as no other substance, except from cork, has demonstrated inhibitory effects on *S. epidermidis*, a Gram-positive bacterium. Furthermore, cork exhibited inhibitory effects against *Pseudomonas aeruginosa*, a Gram-negative bacterium. The potential explanation for the strong antimicrobial properties exhibited by cork could be attributed to its significant phenolic content (**Figure 34**), which is recognized for its

antibacterial properties. The antibacterial effects of phenolic-rich extracts may be attributed to various potential modes of action. The hydroxyl groups possess the ability to establish hydrogen bonds with the proteins present in the bacterial membrane, so inducing alterations in the membrane's permeability and resulting in the demise of the bacterial cell. Additionally, these pathogens have the capability to infiltrate bacterial cells, leading to the coagulation of their internal components (Touati et al., 2015). Previously, Algerian *Quercus suber* L. has been reported for its antibacterial activity on *S. aureus* and *P. aeruginosa* (Touati et al., 2015).

4.3.4.2 Agar-well diffusion method

The antimicrobial activity was studied on the extracts obtained using method 8 and 11 against Gram-positive, *S. aureus* and *S. epidermidis* strains and Gram-negative, *E. coli* strain bacteria using the agar-well diffusion method. The zones of inhibition of the selected extracts for each bacteria are shown in **Table 18**.

Table 18. Zones of inhibition (mm) of selected extracts against Gram-positive and Gram-negative bacteria.

Extract	DES	Bacteria		
		S. aureus (mm)	*S. epidermidis* (mm)	*E. coli* (mm)
DES (Control)	1	6.0	6.0	10.7
	2	6.0	6.0	8.0
Lavender	1	6.0	6.0	10.7
	2	6.0	6.0	8.0
Eucalyptus	1	11.7	11.0	10.0
	2	9.7	9.0	21.7
Thyme	1	8.3	7.0	11.0
	2	8.0	6.0	11.0
Cork	1	9.0	9.0	12.0
	2	8.3	10.0	20.3

The various extracts exhibited varying levels of antibacterial efficacy against the microorganisms that were subjected to testing. The antibacterial activity observed in lavender is not attributed to the lavender itself, but rather to the presence of DES which possesses its own antimicrobial properties. Similarly, a comparable outcome is shown for thyme in DES 2 when tested against *S. epidermidis*, as well as for eucalyptus in DES 1 when evaluated against *E. coli*. The previously documented literature has already presented findings on the antibacterial efficacy of DES, namely those derived from organic acids (Swebocki et al., 2023).

Regarding the remaining extracts, it is observed that there is a notable expansion in the zone of inhibition specifically for DES 1 and DES 2 when exposed solely to the extracts dissolved in these solvents. This suggests that the enhanced antimicrobial activity can be attributed to the presence of bioactive chemicals within each extract. From the three natural extracts tested, eucalyptus showed the highest antimicrobial activity. These results can be explained by the different compounds present in each plant, being that eucalyptus is rich in phenolic compounds (**Figure 34**) which have been shown to possess antimicrobial activity (Touati et al., 2015). In addition to eucalyptus, cork also exhibited inhibitory effects, particularly against *E.coli*, a finding that could not be confirmed in the previous investigation (**Table 17**). It is noteworthy to observe that both of these extracts exhibit significant antibacterial efficacy against Gram-negative bacteria, which, owing to its structural characteristics, presents more resistance to penetration.

4.3.5 Sun Protection Factor (SPF)

Exposure to ultraviolet (UV) light leads to a variety of skin alterations, such as photoaging and other irregularities, which can be attributed to intracellular DNA damage. Hence, protecting against UV radiation is an essential attribute of natural extracts utilized in cosmetic applications. The evaluation of UV protection for several natural extracts was conducted and is depicted in **Figure 40**. The findings are presented in the form of Sun Protection Factor (SPF), which serves as a quantitative assessment of the potency and efficiency of the natural extracts. The greater the numerical value assigned to the SPF, the greater the level of protection provided against harmful UV radiation. The standard sunscreen lotion utilized in this study was Darphin® Soleil SPF 50, a commercially available product. The components that have been extensively researched for their photoprotective effects include phenolic compounds, namely flavonoids. The photoprotective activity of flavonoids against UV radiation can be attributed to their chemical structure, which is characterized by the presence of double bonds in their aromatic rings. Phenols are believed to possess the ability to limit DNA damage by intervening in redox-sensitive signalling cascades and reducing the production of oxygen-free radicals and lipid peroxidation generated by UV radiation (Ebrahimzadeh et al., 2014; Li et al., 2023).

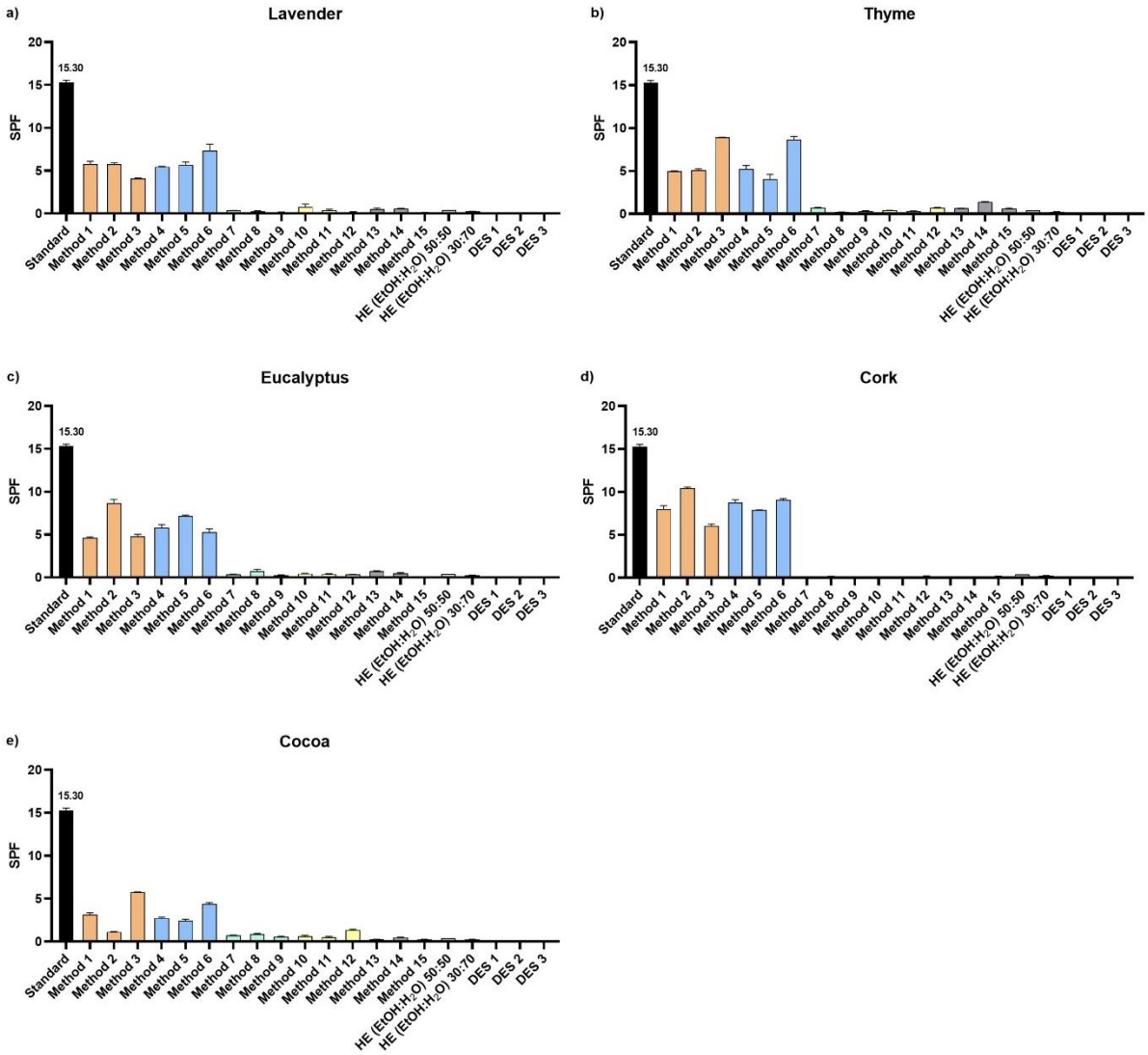


Figure 40. Sun protection factor (SPF) values of all natural extracts extracted with a mechanical impeller (MI) for 30 and 90 minutes and a planetary mixer using HE (EtOH:H_2O) 50:50 and 30:70, and deep eutectic solvent (DES) 1,2 and 3. Sunscreen lotion Darphin® Soleil SPF 50 was used as standard and the samples containing only the solvents were evaluated to infer the role of the matrix. Data is expressed as mean ± SD.

The extracted samples demonstrated SPF values that were comparable to the established benchmark. The cork extract had the highest SPF values, ranging from 6.03 ± 0.23 to 10.43 ± 0.12 for the HE (EtOH:H_2O) 50:50 formulation and from 7.87 ± 0.04 to 9.08 ± 0.15 for the HE (EtOH:H_2O) 30:70 formulation (**Figure 40d**). Thyme and eucalyptus were the other two extracts that exhibited noteworthy photoprotective efficacy subsequent to cork (Figures **40b** and **40c**). The findings align with the TPC results acquired (**Figure 34**), wherein the cork extract exhibited the highest total phenolic content (TPC) in both hydroethanolic (HE) solvents. Eucalyptus and thyme exhibited elevated TPC levels. The results obtained from the total flavonoid content (TFC) analysis, as shown in **Figure 35**, indicate that the cork

extract exhibited the highest TFC in both HE solvents. These findings are consistent with the sun protection factor values. Furthermore, it can be observed that the hydroethanolic extracts exhibited comparatively more potent antioxidant properties, as depicted in **Figures 36** and **37**.

The SPF values of all eutectic extracts were observed to be significantly low, with the majority of cases failing to surpass an SPF value of 1. The obtained results are consistent with the expected results, as the SPF value is directly associated with the quantity of phenols and flavonoids. As depicted in Figures **34** and **35**, the concentration of phenolics and flavonoids in DES is relatively minimal. To achieve enhanced photoprotection, it is imperative to utilize eutectic extracts at significantly elevated quantities inside the cosmetic formulation.

In relation to the extraction methods employed, the derived values exhibited a high degree of similarity, with no method demonstrating a notable distinction. For a long time, tests that are conducted on human volunteers have been used to evaluate the effectiveness of sunscreen (Ebrahimzadeh et al., 2014). This *in vitro* SPF assessment assay is useful for screening tests during product development since it is simple, rapid, and cheap.

4.3.6 Identification of extracts' volatile compounds by gas chromatography-mass spectrometry (GC-MS)

The identification and isolation of bioactive compounds present in plant extracts pose challenges due to their varying polarities. The utilization of gas chromatography-mass spectrometry (GC-MS) enables both qualitative and quantitative analysis of the samples. The composition of the extracts obtained using method 2 and 11 was determined using the GC-MS technique (**Figures 41** and **42**). The analysis of the extracts was hindered by the presence of eutectic. Consequently, the technique of column chromatography was employed to achieve the separation of the various components based on their respective families of compounds.

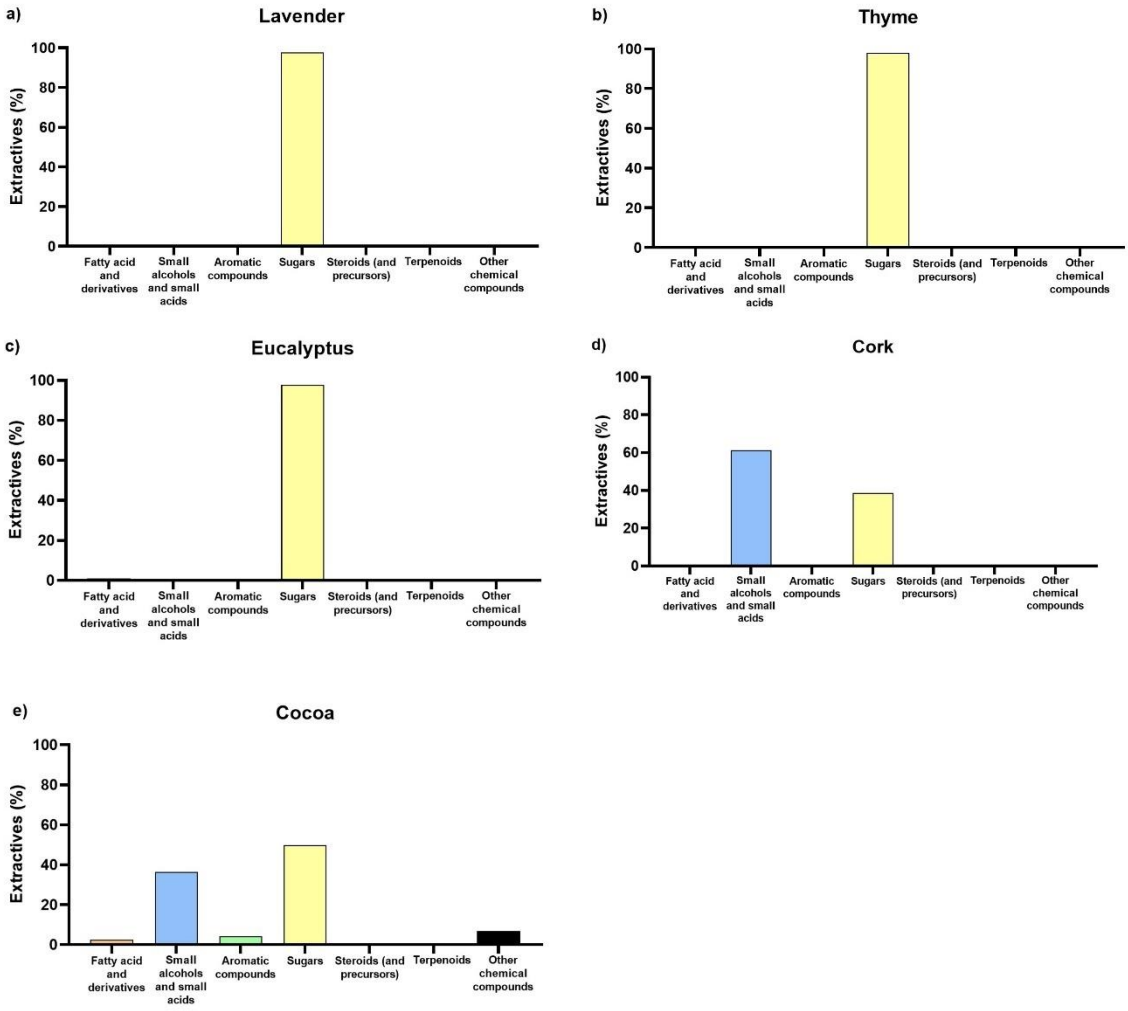


Figure 41. Gas chromatography-mass spectroscopy (GC-MS) analysis of the extracts obtained using method 2.

Differences in the content of the extracts can be observed when employing HE (EtOH:H_2O 50:50) and DES 2 as solvents. Sugars were shown to be the predominant class of chemicals in lavender, thyme, and eucalyptus when using the HE solvent (**Figure 41**). Regarding cork and cocoa, a significant amount of small alcohols and acids were observed (**Figure 41**). The variability in the content of natural extracts was greater when using DES 2. The composition of all extracts mostly consists of sugars, with the presence of small quantities of alcohols and acids. Certain extracts may exhibit the presence of steroids, aromatic chemicals, fatty acids, and terpenoids (**Figure 42**). Moreover, DES 2 exhibits the lowest polarity among eutectic solvents and is capable of extracting substantial quantities of both polar and nonpolar molecules across several classes. DES 2 is composed of lactic acid and is believed to be linked to an extraction process using acid catalysis. This technique facilitates the extraction of significant quantities of bioactive molecules that possess additional value, such as fatty acids and derivatives, aromatic compounds, and terpenoids. While chromatograms can provide valuable insights into the composition of

extracts, the absence of certain chemicals in the chromatograms does not necessarily imply their absence in the extracts. The overlapping of eutectic peaks has the potential to significantly diminish the regions of other compound peaks, hence posing challenges in their accurate identification.

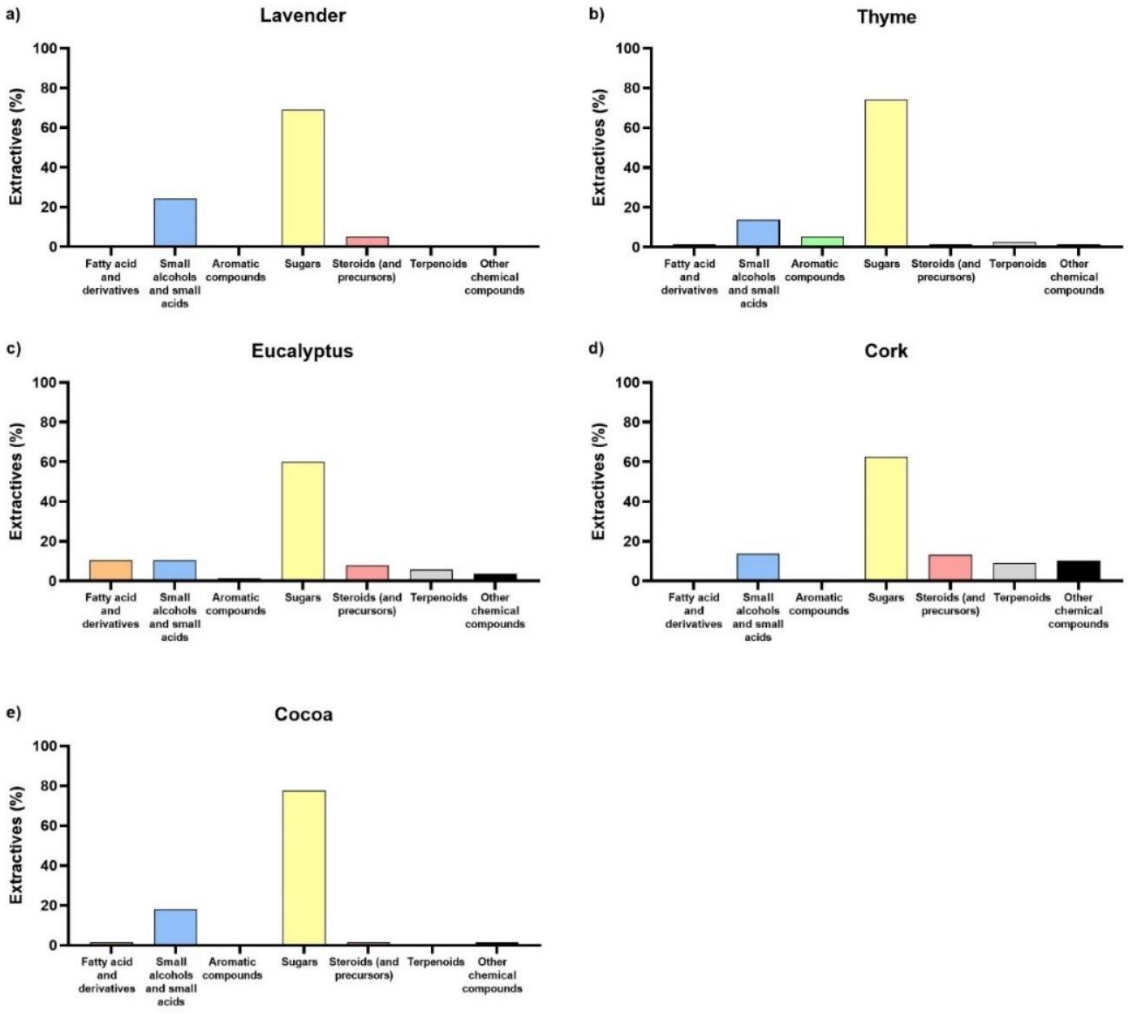


Figure 42. Gas chromatography-mass spectroscopy (GC-MS) analysis of the extracts obtained using method 11.

The application of the GC-MS technology facilitated the segregation of compounds based on their respective families; nonetheless, the identification of individual components remains unattainable. In order to accurately characterize the extracts, it was necessary to conduct HPLC-MS analysis. However, due to time limitations, this study was unable to perform the aforementioned analysis.

4.3.7 Tyrosinase inhibition assay

The presence of an excessive amount of pigmentation on the skin is attributed to the abnormal proliferation of melanocytes and the subsequent activation of melanin synthesis. This phenomenon is

closely associated with elevated expression levels of particular enzymes, notably tyrosinase. The enzyme, which plays a crucial role in the formation of melanin, is often the focus of antiaging drugs. The assessment of tyrosinase inhibitory activity was conducted for all extracts (**Figures 43-47**).

All extracts exhibited notable activity, and the inhibitory action was discovered to be dependent on concentration. The tyrosinase inhibitory activity of the extract was assessed across seven different concentrations. Among these concentrations, the highest concentration of 0.1 mg/mL exhibited the most notable and substantial inhibitory impact. The results indicate that the highest inhibitory activity for lavender was observed at this particular concentration with method 13, resulting in an inhibition rate of 35.9% (**Figure 43e**). Similarly, thyme exhibited the strongest inhibitory activity when the method 2 was applied, resulting in an inhibition rate of 46.0% (**Figure 44a**). Eucalyptus demonstrated the highest inhibitory activity when method 3 was used, resulting in an inhibition rate of 40.1% (**Figure 45a**). Cork exhibited the strongest inhibitory activity when method 4, resulting in an inhibition rate of 38.6% (**Figure 46b**). Lastly, cocoa demonstrated the highest inhibitory activity when method 1 was used, resulting in an inhibition rate of 41.2% (**Figure 47a**). With the exception of the lavender extract, which demonstrated limited inhibitory activity, all other extracts obtained using HE solvents exhibited comparable percentages. Notably, the cocoa extract with HE (EtOH:H_2O) 50:50 solvent displayed inhibitory values ranging from 5.9 ± 0.39% to 41.2 ± 0.24% (**Figure 47a**), while the thyme extracted with HE (EtOH:H_2O) 30:70 solvent exhibited inhibitory values ranging from 9 ± 0.28% to 42.8 ± 0.80% (**Figure 44b**). Regarding the extraction with eutectic solvents, thyme had the highest inhibitory activity when extracted with DES 1 (inhibitory values ranging from 5.7 ± 0.69% to 36.4 ± 0.26%) (**Figure 44c**) and cocoa when extracted with DES 2 and 3 (inhibitory values ranging from 4.7 ± 0.41% to 39.7 ± 0.54% for DES 2 and inhibitory values ranging from 3.6 ± 1.03% to 39.3 ± 0.31% for DES 3) (**Figures 47d** and **47e**). Cocoa and thyme stood out for their tyrosinase inhibitory activity. The capability of cocoa pod extracts to inhibit tyrosinase activity has been previously shown (Abdul Karim et al., 2014). The extract exhibited significant suppression of tyrosinase activity and shown superior inhibitory effects compared to well-established tyrosinase inhibitors such as kojic acid and ascorbic acid. The previous studies have also provided evidence of the tyrosinase inhibitory activity exhibited by the thyme extract (Akin & Saki, 2019).

The mentioned assay is widely recognized as the most favorable choice for conducting preliminary screening tests on newly developed skin-lightening compounds and extracts due to its cost-effectiveness, ability to process a large number of samples efficiently, and rapid analysis capabilities.

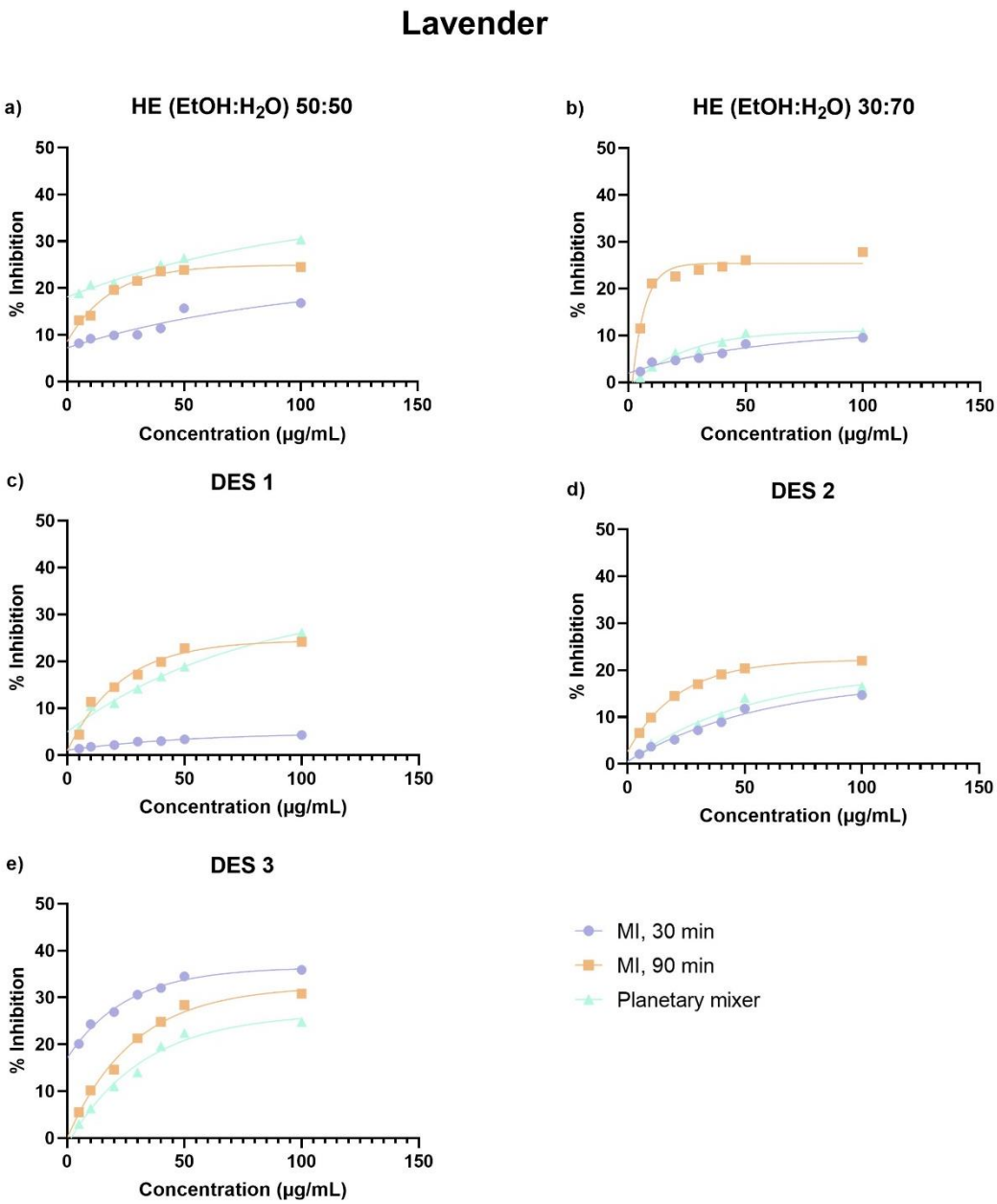


Figure 43. Curves of percentage of tyrosinase inhibition *versus* concentration for the lavender extracts **a)** HE (EtOH:H_2O) 50:50 solvent **b)** HE (EtOH:H_2O) 30:70 solvent **c)** deep eutectic solvent (DES) 1 **d)** DES 2 **e)** DES 3.

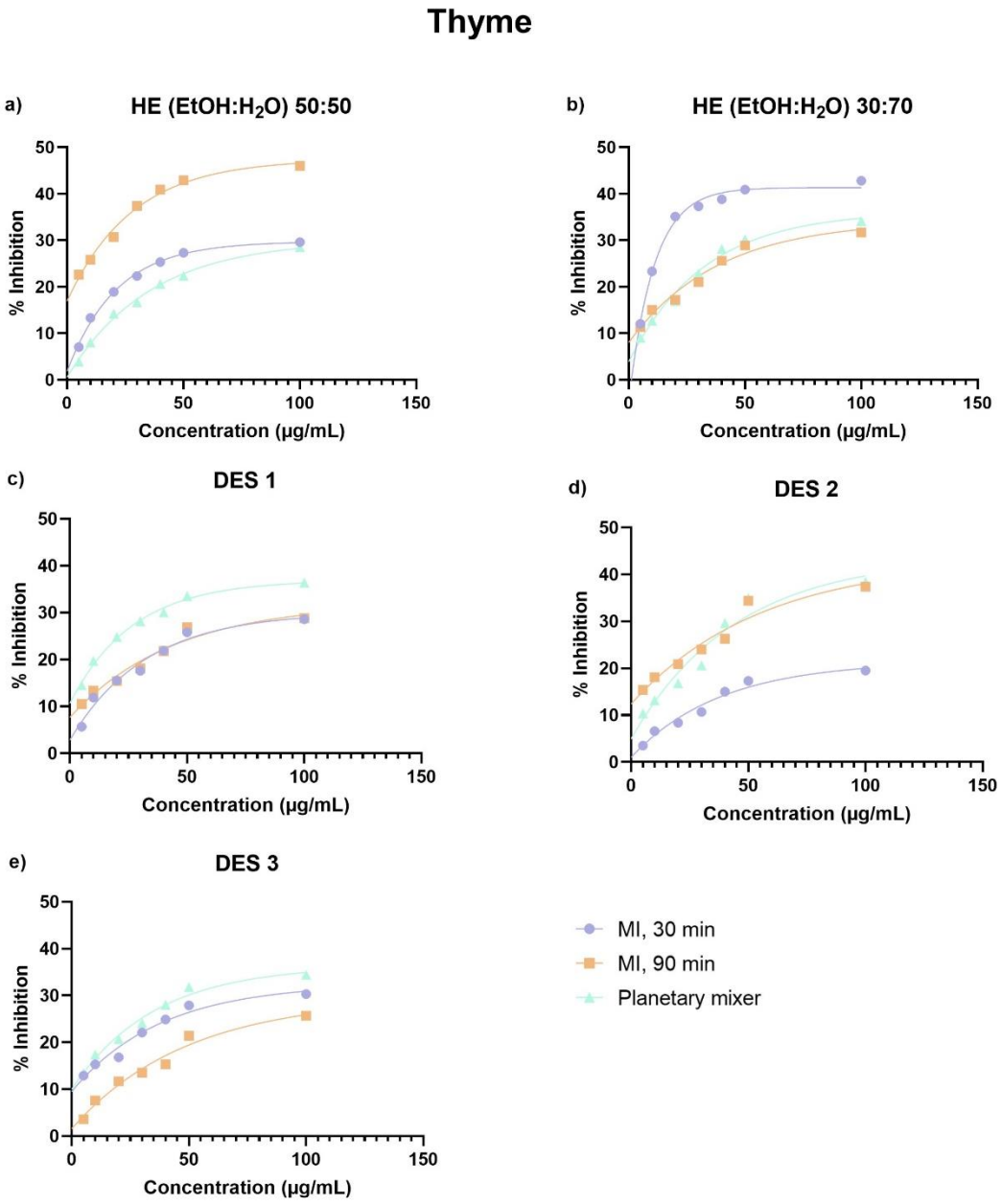


Figure 44. Curves of percentage of tyrosinase inhibition *versus* concentration for the thyme extracts **a)** HE (EtOH:H_2O) 50:50 solvent **b)** HE (EtOH:H_2O) 30:70 solvent **c)** deep eutectic solvent (DES) 1 **d)** DES 2 **e)** DES 3.

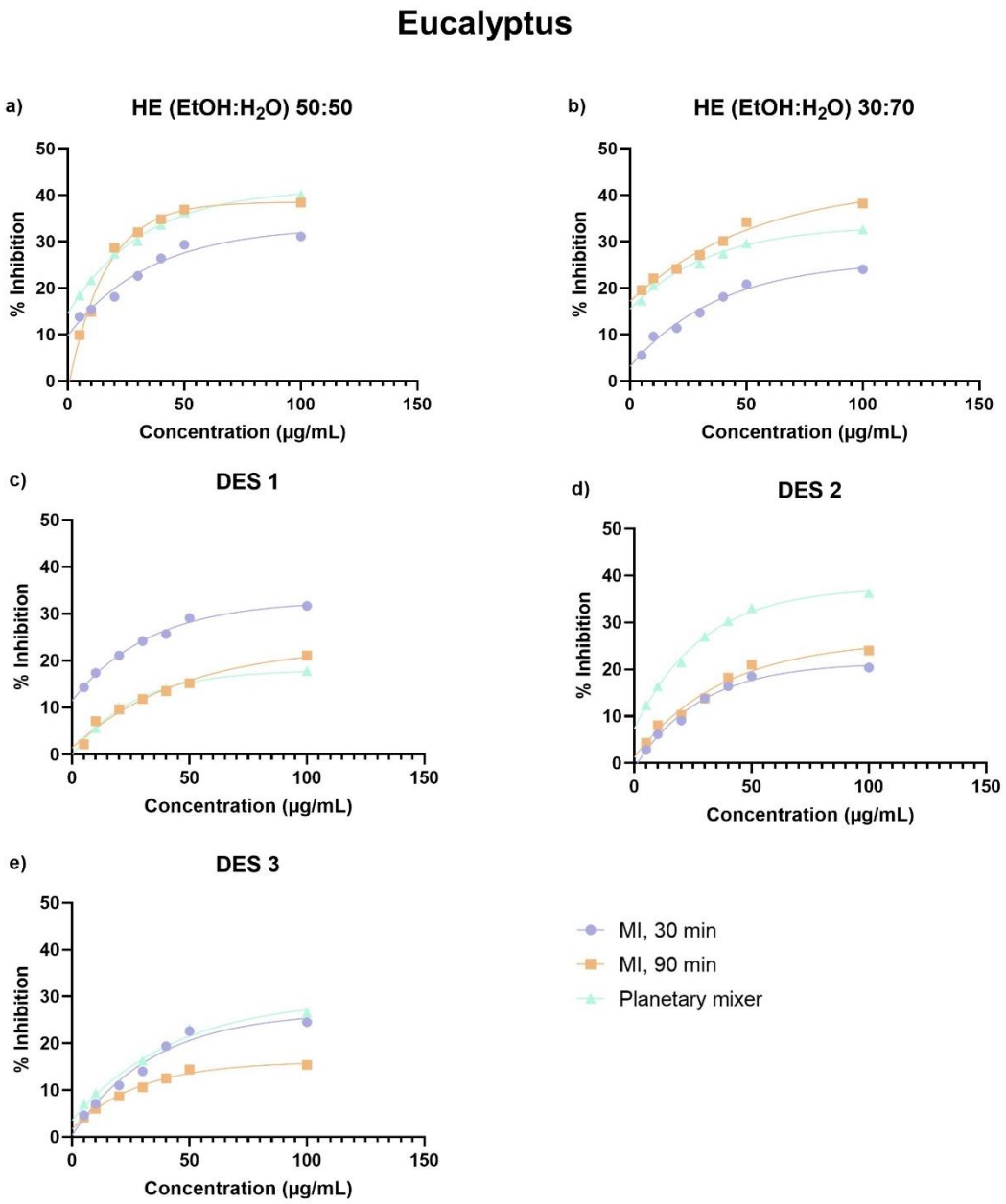


Figure 45. Curves of percentage of tyrosinase inhibition *versus* concentration for the eucalyptus extracts **a)** HE (EtOH:H_2O) 50:50 solvent **b)** HE (EtOH:H_2O) 30:70 solvent **c)** deep eutectic solvent (DES) 1 **d)** DES 2 **e)** DES 3.

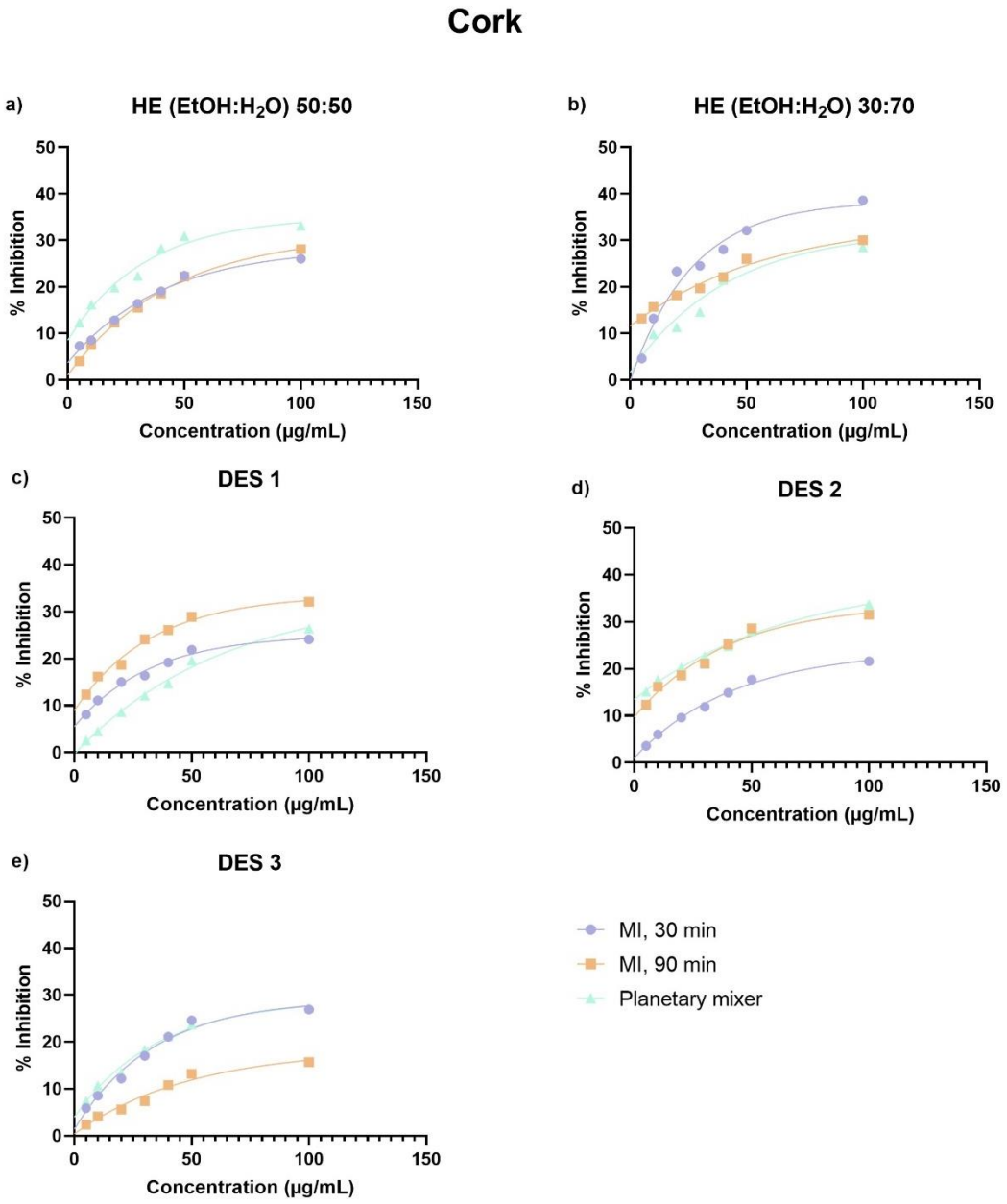


Figure 46. Curves of percentage of tyrosinase inhibition *versus* concentration for the cork extracts **a)** HE (EtOH:H_2O) 50:50 solvent **b)** HE (EtOH:H_2O) 30:70 solvent **c)** deep eutectic solvent (DES) 1 **d)** DES 2 **e)** DES 3.

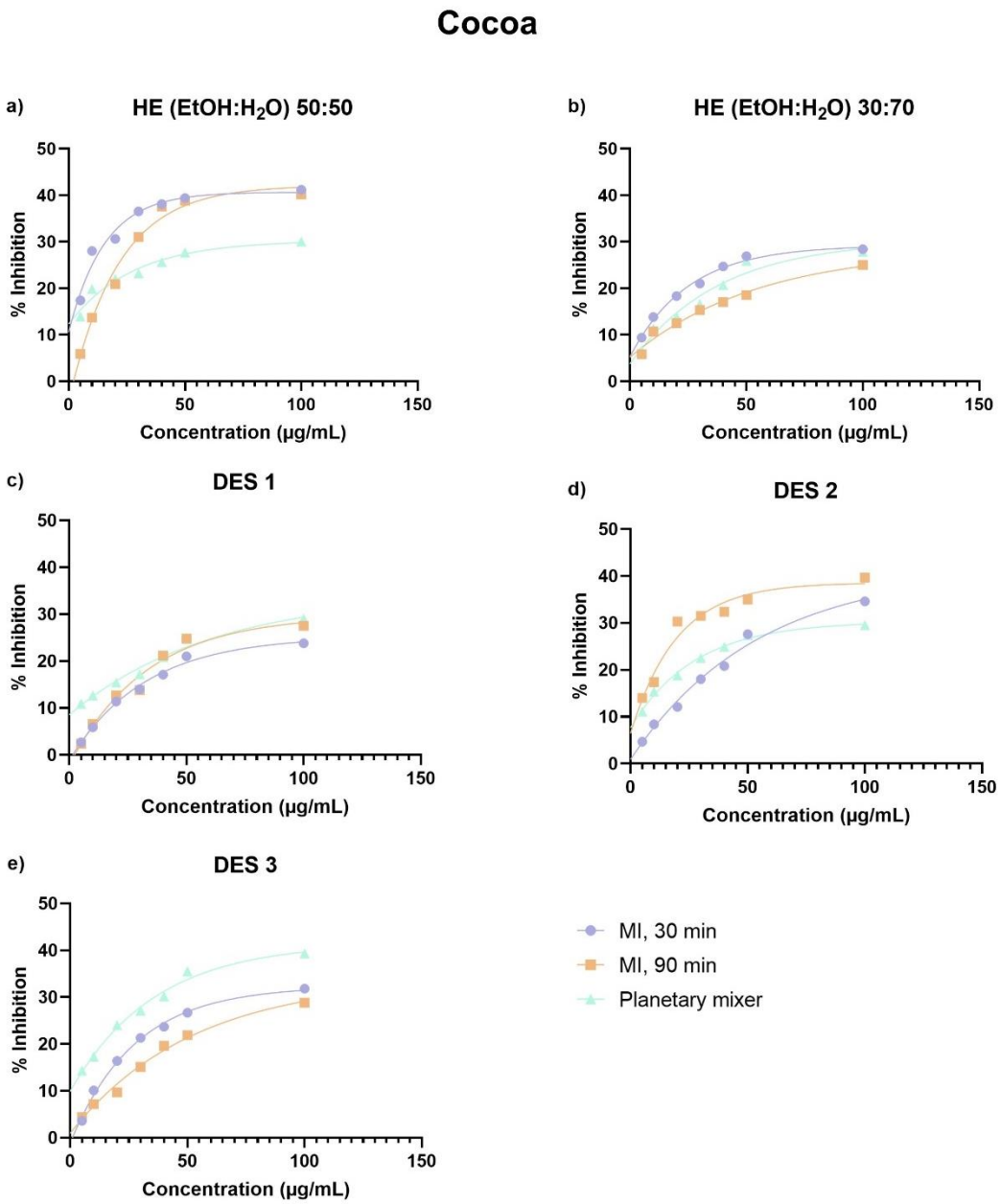


Figure 47. Curves of percentage of tyrosinase inhibition *versus* concentration for the cocoa extracts **a)** HE (EtOH:H_2O) 50:50 solvent **b)** HE (EtOH:H_2O) 30:70 solvent **c)** deep eutectic solvent (DES) 1 **d)** DES 2 **e)** DES 3.

5. CONCLUSIONS AND FUTURE PERSPECTIVES

Based on the experimental findings of this investigation, it can be inferred that the physicochemical characteristics of DES exhibit variability dependent upon the constituent elements they encompass, hence leading to potential variations in their respective applications.

The three deep eutectic solvents (DES) demonstrated favorable extraction yields that were comparable to those achieved with conventional solvents, specifically hydroethanolic mixture solvents (HE mixes). Among the DES tested, DES 3 exhibited the most promising results. Although the planetary mixer is often considered the most effective extraction method, it has been shown that the MI for 30 and 90 minutes can also serve as viable alternatives, yielding extraction results comparable to those of the planetary mixer. The posterior physicochemical characterisation of the extracts allowed for the observation that the composition of plant extracts is influenced by the extraction procedure and, particularly, the choice of solvent. All the extracts examined in this study exhibited noteworthy levels of total phenolic compounds (TPC) and total flavonoid compounds (TFC), with cork extract demonstrating the greatest concentration. On the other hand, eutectic extracts exhibit lower levels of total phenolic content (TPC) and total flavonoid content (TFC), with thyme and eucalyptus extracts displaying the greatest TPC values, while thyme extract demonstrates the highest TFC value. The antioxidant activities of the extracts were assessed using four different assays. The scavenging effect of cork and eucalyptus extracts exhibited the best efficacy for HE extracts in both the DPPH and ABTS experiments. Conversely, cocoa and eucalyptus extracts demonstrated the lowest EC_{50} values among the eutectic extracts. In the FRAP assay, it was observed that lavender extract exhibited the highest level of activity compared to the other herbal extracts. Additionally, eucalyptus extract demonstrated notable activity among the eutectic extracts. Regarding the ferric chelating activity, it was observed that none of the extracts demonstrated noteworthy activity when compared to the standard. The present study aimed to assess the antimicrobial efficacy of specific hydroethanolic and eutectic extracts. Notably, cork extract exhibited significant antimicrobial activity against both Gram-positive and Gram-negative bacteria. Additionally, among the eutectic extracts, eucalyptus extract demonstrated noteworthy effectiveness against *E. coli*. The photoprotective characteristics of the extracts were evaluated by measuring the sun protection factor (SPF), and it was found that cork exhibited the highest SPF value. The gas chromatography-mass spectrometry (GC-MS) study of the chosen extracts revealed variations in the chemical makeup of the extracts when employing different solvents. Finally, an examination was conducted on the tyrosinase inhibitory properties of all the

extracts, revealing that cocoa and thyme had notable inhibition effects in both the hydroalcoholic and eutectic extracts. **Table 19** presents the optimal extraction conditions for each physicochemical parameter determined in each extract. This study demonstrated the efficacy of DES in combination with alternate extraction techniques for the isolation of bioactive chemicals from various natural sources. Nevertheless, the traditional solvents yielded superior outcomes in terms of the analysis of the extract, specifically in relation to the phenolic content and antioxidant tests. However, in terms of the inhibition of tyrosinase, which is the crucial enzyme involved in melanin production, extracts derived from DES have demonstrated significant inhibitory effects. This suggests that there is promising potential for utilizing these extracts in the cosmetic industry to address pigmentary disorders. Among the natural extracts under consideration, cork and eucalyptus exhibited the most promising properties like TPC and TFC, antioxidant and photoprotective properties, antimicrobial activity, and tyrosinase inhibition.

In conclusion, this thesis demonstrated the use and efficiency of simpler and less wasteful extraction methods and newer greener solvents in the extraction of bioactive compounds from natural sources. The five natural extracts were characterized in terms of their physicochemical properties which help understand their chemical composition, bioactivity, and potential applications in cosmetics. In addition to exhibiting antioxidant, photoprotective and antibacterial properties, research on the impact of these natural extracts on tyrosinase inhibition revealed possibilities for future use in the cosmetics industry, specifically for the treatment of pigmentary disorders.

Based on the results obtained, the following suggestions are presented for future work:

- Remove the DES after extraction to better characterize the properties of the natural extracts;
- Characterize the extracts through HPLC-MS to identify individual components;
- Examine the integration of these natural extracts into cosmetic formulations, with a focus on evaluating their efficacy using stability tests, cytotoxicity assessments, and other relevant analyses.

Table 19. Optimized operational conditions for each extract tested and corresponding physicochemical properties.

Natural extract	Optimized conditions
Lavender	**Extraction yield:** method 11 (0.68 g extract/g staring material). **TPC:** method 5 (104.25 mg GAE/g extract) **TFC:** method 2 (646.90 mg QE/g extract) **DPPH:** method 3 (EC_{50} of 1.04 mg/mL) **ABTS:** method 3 (EC_{50} of 69.77 mg/mL)

	FRAP: method 5 (9.96 mg TE/g extract) **Antimicrobial activity:** non-determined **Sun protection factor:** method 6 (7.34) **Tyrosinase inhibition:** method 13 (35.9%)
Thyme	**Extraction yield:** method 8 (0.74 g extract/g starting material) **TPC:** method 4 (165.51 mg GAE/g extract) **TFC:** method 3 (901.80 mg QE/g extract) **DPPH:** method 3 (EC_{50} of 0.70 mg/mL) **ABTS:** method 1 (EC_{50} of 62.42 mg/mL) **FRAP:** method 8 (6.99 mg TE/g extract) **Antimicrobial activity:** method 8 against *S. aureus* **Sun protection factor:** method 3 (8.91) **Tyrosinase inhibition:** method 2 (46.0%)
Eucalyptus	**Extraction yield:** method 8 (0.66 g extract/g starting material) **TPC:** method 3 (286.75 mg GAE/g extract) **TFC:** method 1 (755 mg QE/g extract) **DPPH:** method 3 (EC_{50} of 0.55 mg/mL) **ABTS:** method 3 (EC_{50} of 33.93 mg/mL) **FRAP:** method 7 (9.12 mg TE/g extract) **Antimicrobial activity:** method 11 against *E. coli* **Sun protection factor:** method 2 (8.70) **Tyrosinase inhibition:** method 3 (40.1%)
Cork	**Extraction yield:** method 6 (0.46 g extract/g starting material) **TPC:** method 1 (362.10 mg GAE/g extract) **TFC:** method 5 (1481.50 mg QE/g extract) **DPPH:** method 3 (EC_{50} of 0.35 mg/mL) **ABTS:** method 2 (EC_{50} of 28.84 mg/mL) **FRAP:** method 15 (6.00 mg TE/g extract) **Antimicrobial activity:** method 11 against *E. coli* **Sun protection factor:** method 2 (10.43) **Tyrosinase inhibition:** method 4 (38.6%)
Cocoa	**Extraction yield:** method 12 (0.70 g extract/g starting material) **TPC:** method 1 (142.31 mg GAE/g extract)

	TFC: method 1 (932.15 mg QE/g extract) **DPPH:** method 1 (EC_{50} of 0.85 mg/mL) **ABTS:** method 1 (EC_{50} of 49.23 mg/mL) **FRAP:** method 14 (7.90 mg TE/g extract) **Antimicrobial activity:** non-determined **Sun protection factor:** method 3 (5.76) **Tyrosinase inhibition:** method 1 (41.2%)

6. REFERENCES

Abdul Karim, A., Azlan, A., Ismail, A., Hashim, P., Abd Gani, S. S., Zainudin, B. H., & Abdullah, N. A. (2014). Phenolic composition, antioxidant, anti-wrinkles and tyrosinase inhibitory activities of cocoa pod extract. *BMC Complementary and Alternative Medicine*, *14*(1), 381. https://doi.org/10.1186/1472-6882-14-381

Akin, M., & Saki, N. (2019). Antimicrobial, DPPH scavenging and tyrosinase inhibitory activities of Thymus vulgaris, Helichrysum arenarium and Rosa damascena mill. Ethanol extracts by using TLC bioautography and chemical screening methods. *Journal of Liquid Chromatography & Related Technologies*, *42*(7–8), 204–216. https://doi.org/10.1080/10826076.2019.1591977

Allami, R., Mouhamad, R., Abdulateef, S., & Al-Khafaji, K. (2020). Antimicrobial Activity of Herbal Mixture Extract Combination on Microorganisms. *Bionatura*, *5*. https://doi.org/10.21931/RB/2020.05.04.11

Álvarez-Martínez, F. J., Barrajón-Catalán, E., Herranz-López, M., & Micol, V. (2021). Antibacterial plant compounds, extracts and essential oils: An updated review on their effects and putative mechanisms of action. *Phytomedicine*, *90*, 153626. https://doi.org/10.1016/j.phymed.2021.153626

Álvarez-Martínez, F. J., Rodríguez, J. C., Borrás-Rocher, F., Barrajón-Catalán, E., & Micol, V. (2021). The antimicrobial capacity of Cistus salviifolius and Punica granatum plant extracts against clinical pathogens is related to their polyphenolic composition. *Scientific Reports*, *11*(1), Article 1. https://doi.org/10.1038/s41598-020-80003-y

Amawi, H., Ashby, C. R., Samuel, T., Peraman, R., & Tiwari, A. K. (2017). Polyphenolic Nutrients in Cancer Chemoprevention and Metastasis: Role of the Epithelial-to-Mesenchymal (EMT) Pathway. *Nutrients*, *9*(8), Article 8. https://doi.org/10.3390/nu9080911

Awad, A. M., Kumar, P., Ismail-Fitry, M. R., Jusoh, S., Ab Aziz, M. F., & Sazili, A. Q. (2021). Green Extraction of Bioactive Compounds from Plant Biomass and Their Application in Meat as Natural Antioxidant. *Antioxidants*, *10*(9), 1465. https://doi.org/10.3390/antiox10091465

Azevedo, J., Lopes, P., Mateus, N., & de Freitas, V. (2022). Cork, a Natural Choice to Wine? *Foods*, *11*(17), Article 17. https://doi.org/10.3390/foods11172638

Batiha, G. E.-S., Teibo, J. O., Wasef, L., Shaheen, H. M., Akomolafe, A. P., Teibo, T. K. A., Al-kuraishy, H. M., Al-Garbeeb, A. I., Alexiou, A., & Papadakis, M. (2023). A review of the bioactive components and pharmacological properties of Lavandula species. *Naunyn-Schmiedeberg's Archives of Pharmacology*, *396*(5), 877–900. https://doi.org/10.1007/s00210-023-02392-x

Benzie, I. F., & Strain, J. J. (1996). The ferric reducing ability of plasma (FRAP) as a measure of 'antioxidant power': The FRAP assay. *Analytical Biochemistry*, *239*(1), 70–76. https://doi.org/10.1006/abio.1996.0292

Bibi Sadeer, N., Montesano, D., Albrizio, S., Zengin, G., & Mahomoodally, M. F. (2020). The Versatility of Antioxidant Assays in Food Science and Safety—Chemistry, Applications, Strengths, and Limitations. *Antioxidants*, *9*(8), Article 8. https://doi.org/10.3390/antiox9080709

bio10 forte L-tigo. Intensive depigmenting treatment. (n.d.). Bella Aurora. Retrieved 7 October 2023, from https://bella-aurora.com/eu-en/bella-aurora/888-bio10-forte-l-tigo-intensive-depigmenting-treatment.html

Blainski, A., Lopes, G. C., & de Mello, J. C. P. (2013). Application and Analysis of the Folin Ciocalteu Method for the Determination of the Total Phenolic Content from Limonium Brasiliense L. *Molecules*, *18*(6), 6852–6865. https://doi.org/10.3390/molecules18066852

Boo, Y. C. (2020). Up- or Downregulation of Melanin Synthesis Using Amino Acids, Peptides, and Their Analogs. *Biomedicines*, *8*(9), Article 9. https://doi.org/10.3390/biomedicines8090322

Boo, Y. C. (2021). Arbutin as a Skin Depigmenting Agent with Antimelanogenic and Antioxidant Properties. *Antioxidants*, *10*(7), Article 7. https://doi.org/10.3390/antiox10071129

Braithwaite, A., & Smith, F. J. (1999). *Chromatographic Methods*. Springer Netherlands. https://doi.org/10.1007/978-94-011-0599-6

Brand-Williams, W., Cuvelier, M. E., & Berset, C. (1995). Use of a free radical method to evaluate antioxidant activity. *LWT - Food Science and Technology*, *28*(1), 25–30. https://doi.org/10.1016/S0023-6438(95)80008-5

Carriço, C., Ribeiro, H. M., & Marto, J. (2018). Converting cork by-products to ecofriendly cork bioactive ingredients: Novel pharmaceutical and cosmetics applications. *Industrial Crops and Products*, *125*, 72–84. https://doi.org/10.1016/j.indcrop.2018.08.092

Castellano-Pellicena, I., Morrison, C. G., Bell, M., O'Connor, C., & Tobin, D. J. (2021). Melanin Distribution in Human Skin: Influence of Cytoskeletal, Polarity, and Centrosome-Related Machinery of Stratum basale Keratinocytes. *International Journal of Molecular Sciences*, *22*(6), Article 6. https://doi.org/10.3390/ijms22063143

Cefali, L. C., Franco, J. G., Nicolini, G. F., Ataide, J. A., & Mazzola, P. G. (2019). In vitro antioxidant activity and solar protection factor of blackberry and raspberry extracts in topical formulation. *Journal of Cosmetic Dermatology*, *18*(2), 539–544. https://doi.org/10.1111/jocd.12842

Chemat, F., Abert Vian, M., Ravi, H. K., Khadhraoui, B., Hilali, S., Perino, S., & Fabiano Tixier, A.-S. (2019). Review of Alternative Solvents for Green Extraction of Food and Natural Products: Panorama, Principles, Applications and Prospects. *Molecules*, *24*(16), 3007. https://doi.org/10.3390/molecules24163007

Chuo, S. C., Nasir, H. M., Mohd-Setapar, S. H., Mohamed, S. F., Ahmad, A., Wani, W. A., Muddassir, Mohd., & Alarifi, A. (2022). A Glimpse into the Extraction Methods of Active Compounds from Plants. *Critical Reviews in Analytical Chemistry*, *52*(4), 667–696. https://doi.org/10.1080/10408347.2020.1820851

Cichorek, M., Wachulska, M., Stasiewicz, A., & Tymińska, A. (2013). Skin melanocytes: Biology and development. *Advances in Dermatology and Allergology/Postępy Dermatologii I Alergologii*, *30*(1), 30–41. https://doi.org/10.5114/pdia.2013.33376

Crozier, A., Jaganath, I., & Clifford, M. (2009). ChemInform Abstract: Dietary Phenolics: Chemistry, Bioavailability and Effects on Health. *Natural Product Reports*, *26*, 1001–1043. https://doi.org/10.1039/b802662a

Cunha, S. C., & Fernandes, J. O. (2018). Extraction techniques with deep eutectic solvents. *TrAC Trends in Analytical Chemistry*, *105*, 225–239. https://doi.org/10.1016/j.trac.2018.05.001

Dai, Y., Witkamp, G.-J., Verpoorte, R., & Choi, Y. (2015). Tailoring properties of natural deep eutectic solvents with water to facilitate their applications. *Food Chemistry*, *187*. https://doi.org/10.1016/j.foodchem.2015.03.123

Das, K., & Gezici, S. (2018). Secondary plant metabolites, their separation and identification, and role in human disease prevention. *Annals of Phytomedicine: An International Journal*, *7*, 13–24. https://doi.org/10.21276/ap.2018.7.2.3

Diem Vitamin C Pigment-Correcting Water Cream 60ml. (n.d.). Antipodes New Zealand. Retrieved 26 September 2023, from https://antipodesnature.com/products/diem-vitamin-c-pigment-correcting-water-cream-60ml

Dini, I., & Laneri, S. (2021). The New Challenge of Green Cosmetics: Natural Food Ingredients for Cosmetic Formulations. *Molecules (Basel, Switzerland)*, *26*(13), 3921. https://doi.org/10.3390/molecules26133921

Dinis, T. C. P., Madeira, V. M. C., & Almeida, L. M. (1994). Action of Phenolic Derivatives (Acetaminophen, Salicylate, and 5-Aminosalicylate) as Inhibitors of Membrane Lipid Peroxidation and as Peroxyl Radical Scavengers. *Archives of Biochemistry and Biophysics*, *315*(1), 161–169. https://doi.org/10.1006/abbi.1994.1485

D'Mello, S. A. N., Finlay, G. J., Baguley, B. C., & Askarian-Amiri, M. E. (2016). Signaling Pathways in Melanogenesis. *International Journal of Molecular Sciences*, *17*(7), 1144. https://doi.org/10.3390/ijms17071144

Dobros, N., Zawada, K., & Paradowska, K. (2022). Phytochemical Profile and Antioxidant Activity of Lavandula angustifolia and Lavandula x intermedia Cultivars Extracted with Different Methods. *Antioxidants*, *11*(4), 711. https://doi.org/10.3390/antiox11040711

Drira, R., & Sakamoto, K. (2015). Isosakuranetin, a 4'-O-methylated flavonoid, stimulates melanogenesis in B16BL6 murine melanoma cells. *Life Sciences*, *143*, 43–49. https://doi.org/10.1016/j.lfs.2015.10.009

Duan, L., Dou, L.-L., Guo, L., Li, P., & Liu, E.-H. (2016, March 22). *Comprehensive Evaluation of Deep Eutectic Solvents in Extraction of Bioactive Natural Products* (world) [Research-article]. ACS Publications; American Chemical Society. https://doi.org/10.1021/acssuschemeng.6b00091

Ebrahimzadeh, M. A., Enayatifard, R., Khalili, M., Ghaffarloo, M., Saeedi, M., & Yazdani Charati, J. (2014). Correlation between Sun Protection Factor and Antioxidant Activity, Phenol and Flavonoid Contents of some Medicinal Plants. *Iranian Journal of Pharmaceutical Research : IJPR*, *13*(3), 1041–1047.

El-Nashar, H. A. S., El-Din, M. I. G., Hritcu, L., & Eldahshan, O. A. (2021). Insights on the Inhibitory Power of Flavonoids on Tyrosinase Activity: A Survey from 2016 to 2021. *Molecules*, *26*(24), 7546. https://doi.org/10.3390/molecules26247546

Ezzat, S. M., El Bishbishy, M. H., El Kersh, D. M., Zayed, A., Salem, M. A., & Salama, M. M. (2021). Chapter 7—Herbal cosmeticology. In C. Egbuna, A. P. Mishra, & M. R. Goyal (Eds.), *Preparation of Phytopharmaceuticals for the Management of Disorders* (pp. 129–168). Academic Press. https://doi.org/10.1016/B978-0-12-820284-5.00022-8

Farris, P. (2007). Idebenone, green tea, and Coffeeberry extract: New and innovative antioxidants. *Dermatologic Therapy*, *20*(5), 322–329. https://doi.org/10.1111/j.1529-8019.2007.00146.x

Fernandes, A., Fernandes, I., Cruz, L., Mateus, N., Cabral, M., & de Freitas, V. (2009). Antioxidant and Biological Properties of Bioactive Phenolic Compounds from Quercus suber L. *Journal of Agricultural and Food Chemistry*, *57*(23), 11154–11160. https://doi.org/10.1021/jf902093m

Fiocco, D., Fiorentino, D., Frabboni, L., Benvenuti, S., Orlandini, G., Pellati, F., & Gallone, A. (2011). Lavender and peppermint essential oils as effective mushroom tyrosinase inhibitors: A basic study. *Flavour and Fragrance Journal*, *26*(6), 441–446. https://doi.org/10.1002/ffj.2072

Freitas, D. S., Rocha, D., Castro, T. G., Noro, J., Castro, V. I. B., Teixeira, M. A., Reis, R. L., Cavaco-Paulo, A., & Silva, C. (2022). Green Extraction of Cork Bioactive Compounds Using Natural Deep Eutectic Mixtures. *ACS Sustainable Chemistry & Engineering*, *10*(24), 7974–7989. https://doi.org/10.1021/acssuschemeng.2c01422

Fu, C., Chen, J., Lu, J., Yi, L., Tong, X., Kang, L., Pei, S., Ouyang, Y., Jiang, L., Ding, Y., Zhao, X., Li, S., Yang, Y., Huang, J., & Zeng, Q. (2020). Roles of inflammation factors in melanogenesis. *Molecular Medicine Reports*, *21*(3), 1421–1430. https://doi.org/10.3892/mmr.2020.10950

Garcia, L. B., Pires, G. A., Oliveira, D. A. J., Silva, L. A. O., Gomes, A. F., Amaral, J. G., Pereira, G. R., & Ruela, A. L. M. (2021). Incorporation of glycolic extract of cocoa beans (Theobroma cacao L.) into microemulsions and emulgels for skincare. *Industrial Crops and Products*, *161*, 113181. https://doi.org/10.1016/j.indcrop.2020.113181

Garcia-Salas, P., Morales-Soto, A., Segura Carretero, A., & Fernández-Gutiérrez, A. (2010). Phenolic-Compound-Extraction Systems for Fruit and Vegetable Samples. *Molecules (Basel, Switzerland)*, *15*, 8813–8826. https://doi.org/10.3390/molecules15128813

Gaweł-Bęben, K., Strzępek-Gomółka, M., Czop, M., Sakipova, Z., Głowniak, K., & Kukula-Koch, W. (2020). Achillea millefolium L. and Achillea biebersteinii Afan. Hydroglycolic Extracts–Bioactive Ingredients for Cosmetic Use. *Molecules*, *25*(15), 3368. https://doi.org/10.3390/molecules25153368

Gulcin, İ. (2020). Antioxidants and antioxidant methods: An updated overview. *Archives of Toxicology*, *94*(3), 651–715. https://doi.org/10.1007/s00204-020-02689-3

Gullón, B., Muñiz-Mouro, A., Lú-Chau, T. A., Moreira, M. T., Lema, J. M., & Eibes, G. (2019). Green approaches for the extraction of antioxidants from eucalyptus leaves. *Industrial Crops and Products*, *138*, 111473. https://doi.org/10.1016/j.indcrop.2019.111473

Habán, M., Korczyk-Szabó, J., Čerteková, S., & Ražná, K. (2023). Lavandula Species, Their Bioactive Phytochemicals, and Their Biosynthetic Regulation. *International Journal of Molecular Sciences*, *24*(10), Article 10. https://doi.org/10.3390/ijms24108831

Han, Y. K., Park, Y. J., Ha, Y. M., Park, D., Lee, J. Y., Lee, N., Yoon, J. H., Moon, H. R., & Chung, H. Y. (2012). Characterization of a novel tyrosinase inhibitor, (2RS,4R)-2-(2,4-dihydroxyphenyl)thiazolidine-4-carboxylic acid (MHY384). *Biochimica et Biophysica Acta*, *1820*(4), 542–549. https://doi.org/10.1016/j.bbagen.2012.01.001

Hemeg, H. A., Moussa, I. M., Ibrahim, S., Dawoud, T. M., Alhaji, J. H., Mubarak, A. S., Kabli, S. A., Alsubki, R. A., Tawfik, A. M., & Marouf, S. A. (2020). Antimicrobial effect of different herbal plant extracts against different microbial population. *Saudi Journal of Biological Sciences*, *27*(12), 3221–3227. https://doi.org/10.1016/j.sjbs.2020.08.015

Hernandez, D. F., Cervantes, E. L., Luna-Vital, D. A., & Mojica, L. (2021). Food-derived bioactive compounds with anti-aging potential for nutricosmetic and cosmeceutical products. *Critical Reviews in Food Science and Nutrition*, *61*(22), 3740–3755. https://doi.org/10.1080/10408398.2020.1805407

Hidayah, H., Amal, S., Yuniarsih, N., Farhamzah, F., Kusumawati, A., Gunarti, N., Abriyani, E., Mursal, I., Sundara, A., & Alkandahri, M. (2023). Sun Protection Factor Activity of Jamblang Leaves Serum Extract (Syzygium cumini). *Pharmacognosy Journal*, *15*, 134–140. https://doi.org/10.5530/pj.2023.15.18

Hsu, C.-K., Chang, C.-T., Lu, H.-Y., & Chung, Y.-C. (2007). Inhibitory effects of the water extracts of Lavendula sp. On mushroom tyrosinase activity. *Food Chemistry*, *105*(3), 1099–1105. https://doi.org/10.1016/j.foodchem.2007.02.008

Identify, explore and share your observations of wild plants. (n.d.). Retrieved 19 October 2023, from https://identify.plantnet.org/

Idris, M., Yelwa, A., & Muhammad, A. (2021). Phytochemical Screening, Cytotoxicity and Antioxidant Activities of Leaves Extracts from Eucalyptus citriodora. *Journal of Tropical Pharmacy and Chemistry*, *5*, 165–173. https://doi.org/10.25026/jtpc.v5i3.280

Ilmi, H. M., Elya, B., & Handayani, R. (2020). ASSOCIATION BETWEEN TOTAL PHENOL AND FLAVONOID CONTENTS IN ARTOCARPUS HETEROPHYLLUS (JACKFRUIT) BARK AND LEAF EXTRACTS AND LIPOXYGENASE INHIBITION. *International Journal of Applied Pharmaceutics*, 252–256. https://doi.org/10.22159/ijap.2020.v12s1.FF055

Ilyasov, I. R., Beloborodov, V. L., Selivanova, I. A., & Terekhov, R. P. (2020). ABTS/PP Decolorization Assay of Antioxidant Capacity Reaction Pathways. *International Journal of Molecular Sciences*, *21*(3), 1131. https://doi.org/10.3390/ijms21031131

Jeon, N.-J., Kim, Y.-S., Kim, E.-K., Dong, X., Lee, J.-W., Park, J.-S., Shin, W.-B., Moon, S.-H., Jeon, B.-T., & Park, P.-J. (2018). Inhibitory effect of carvacrol on melanin synthesis via suppression of tyrosinase expression. *Journal of Functional Foods*, *45*, 199–205. https://doi.org/10.1016/j.jff.2018.03.043

Jovanović, A. A., Đorđević, V. B., Zdunić, G. M., Pljevljakušić, D. S., Šavikin, K. P., Gođevac, D. M., & Bugarski, B. M. (2017). Optimization of the extraction process of polyphenols from Thymus serpyllum L. herb using maceration, heat- and ultrasound-assisted techniques. *Separation and Purification Technology*, *179*, 369–380. https://doi.org/10.1016/j.seppur.2017.01.055

Katz, D. L., Doughty, K., & Ali, A. (2011). Cocoa and Chocolate in Human Health and Disease. *Antioxidants & Redox Signaling*, *15*(10), 2779–2811. https://doi.org/10.1089/ars.2010.3697

Kaur, S., & Ubeyitogullari, A. (2023). Extraction of phenolic compounds from rice husk via ethanol-water-modified supercritical carbon dioxide. *Heliyon*, *9*(3), e14196. https://doi.org/10.1016/j.heliyon.2023.e14196

Khaleel, C., Tabanca, N., & Buchbauer, G. (2018). α-Terpineol, a natural monoterpene: A review of its biological properties. *Open Chemistry*, *16*(1), 349–361. https://doi.org/10.1515/chem-2018-0040

Lee, S. Y., Baek, N., & Nam, T. (2016). Natural, semisynthetic and synthetic tyrosinase inhibitors. *Journal of Enzyme Inhibition and Medicinal Chemistry*, *31*(1), 1–13. https://doi.org/10.3109/14756366.2015.1004058

Lepe, V., Moncada, B., Castanedo-Cazares, J. P., Torres-Alvarez, M. B., Ortiz, C. A., & Torres-Rubalcava, A. B. (2003). A double-blind randomized trial of 0.1% tacrolimus vs 0.05% clobetasol for the treatment of childhood vitiligo. *Archives of Dermatology*, *139*(5), 581–585. https://doi.org/10.1001/archderm.139.5.581

Lesage-Meessen, L., Bou, M., Sigoillot, J.-C., Faulds, C. B., & Lomascolo, A. (2015). Essential oils and distilled straws of lavender and lavandin: A review of current use and potential application in white biotechnology. *Applied Microbiology and Biotechnology*, *99*(8), 3375–3385. https://doi.org/10.1007/s00253-015-6511-7

Li, L., Chong, L., Huang, T., Ma, Y., Li, Y., & Ding, H. (2023). Natural products and extracts from plants as natural UV filters for sunscreens: A review. *Animal Models and Experimental Medicine*, *6*(3), 183–195. https://doi.org/10.1002/ame2.12295

Liu, J.-K. (2022). Natural products in cosmetics. *Natural Products and Bioprospecting*, *12*(1), 40. https://doi.org/10.1007/s13659-022-00363-y

Magalhães, L. M., Almeida, M. I. G. S., Barreiros, L., Reis, S., & Segundo, M. A. (2012). Automatic Aluminum Chloride Method for Routine Estimation of Total Flavonoids in Red Wines and Teas. *Food Analytical Methods*, *5*(3), 530–539. https://doi.org/10.1007/s12161-011-9278-1

Mansur, J. S., Breder, M. N. R., Mansur, M. C. A., & Azulay, R. D. (1986). Determinação do fator de proteção solar por espectrofotometria. *An Bras Dermatol Rio De Janeiro*, *61*, 121–124.

Mapoung, S., Semmarath, W., Arjsri, P., Umsumarng, S., Srisawad, K., Thippraphan, P., Yodkeeree, S., & Limtrakul (Dejkriengkraikul), P. (2021). Determination of Phenolic Content, Antioxidant Activity, and Tyrosinase Inhibitory Effects of Functional Cosmetic Creams Available on the Thailand Market. *Plants*, *10*(7), 1383. https://doi.org/10.3390/plants10071383

Martin, M. Á., & Ramos, S. (2021). Impact of cocoa flavanols on human health. *Food and Chemical Toxicology*, *151*, 112121. https://doi.org/10.1016/j.fct.2021.112121

Masum, M. N., Yamauchi, K., & Mitsunaga, T. (2019). Tyrosinase Inhibitors from Natural and Synthetic Sources as Skin-lightening Agents. *Reviews in Agricultural Science*, *7*, 41–58. https://doi.org/10.7831/ras.7.41

Mazière, C., Dantin, F., Dubois, F., Santus, R., & Mazière, J. (2000). Biphasic effect of UVA radiation on STAT1 activity and tyrosine phosphorylation in cultured human keratinocytes. *Free Radical Biology & Medicine*, *28*(9), 1430–1437. https://doi.org/10.1016/s0891-5849(00)00264-1

Mejía-Giraldo, J. C., Henao-Zuluaga, K., Gallardo, C., Atehortúa, L., & Puertas-Mejía, M. A. (2016). Novel In Vitro Antioxidant and Photoprotection Capacity of Plants from High Altitude Ecosystems of Colombia. *Photochemistry and Photobiology*, *92*(1), 150–157. https://doi.org/10.1111/php.12543

Mokhtari, R., Kazemi Fard, M., Rezaei, M., Moftakharzadeh, S. A., & Mohseni, A. (2023). Antioxidant, Antimicrobial Activities, and Characterization of Phenolic Compounds of Thyme (*Thymus vulgaris* L.), Sage (*Salvia officinalis* L.), and Thyme–Sage Mixture Extracts. *Journal of Food Quality*, *2023*, e2602454. https://doi.org/10.1155/2023/2602454

Moreira, P., Sousa, F. J., Matos, P., Brites, G. S., Gonçalves, M. J., Cavaleiro, C., Figueirinha, A., Salgueiro, L., Batista, M. T., Branco, P. C., Cruz, M. T., & Pereira, C. F. (2022). Chemical Composition and Effect against Skin Alterations of Bioactive Extracts Obtained by the Hydrodistillation of Eucalyptus globulus Leaves. *Pharmaceutics*, *14*(3), 561. https://doi.org/10.3390/pharmaceutics14030561

Muddathir, A. M., Yamauchi, K., Batubara, I., Mohieldin, E. A. M., & Mitsunaga, T. (2017). Anti-tyrosinase, total phenolic content and antioxidant activity of selected Sudanese medicinal plants. *South African Journal of Botany*, *109*, 9–15. https://doi.org/10.1016/j.sajb.2016.12.013

Munteanu, I. G., & Apetrei, C. (2021). Analytical Methods Used in Determining Antioxidant Activity: A Review. *International Journal of Molecular Sciences*, *22*(7), 3380. https://doi.org/10.3390/ijms22073380

Muzaffer, U., Paul, V. I., Prasad, N. R., Karthikeyan, R., & Agilan, B. (2018). Protective effect of Juglans regia L. against ultraviolet B radiation induced inflammatory responses in human epidermal keratinocytes. *Phytomedicine*, *42*, 100–111. https://doi.org/10.1016/j.phymed.2018.03.024

Nabet, N., Gilbert-López, B., Madani, K., Herrero, M., Ibáñez, E., & Mendiola, J. A. (2019). Optimization of microwave-assisted extraction recovery of bioactive compounds from Origanum glandulosum and Thymus fontanesii. *Industrial Crops and Products*, *129*, 395–404. https://doi.org/10.1016/j.indcrop.2018.12.032

Namukobe, J., Sekandi, P., Byamukama, R., Murungi, M., Nambooze, J., Ekyibetenga, Y., Nagawa, C. B., & Asiimwe, S. (2021). Antibacterial, antioxidant, and sun protection potential of selected ethno medicinal plants used for skin infections in Uganda. *Tropical Medicine and Health*, *49*(1), 49. https://doi.org/10.1186/s41182-021-00342-y

Napagoda, M. T., Malkanthi, B. M. A. S., Abayawardana, S. A. K., Qader, M. M., & Jayasinghe, L. (2016). Photoprotective potential in some medicinal plants used to treat skin diseases in Sri Lanka. *BMC Complementary and Alternative Medicine*, *16*, 479. https://doi.org/10.1186/s12906-016-1455-8

Nascimento, G. G. F., Locatelli, J., Freitas, P. C., & Silva, G. L. (2000). Antibacterial activity of plant extracts and phytochemicals on antibiotic-resistant bacteria. *Brazilian Journal of Microbiology*, *31*, 247–256. https://doi.org/10.1590/S1517-83822000000400003

Nayim, P., Mbaveng, A. T., Wamba, B. E. N., Fankam, A. G., Dzotam, J. K., & Kuete, V. (2018). Antibacterial and Antibiotic-Potentiating Activities of Thirteen Cameroonian Edible Plants against Gram-Negative Resistant Phenotypes. *The Scientific World Journal*, *2018*, e4020294. https://doi.org/10.1155/2018/4020294

Nazzaro, F., Fratianni, F., De Martino, L., Coppola, R., & De Feo, V. (2013). Effect of Essential Oils on Pathogenic Bacteria. *Pharmaceuticals*, *6*(12), 1451–1474. https://doi.org/10.3390/ph6121451

Ndiaye, M., Philippe, C., Mukhtar, H., & Ahmad, N. (2011). The grape antioxidant resveratrol for skin disorders: Promise, prospects, and challenges. *Archives of Biochemistry and Biophysics*, *508*(2), 164–170. https://doi.org/10.1016/j.abb.2010.12.030

Niacinamide 10% + Zinc 1% | The Ordinary. (n.d.). Retrieved 26 September 2023, from https://theordinary.com/en-us/niacinamide-10-zinc-1-serum-100436.html

Nieto, G. (2020). A Review on Applications and Uses of Thymus in the Food Industry. *Plants*, *9*(8), Article 8. https://doi.org/10.3390/plants9080961

Niu, C., & Aisa, H. A. (2017). Upregulation of Melanogenesis and Tyrosinase Activity: Potential Agents for Vitiligo. *Molecules : A Journal of Synthetic Chemistry and Natural Product Chemistry*, *22*(8), 1303. https://doi.org/10.3390/molecules22081303

OLIVIA QUIDO FIRM & FADE | Skin Lightener Cream – O SKIN Pharmaceutical. (n.d.). Retrieved 26 September 2023, from https://firmandfade.com/product/ff1/

Pachuau, L., & Chhakchhuak, M. (2013). Determination of Sun Protection Factor (SPF) number of some aqueous herbal extracts. *Journal of Applied Pharmaceutical Science*, *3*, 150–151. https://doi.org/10.7324/JAPS.2013.3925

Pahari, T., Chattopadhyay, K., Mukherjee, S., & Jana, S. (2020). A Review on a Bio-Synthetic Pathway: Melanogenesis. *International Journal of Current Microbiology and Applied Sciences*, *9*(5), 2372–2385. https://doi.org/10.20546/ijcmas.2020.905.270

Park, J. W., Ha, Y. M., Moon, K. M., Kim, S. R., Jeong, H. O., Park, Y. J., Lee, H. J., Park, J. Y., Song, Y. M., Chun, P., Byun, Y., Moon, H. R., & Chung, H. Y. (2013). De novo tyrosinase inhibitor: 4-(6,7-Dihydro-5H-indeno[5,6-d]thiazol-2-yl) benzene-1,3-diol (MHY1556). *Bioorganic and Medicinal Chemistry Letters*, *23*(14), 4172–4176. https://doi.org/10.1016/j.bmcl.2013.05.029

Park, W.-S., Kwon, O., Yoon, T.-J., & Chung, J. H. (2014). Anti-graying effect of the extract of Pueraria thunbergiana via upregulation of cAMP/MITF-M signaling pathway. *Journal of Dermatological Science*, *75*(2), 153–155. https://doi.org/10.1016/j.jdermsci.2014.05.003

Pena-Pereira, F., & De La Calle, I. (2018). *Solvents/Eutectic Solvents*. https://doi.org/10.1016/B978-0-12-409547-2.14020-X

Pena-Pereira, F., & Namieśnik, J. (2014). Ionic Liquids and Deep Eutectic Mixtures: Sustainable Solvents for Extraction Processes. *ChemSusChem*, *7*(7), 1784–1800. https://doi.org/10.1002/cssc.201301192

Phasha, V., Senabe, J., Ndzotoyi, P., Okole, B., Fouche, G., & Chuturgoon, A. (2022). Review on the Use of Kojic Acid—A Skin-Lightening Ingredient. *Cosmetics*, *9*(3), Article 3. https://doi.org/10.3390/cosmetics9030064

Pillaiyar, T., Manickam, M., & Jung, S.-H. (2017). Downregulation of melanogenesis: Drug discovery and therapeutic options. *Drug Discovery Today*, *22*(2), 282–298. https://doi.org/10.1016/j.drudis.2016.09.016

Pretzler, M., Bijelic, A., & Rompel, A. (2017). Heterologous expression and characterization of functional mushroom tyrosinase (AbPPO4). *Scientific Reports*, *7*(1), 1810. https://doi.org/10.1038/s41598-017-01813-1

Radošević, K., Ćurko, N., Gaurina Srček, V., Cvjetko Bubalo, M., Tomašević, M., Kovačević Ganić, K., & Radojčić Redovniković, I. (2016). Natural deep eutectic solvents as beneficial extractants for enhancement of plant extracts bioactivity. *LWT*, *73*, 45–51. https://doi.org/10.1016/j.lwt.2016.05.037

Radulescu, C., Buruleanu, L., Georgescu, A., & Dulama, I. (2019). *Correlation between Enzymatic and Non-Enzymatic Antioxidants in Several Edible Mushrooms Species*. https://doi.org/10.5772/intechopen.82578

Ramalho, S., Gualberto, N., Santos Leite Neta, M., Batista, R., Araújo, S., Moreira, J., & Narain, N. (2014). Catechin and Epicatechin Contents in Wines Obtained from Brazilian Exotic Tropical Fruits. *Food and Nutrition Sciences*, *05*, 449–457. https://doi.org/10.4236/fns.2014.55053

Rangel, J. C., Benavides Lozano, J., Heredia, J. B., Cisneros-Zevallos, L., & Jacobo-Velázquez, D. (2013). The Folin-Ciocalteu assay revisited: Improvement of its specificity for total phenolic content determination. *Analytical Methods*, *5*, 5990. https://doi.org/10.1039/c3ay41125g

Rao, H. & Lakshmi. (2012). Therapeutic Applications of Almonds (Prunus amygdalus L): A Review. *Journal of Clinical and Diagnostic Research*, *6*, 130–135.

Rathod, N. B., Kulawik, P., Ozogul, F., Regenstein, J. M., & Ozogul, Y. (2021). Biological activity of plant-based carvacrol and thymol and their impact on human health and food quality. *Trends in Food Science & Technology*, *116*, 733–748. https://doi.org/10.1016/j.tifs.2021.08.023

Re, R., Pellegrini, N., Proteggente, A., Pannala, A., Yang, M., & Rice-Evans, C. (1999). Antioxidant activity applying an improved ABTS radical cation decolorization assay. *Free Radical Biology & Medicine*, *26*(9–10), 1231–1237. https://doi.org/10.1016/s0891-5849(98)00315-3

Rovetto, L. J., & Aieta, N. V. (2017). Supercritical carbon dioxide extraction of cannabinoids from Cannabis sativa L. *The Journal of Supercritical Fluids*, *129*, 16–27. https://doi.org/10.1016/j.supflu.2017.03.014

Ruesgas-Ramón, M., Figueroa-Espinoza, M. C., & Durand, E. (2017, April 26). *Application of Deep Eutectic Solvents (DES) for Phenolic Compounds Extraction: Overview, Challenges, and Opportunities* (world) [Review-article]. ACS Publications; American Chemical Society. https://doi.org/10.1021/acs.jafc.7b01054

Rumpf, J., Burger, R., & Schulze, M. (2023). Statistical evaluation of DPPH, ABTS, FRAP, and Folin-Ciocalteu assays to assess the antioxidant capacity of lignins. *International Journal of Biological Macromolecules*, *233*, 123470. https://doi.org/10.1016/j.ijbiomac.2023.123470

Sakkas, H., & Papadopoulou, C. (2017). Antimicrobial Activity of Basil, Oregano, and Thyme Essential Oils. *Journal of Microbiology and Biotechnology*, *27*(3), 429–438. https://doi.org/10.4014/jmb.1608.08024

Sánchez-Ferrer, A., Rodríguez-López, J. N., García-Cánovas, F., & García-Carmona, F. (1995). Tyrosinase: A comprehensive review of its mechanism. *Biochimica Et Biophysica Acta*, *1247*(1), 1–11. https://doi.org/10.1016/0167-4838(94)00204-t

Santos, J. S., Alvarenga Brizola, V. R., & Granato, D. (2017). High-throughput assay comparison and standardization for metal chelating capacity screening: A proposal and application. *Food Chemistry*, *214*, 515–522. https://doi.org/10.1016/j.foodchem.2016.07.091

Santos, S. A. O., Pinto, P. C. R. O., Silvestre, A. J. D., & Neto, C. P. (2010). Chemical composition and antioxidant activity of phenolic extracts of cork from Quercus suber L. *Industrial Crops and Products*, *31*(3), 521–526. https://doi.org/10.1016/j.indcrop.2010.02.001

Santos, S. A. O., Villaverde, J. J., Sousa, A. F., Coelho, J. F. J., Neto, C. P., & Silvestre, A. J. D. (2013). Phenolic composition and antioxidant activity of industrial cork by-products. *Industrial Crops and Products*, *47*, 262–269. https://doi.org/10.1016/j.indcrop.2013.03.015

Sarkar, R., Arora, P., & Garg, K. V. (2013). Cosmeceuticals for Hyperpigmentation: What is Available? *Journal of Cutaneous and Aesthetic Surgery*, *6*(1), 4–11. https://doi.org/10.4103/0974-2077.110089

Sasikumar, J. M., Erba, O., & Egigu, M. C. (2020). In vitro antioxidant activity and polyphenolic content of commonly used spices from Ethiopia. *Heliyon*, *6*(9), e05027. https://doi.org/10.1016/j.heliyon.2020.e05027

Sato, K., & Toriyama, M. (2009). Depigmenting Effect of Catechins. *Molecules*, *14*(11), 4425–4432. https://doi.org/10.3390/molecules14114425

Satooka, H., & Kubo, I. (2011). Effects of Thymol on Mushroom Tyrosinase-Catalyzed Melanin Formation. *Journal of Agricultural and Food Chemistry*, *59*(16), 8908–8914. https://doi.org/10.1021/jf2014149

Sayre, R. M., Agin, P. P., LeVee, G. J., & Marlowe, E. (1979). A Comparison of in Vivo and in Vitro Testing of Sunscreening Formulas. *Photochemistry and Photobiology*, *29*(3), 559–566. https://doi.org/10.1111/j.1751-1097.1979.tb07090.x

Sharifi-Rad, M., Varoni, E. M., Iriti, M., Martorell, M., Setzer, W. N., Del Mar Contreras, M., Salehi, B., Soltani-Nejad, A., Rajabi, S., Tajbakhsh, M., & Sharifi-Rad, J. (2018). Carvacrol and human health: A comprehensive review. *Phytotherapy Research: PTR*, *32*(9), 1675–1687. https://doi.org/10.1002/ptr.6103

Shraim, A. M., Ahmed, T. A., Rahman, M. M., & Hijji, Y. M. (2021). Determination of total flavonoid content by aluminum chloride assay: A critical evaluation. *LWT*, *150*, 111932. https://doi.org/10.1016/j.lwt.2021.111932

Silpa-archa, N., Kohli, I., Chaowattanapanit, S., Lim, H. W., & Hamzavi, I. (2017). Postinflammatory hyperpigmentation: A comprehensive overview: Epidemiology, pathogenesis, clinical presentation, and noninvasive assessment technique. *Journal of the American Academy of Dermatology*, *77*(4), 591–605. https://doi.org/10.1016/j.jaad.2017.01.035

Singh, M., Agarwal, S., Agarwal, M., & R, R. (2020). *Benefits of Theobroma cacao and Its Phytocompounds as Cosmeceuticals* (pp. 509–521). https://doi.org/10.1007/978-981-15-1761-7_21

Singleton, V. L., & Rossi, J. A. (1965). Colorimetry of Total Phenolics with Phosphomolybdic-Phosphotungstic Acid Reagents. *American Journal of Enology and Viticulture*, *16*(3), 144–158. https://doi.org/10.5344/ajev.1965.16.3.144

Skoog, D. A., Holler, F. J., & Crouch, S. R. (2017). *Principles of Instrumental Analysis*. Cengage Learning.

Slominski, R. M., Sarna, T., Płonka, P. M., Raman, C., Brożyna, A. A., & Slominski, A. T. (2022). Melanoma, Melanin, and Melanogenesis: The Yin and Yang Relationship. *Frontiers in Oncology*, *12*, 842496. https://doi.org/10.3389/fonc.2022.842496

Solano, F. (2020). Photoprotection and Skin Pigmentation: Melanin-Related Molecules and Some Other New Agents Obtained from Natural Sources. *Molecules*, *25*(7), Article 7. https://doi.org/10.3390/molecules25071537

Soto-Armenta, L. C., Sacramento-Rivero, J. C., Ruiz-Mercado, C. A., Lope-Navarrete, M. C., & Rocha-Uribe, J. A. (2019). Extraction yield and kinetic study of Lippia graveolens with supercritical CO2. *The Journal of Supercritical Fluids*, *145*, 205–210. https://doi.org/10.1016/j.supflu.2018.12.018

Stephens, N. M., & Smith, E. A. (2022). Structure of Deep Eutectic Solvents (DESs): What We Know, What We Want to Know, and Why We Need to Know It. *Langmuir*, *38*(46), 14017–14024. https://doi.org/10.1021/acs.langmuir.2c02116

Stobiecka, M., Król, J., & Brodziak, A. (2022). Antioxidant Activity of Milk and Dairy Products. *Animals*, *12*(3), Article 3. https://doi.org/10.3390/ani12030245

Sugimoto, K., Nakagawa, K., Hayashi, S., Amakura, Y., Yoshimura, M., Yoshida, T., Yamaji, R., Nakano, Y., & Inui, H. (2009). Hydrolyzable Tannins as Antioxidants in the Leaf Extract of *Eucalyptus globulus* Possessing Tyrosinase and Hyaluronidase Inhibitory Activities. *Food Science and Technology Research*, *15*(3), 331–336. https://doi.org/10.3136/fstr.15.331

Surbhi, Kumar, A., Singh, S., Kumari, P., & Rasane, P. (2021). Eucalyptus: Phytochemical composition, extraction methods and food and medicinal applications. *Advances in Traditional Medicine*. https://doi.org/10.1007/s13596-021-00582-7

Swebocki, T., Barras, A., Abderrahmani, A., Haddadi, K., & Boukherroub, R. (2023). Deep Eutectic Solvents Comprising Organic Acids and Their Application in (Bio)Medicine. *International Journal of Molecular Sciences*, *24*(10), Article 10. https://doi.org/10.3390/ijms24108492

Thawabteh, A. M., Jibreen, A., Karaman, D., Thawabteh, A., & Karaman, R. (2023). Skin Pigmentation Types, Causes and Treatment—A Review. *Molecules*, *28*(12), Article 12. https://doi.org/10.3390/molecules28124839

Touati, R., Santos, S. A. O., Rocha, S. M., Belhamel, K., & Silvestre, A. J. D. (2015). The potential of cork from Quercus suber L. grown in Algeria as a source of bioactive lipophilic and phenolic compounds. *Industrial Crops and Products*, *76*, 936–945. https://doi.org/10.1016/j.indcrop.2015.07.074

Wiegand, I., Hilpert, K., & Hancock, R. E. W. (2008). Agar and broth dilution methods to determine the minimal inhibitory concentration (MIC) of antimicrobial substances. *Nature Protocols*, *3*(2), 163–175. https://doi.org/10.1038/nprot.2007.521

Zárate, R., Portillo, E., Teixidó, S., Carvalho, M. A. A. P. de, Nunes, N., Ferraz, S., Seca, A. M. L., Rosa, G. P., & Barreto, M. C. (2020). Pharmacological and Cosmeceutical Potential of Seaweed Beach-Casts of Macaronesia. *Applied Sciences*, *10*(17), Article 17. https://doi.org/10.3390/app10175831

Zhang, Q.-W., Lin, L.-G., & Ye, W.-C. (2018). Techniques for extraction and isolation of natural products: A comprehensive review. *Chinese Medicine*, *13*(1), 20. https://doi.org/10.1186/s13020-018-0177-x

Zhao, P., Park, N. H., Alam, M. B., & Lee, S.-H. (2022). Fuzhuan Brick Tea Boosts Melanogenesis and Prevents Hair Graying through Reduction of Oxidative Stress via NRF2-HO-1 Signaling. *Antioxidants*, *11*(3), 599. https://doi.org/10.3390/antiox11030599

Zhishen, J., Mengcheng, T., & Jianming, W. (1999). The determination of flavonoid contents in mulberry and their scavenging effects on superoxide radicals. *Food Chemistry*, *64*(4), 555–559. https://doi.org/10.1016/S0308-8146(98)00102-2

Zhou, D., Liu, Z.-H., Wang, D.-M., Li, D.-W., Yang, L.-N., & Wang, W. (2019). Chemical composition, antibacterial activity and related mechanism of valonia and shell from Quercus variabilis Blume (Fagaceae) against Salmonella paratyphi a and Staphylococcus aureus. *BMC Complementary and Alternative Medicine*, *19*(1), 271. https://doi.org/10.1186/s12906-019-2690-6

Zhu, Y., Wang, S., Lin, F., Li, Q., & Xu, A. (2014). The therapeutic effects of EGCG on vitiligo. *Fitoterapia*, *99*, 243–251. https://doi.org/10.1016/j.fitote.2014.08.007

Zolghadri, S., Bahrami, A., Hassan Khan, M. T., Munoz-Munoz, J., Garcia-Molina, F., Garcia-Canovas, F., & Saboury, A. A. (2019). A comprehensive review on tyrosinase inhibitors. *Journal of Enzyme Inhibition and Medicinal Chemistry*, *34*(1), 279–309. https://doi.org/10.1080/14756366.2018.1545767